Optimized Energy Management for Electric Vehicles and Infrastructures

Yassir Dahmane

THÈSE DE DOCTORAT DE

L'ÉCOLE CENTRALE DE NANTES

ÉCOLE DOCTORALE N° 601
Mathématiques et Sciences et Technologies de l'Information et de la Communication
Spécialité : *Génie électrique*

Par

Yassir DAHMANE

«Gestion d'énergie optimisée étendue véhicules infrastructures»

Thèse présentée et soutenue à l'École Centrale de Nantes, le 16 décembre 2020
Unité de recherche : UMR 6004, Laboratoire des Sciences du Numèrique de Nantes (LS2N)

Rapporteurs avant soutenance :

Delphine RIU	Professeur des universités, Grenoble INP
Mickaël HILAIRET	Professeur des universités, Université de Franche-Comté, Belfort

Composition du Jury :

Président :	Jean-Pierre BARBOT	Professeur des universités, ENSEA Cergy-Pontoise, QUARTZ
Examinateur :	Hervé GUEGUEN	Professeur, Centrale Supelec, Cesson-Sévigné
Dir. de thèse :	Malek GHANES	Professeur des universités, École Centrale de Nantes
Co-encadrant :	Raphaël CHENOUARD	Maître de conférences, École Centrale de Nantes

Invité(s) :
Mario ALVARADO-RUIZ Docteur, Technocentre Renault, Guyancourt

Remerciement

Ce travail de thèse est le fruit d'une collaboration entre le laboratoire LS2N à Centrale Nantes (CN) et le groupe automobile REANULT à partir d'octobre 2017. Ce travail est dans le cadre d'une Chaire entre Centrale Nantes et RENAULT visant à renforcer l'excellence des véhicules électriques et hybrides REANULT en terme de fiabilité et performance énergétique, développement l'innovation de rupture sur les groupes motopropulseurs par des techniques de commande et d'observation avancées.

Mes premiers remerciements s'adressent de droit à mon directeur de Thèse, Mr. Malek GHANES. Je t'exprime ma gratitude et te remercie chaleureusement. Merci Malek pour m'avoir fait confiance, m'avoir laissé autant de liberté dans mes travaux de recherches, pour tes conseils avisés, ton formidable côté humain et nos discussions diverses et variées. J'ai réellement apprécié d'apprendre et de travailler à tes côtés. Merci Malek de m'avoir toujours encouragé et soutenu notamment lors des moments les plus difficiles de ces trois années de Thèse. Tu n'étais pas en réalité qu'un directeur de Thèse pour moi, je considère plutôt que tu représentes un vrai savoir-faire, là où on apprend la rigueur, et un vrai savoir-être là où on apprend la sagesse et le bon sens.

Je remercie mon co-encadrant Mr. Raphaël CHENOUARD. Ton expérience, tes explications et tes conseils scientifiques m'ont été d'une grande importance. Merci également pour tes critiques constructives et positives à l'égard de mes rédactions, du manuscrit et de la présentation de ma soutenance.

J'ai été honoré par un jury de Thèse constitué de personnalités scientifiques qui ont pris le temps d'analyser mon travail. À ce titre, j'exprime ma profonde gratitude à Mr. Jean-Pierre BARBOT Professeur des Universités, ENSEA Cergy-Pontoise QUARTZ, pour avoir accepté la présidence du jury.

Mes sincères remerciements s'adressent à Mme. Delphine RIU Professeur des Universités à INP Grenoble, G2Elab et à Mr. Mickaël HILAIRET Professeur des Universités à Université de Franche-Comté, FEMTO-ST pour m'avoir fait l'honneur d'accepter d'être rapporteurs de ce travail. J'ai apprécié vos remarques pertinentes et vos questions qui ont montrées vos intérêts vis-à-vis de cette thématique. Je remercie Mr. Hervé GUEGUEN Professeur à Centrale Supélec, IETR, pour avoir accepté de faire partie du jury en tant qu'examinateur.

Un grand Merci très particulier à mon directeur de Thèse, Mr. Malek GHANES et à mes co-encadrants Mr. Raphaël CHENOUARD et Mr. Mario ALVARADO-RUIZ, qui m'ont secoué, soutenu et encouragé tout au long de ces trois années de thèse. Merci pour avoir tenté de me tirer vers le meilleur ; j'espère avoir pu vous proposer un travail à la hauteur de vos attentes.

Avec de ce mot de remerciement, je tiens à exprimer ma volonté de poursuivre notre collaboration autour de ces thématiques passionnantes sur les batteries, les véhicules électriques, l'optimisation et les Smart Grids.

Du coté de Renault, j'ai sans doute beaucoup de gens à remercier du fond du cœur pour leur aide et leur présence dans ma vie de Thèse. Tous mes remerciements s'adressent d'abord à mes responsables côtés de Renault Mr. Ahmed KETFI-CHERIF et Mr. Abdelmalek MAALOUM qui m'ont fait confiance et cru en moi depuis mes tous premiers pas à Renault. Je dois dire Ahmed et Abdelmalek sont un exemple pour moi en étant tellement professionnel et humain à la fois. Je retiens d'eux des qualités d'un manager très diplomate, multitâche, ouvert, très souriant et assez ferme à la fois. En gardant l'ordre chronologique, je remercie mon encadrant du coté de Renault Mario ALVARADO-RUIZ. Là aussi, je retiens de nombreuses qualités aussi bien techniques qu'humaines. Je retiendrai ses remarques pertinentes et ses conseils avisés tout au long de mon projet de Thèse. Je tiens à remercier mes amis au Technocentre de Renault et mes anciens camarades d'école d'ingénieurs, Abdelaziz BOUZIANI et Othman ZOUITA de leur aide pendant mes déplacements au Techocentre de Renault.

Un grand merci également à Mr. Mohamed Fouad BENKHORIS et Mr. Hervé GUEGUEN qui ont participé au comité de suivi de ma thèse tout au long de ces trois dernières années. Grace à leurs orientations et à leurs propositions pertinentes, j'ai pu avancer sur plusieurs parties de ce travail de thèse.

Dans la continuité, un grand merci également à Mme Christine THABARD et Mme Virginie DUPONT de leur aide dans les procédures administratives et mes déplacements professionnelles tout le long de de mes trois ans de Thèse.

Un grand merci à Mr. Maël VILLENEUVE de son support informatique et son assistance technique surtout pendant la panne de mon disque dur.

Mes remerciements s'adressent de la même façon, à tous mes amis du laboratoire qui m'ont précieusement aidé et encouragé pendant ces dernières années et avec lesquels je passe des très bons moments au laboratoire dans lesquels je me déconnecte pour quelques instants de mes travaux de Thèse.

J'ai enfin l'honneur d'adresser mes remerciements les plus profonds à ma famille proche. Recevez toute ma gratitude, ma reconnaissance totale et tous mes sincères remerciements. C'est grâce à vous que j'ai réussi à accomplir un tel travail, je vous le dédie donc de droit.

À toutes les personnes que j'aime et qui me sont chères.

À mon frère, merci à toi très cher frère. Tu es mon ami et mon âme sœur. À qui je peux me confier, tu as une place exceptionnelle dans ma vie, de tous les autres. Un lien différent que nul ne modifiera.

À ma femme, merci infiniment pour ton soutien, ta compréhension et ton amour. Tes sourires suffisent à mon bonheur. Il n'y a pas de mots suffisamment forts pour t'exprimer mon amour. Je te serai éternellement reconnaissant d'avoir été à mes coté durant ce travail.

À mon très cher Papa, merci à toi pour les valeurs que tu m'as inculquées. C'est en prenant exemple sur toi que je m'efforce chaque jour d'être un bon mari.
À ma très chère Maman, merci à toi pour ton éducation, sans toi cette réalisation aurait été impossible. Trouve la réalisation de ce travail, l'aboutissement de tes efforts et tes sacrifices. Je te dédie donc personnellement cette Thèse et je t'adresse ma plus affectueuse gratitude.

Resumé

Titre: Gestion d'énergie optimisée des véhicules électrique et infrastructures

Resumé: Cette thèse de doctorat s'inscrit dans le cadre de la chaire Renault/Centrale Nantes sur l'amélioration des performances des véhicules électriques (EV/HEV). Elle est dédiée à la problématique de la gestion de la recharge des véhicules électriques, en utilisant des algorithmes d'optimisation et des stratégies de recharge intelligentes. Dans ce cadre, plusieurs contributions ont été proposées sur les sujets de la recharge intelligente d'une voiture électrique et la gestion de la recharge d'une flotte de véhicules électriques, en considérant les contraintes de mobilités (SOC désiré à la fin de la recharge et heure de départ), la température des batteries Li-ion, les infrastructures de recharge, et le réseau électrique.

Sur le sujet de la recharge intelligente d'une voiture électrique, les contributions se sont concentrées sur le développement des algorithmes embarqués permettant la planification du profil de la puissance de recharge afin de réduire le coût de la recharge. Les algorithmes proposés prennent en compte les besoins de mobilités des utilisateurs de véhicules électriques, et l'effet de la température sur la puissance de recharge des batteries Li-ion. Sur le sujet de la gestion de recharge de flotte de véhicules, les contributions portent essentiellement sur les algorithmes centralisés dans les stations de recharge de véhicules électriques. Un algorithme de recharge unidirectionnelle a été proposé afin d'évaluer le nombre optimal de véhicules électriques à recharger avec un bon niveau de satisfaction des contraintes de mobilités et sans aucun renforcement de l'infrastructure. Le passage à l'algorithme bidirectionnel est fait grâce à l'exploitation de la fonctionnalité V2G qui permettra la participation des véhicules électriques dans la régulation de fréquence.

Les contributions proposées sur le premier sujet ont l'avantage d'augmenter la précision d'estimation de SOC final en très basse température, et d'être embarquable sur le véhicule grâce à la légèreté des algorithmes et la rapidité d'exécution. D'autre part, les algorithmes de gestion de recharge de flotte de véhicules permettent une intégration des véhicules électriques à grande échelle sur le réseau et montrent le potentiel des voitures électriques dans la contribution à la stabilité du réseau électrique.

Les algorithmes et les stratégies développées ont été testés en simulation et seront testés sur un système de recharge de voiture électrique. Les résultats obtenus ont permis de mettre en évidence l'avantage de la recharge intelligente sur la réduction des coûts, les bienfaits sur le réseau et l'importance de la gestion de la recharge des flottes de véhicules électriques dans développement des services réseaux.

Mots clés: Voiture électrique, optimisation, batteries Li-ion, effet de la température, algorithmes de planification, gestion d'énergie de flotte, réseau intelligent, V2G, régulation de fréquence.

Abstract

Title: Optimized Energy Management for Electric Vehicles and Infrastructures

Abstract: This PhD thesis is part of the Renault/Centrale Nantes chair on improving the performance of electric vehicles (EV/PHEV). It is dedicated to the problem of the charging management of electric vehicles, using optimization algorithms and smart charging strategies. In this framework, several contributions have been proposed on the topics of smart charging of an EV and the smart energy management of an EV fleet, considering the mobility constraints (desired SOC at the end of the charging and departure time), the temperature of the Li-ion batteries, the charging infrastructures, and the power grid.

On the subject of smart charging of an EV, the contributions focused on the development of embedded algorithms allowing the scheduling of the charging power profile in order to reduce the charging cost. The proposed algorithms take into account the mobility needs of electric vehicle users, and the effect of temperature on the charging power of Li-ion batteries. On the subject of fleet energy management, the contributions focus on centralized algorithms in electric vehicle charging stations. An unidirectional recharging algorithm has been proposed in order to evaluate the optimal number of electric vehicles to be recharged with a good level of satisfaction of mobility constraints and without any infrastructure reinforcement. The switch to the bidirectional algorithm is due to the exploitation of the V2G functionality, which will allow the participation of electric vehicles in frequency regulation.

The proposed contributions on the first topic have the advantage of increasing the estimation accuracy of final SOC in very low temperature, and to be embedded on the EV due to the low computational capacity of the algorithms and the speed of execution. On the other hand, the EV fleet charging management algorithms allow the possibility of large-scale integration of electric vehicles on the grid and show the potential of EVs in contributing to the stability of the power grid by offering ancillary services such as frequency regulation.

The algorithms and strategies developed have been tested in simulation and will be tested on an EV charging system. The results obtained have highlighted the benefits of smart charging on cost reduction and grid benefits and the importance of electric vehicle fleet charging management in the development of grid services.

Keywords: Electric vehicle, optimization, Li-ion battery charging, temperature effect, scheduling algorithms, EV fleet energy management, smart grid, V2G, frequency regulation.

Contents

List of Figures

List of Tables

1

General Introduction

1.1 General Objectives and Problem Statement

Climate and weather conditions are changing across the planet resulting in extreme weather events such as long heat waves, more violent thunderstorms, rare but abundant rainfall. In the last two centuries, the human use of fossil fuels has increased, causing the increase of CO_2 emissions. The increase of greenhouse gas emissions in the world has contributed to a rise of the average global temperature [11].

At a critical time when global emissions are expected to decrease, emissions from transport are increasing, resulting from a higher overall volume of travel. The transport sector emissions also expected to grow at a faster rate than that from any other sector, representing more than 24% of global CO_2 emissions in 2017 [12].

The decarbonization of the transport sector represents a big challenge to meet the Paris agreement and other global goals on climate change. In terms of transport' mode, CO_2 emissions have increased in international aviation and maritime transport, but the majority of transport greenhouse gas emissions come from road vehicles with 74% contribution [12]. Thus, the electrification of road vehicles is an important part of the solution towards an ecological transport model with zero-emission. Due to their low climate impact over their life cycle, electric vehicles (EVs) can make the ecological transition faster and easier.

With the development of electric motor technology in the last century, direct current machines, permanent magnet synchronous motors and induction motors have reached enough maturity to meet the requirement of the EV manufacturers on the term of power efficiency, robustness, reliability, and cost. Moreover, a highly efficient drive motor has been developed with good efficiency and very good precision due to the technological advance in semiconductors and transistors [13]. Allowing both accurate and robust control of the electric motor not only in traction mode but also in breaking mode, using the electric motor as generator and enabling the energy recovery to the battery.

The charging of the battery can be possible with the development of new chemistries allowing the charging and discharging of the batteries [1]. In 1859, Gaston Plante invented the lead-acid battery, the first battery that could be recharged by applying a reverse current flow through it. This invention enabled the development of other battery technologies such as nickel-cadmium (NiCd), and nickel metal hybride (NiMH) as shown in Figure 1.1.

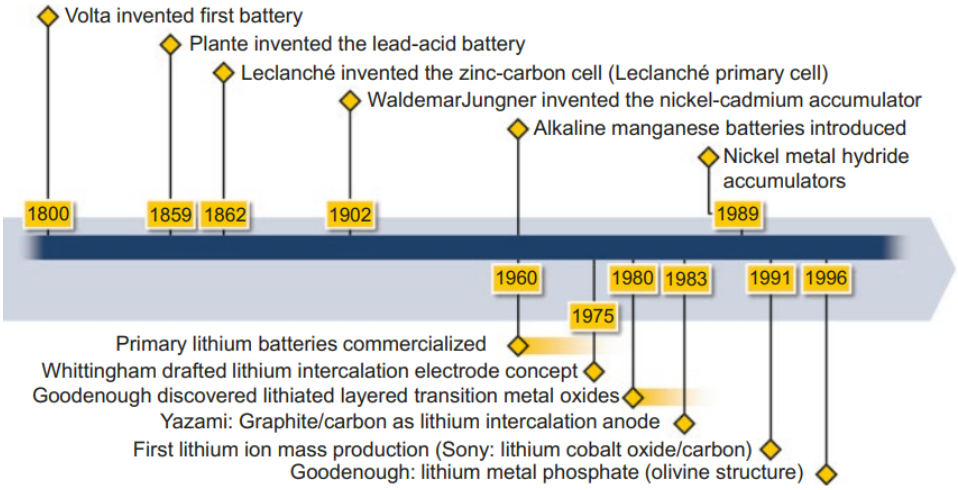

Figure 1.1 – The battery timeline [1]

In 1980, Rachid Yazami [14] was the first, to succeed in intercalating lithium into a graphite electrode without loss of metal. This electrode made it possible to convert the lithium battery into a rechargeable battery. At the same time, a cathode was developed by John Goodenough [15], which enabled Akira Yoshino, five years later, to produce the first prototype of the lithium ion (Li-ion) battery and open up the doors to world markets in 1991. This work jointly led to the development of the first rechargeable lithium battery. Since then, Li-ion batteries have continued to evolve in terms of their chemical composition, energy density, etc.

All technological progress in motors, controllers, and batteries have made it possible. Today, almost all car manufacturers commercialize EVs. Several types of EVs exist in the market, hybrid electric vehicles (HEVs), plug-in hybrid electric vehicles (PHEVs), and battery electric vehicles (BEVs).

The two major battery technologies used in EVs are NiMH and Li-ion. Almost, all HEVs available in the market today use Li-ion batteries because of the maturity of Li-ion technology. Due to the high specific energy, high power density, and cost decreasing, the adoption of Li-ion batteries is expected to grow fast in EVs, particularly in rechargeable EVs (PHEVs and BEVs). Moreover, classical cell systems such as lead-acid, NiCd or NiMH are based on a single chemistry, in contrast to Li-ion batteries that could be produced by several active materials. The combining of lithium with other type of active materials determine the internal characteristics of the Li-ion cells in term of specific energy, power density, temperature sensitivity, internal resistance, and nominal voltage. There are several examples of Li-ion battery chemistry: Lithium cobalt oxide ($LiCoO_2$), lithium iron phosphate ($LiFePO_4$) and lithium titanate ($Li_4Ti_5O_{12}$) [1].

In parallel of the development of EVs technology, countries are interested to convert their internal combustion engine vehicle (ICEV) fleets to electric fleets in order to reduce their greenhouse gas emissions. Placing the promise of an environmentally sustainable transportation system, many countries support of the development of the EVs through conversion bonus, aids for the purchase and subsidies. Therefore, the electric vehicle market is on the rise [2], specially the EV market in North America, China and Europe (see Figure 1.2).

The range of EVs has increased significantly in the last five years. The range hits the mark of 1000 km for the Tesla Roadster for a single charge, 600 km for Tesla Model S LR in WLTP driving cycle, 515 km for Tesla Model 3 Long Range, 451 km for Kia e-Niro, 413 km for Hyundai Kona Electric, 395 km for Renault Zoé ZE 50, and 360 km for Nissan Leaf Plus. The fear of loosing autonomy called range anxiety was the main focus of discussions on EVs is now in the past. Despite the incentives for the purchase of EVs, the development of the battery

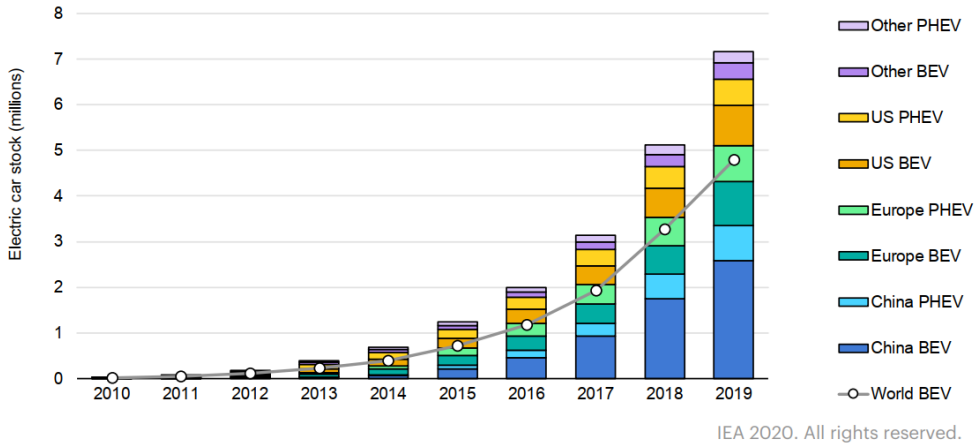

Figure 1.2 – Global electric car stock, 2010-2019 [2]

technology and the increasing range of EVs, the current big challenge for EVs is the charging time. Nowadays, the topic of EV's charging time is getting more attention. The charging time depends on several parameters such as the charging power available and the capacity of the batteries. The duration of the charging process can take 30 min for a fast charging point to many hours in slow charging mode.

The key drivers of the prevalence of domestic charging are convenience, profitability and various supportive policies (such as preferential tariffs, equipment incentives and discounts). Figure 1.3 shows that in 2019, there were about 7.3 million chargers worldwide, of which about 6.5 million were slow chargers for private light vehicles in homes, multi-dwelling buildings and workplaces [2]. The charging infrastructure for electric vehicles will continue to expand.

The home charging can make the EVs more profitable by using vehicle to grid (V2G) and vehicle to home (V2H) features. The owners of EVs can reduce their electricity bill by using the energy stored in the battery to supply the grid or their home in the moment of high energy tariffs like peak hours. By doing so, EVs should schedule the charging to avoid high energy prices periods by using the smart charging concept. With this feature, the EV can manage the charging by shifting the charging from high demand periods (evening charging) when the energy is more expensive to the night charging when the energy prices are more interesting. Moreover, the V2G and V2H features can encourage the purchase of EVs by decreasing the total acquisition cost due to the economic profit from V2G and V2H in high energy price periods.

While the EVs night charging can offer a lot of benefits to both EV owners and the power grid, a major problem occurs especially with Li-ion batteries at night charging when the temperature drops to subzero temperatures in certain regions. Due to the higher sensitivity of the Li-ion battery to the temperature compared to other battery technologies, subzero temperatures decrease the power acceptance, increase the internal resistance of the Li-ion batteries, causing the raising of the Joules power losses, decreasing the efficiency of the charging, and affecting the State of Health (SOH) of the Li-ion batteries [16]. On the other side, high temperatures increase power acceptance of the battery thus facilitate high depth of discharge (DOD) of Li-ion therefore battery lifetime decreases rapidly, causing premature ageing and leakages on the Li-ion batteries [17]. Considering the effect of temperature on the Li-ion batteries is an important topic that makes the EVs suitable to any climate condition and can extend the batteries' lifespan.

Over the coming decade, several challenges will emerge because of the increasing of the penetration level of EVs (PHEV, BEV) in the power grid, and the increasing of the number of

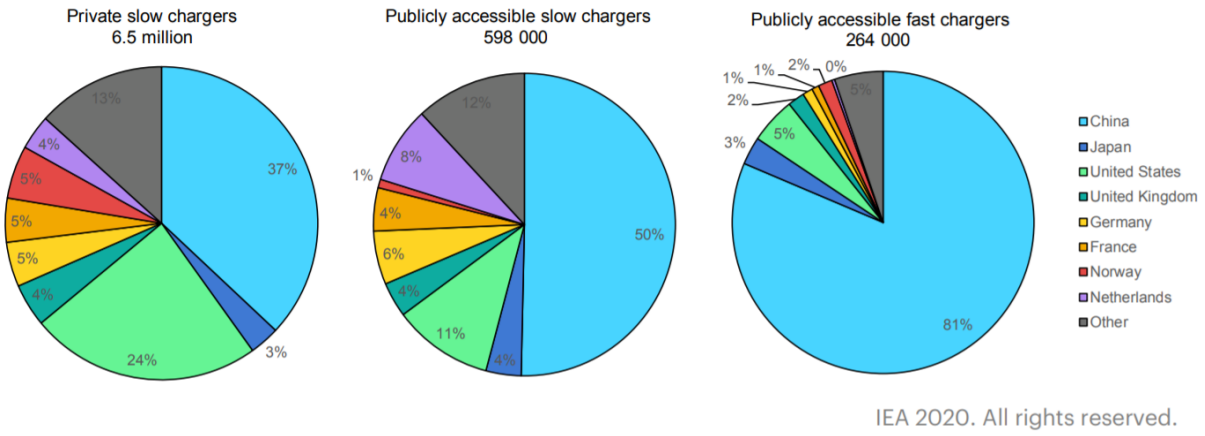

Figure 1.3 – Private and publicly accessible chargers by country, 2019 [2]

private and public charging points. Being able to adjust their charging power on peak hours demand, EVs' smart charging can provide several flexibility services to the power grid. EV fleets can be considered as an energy storage system (ESS) that can supply the grid during high power demand and can be charged during extra power production periods. Moreover, EVs can operate in several timescales from milliseconds to long charging periods, due to the high power density of Li-ion batteries and their fast dynamics. With V2G technology, EVs can provide ancillary services to the power grid like spinning reserve, active/reactive power support, load leveling, peak load shaving, power factor correction and voltage regulation. One of the most common services that EV fleets can offer is the control of grid frequency [18]. The management and the coordination of the charging is a big challenge to ensure the stability of the power grid, support the deployment of renewable energy and guarantee the energy requirement of the EVs' users.

In the literature various charging strategies have been proposed that could be groupped as centralized [19–22] and decentralized [23–26]. The centralized strategies carry out the charging from a system level viewpoint and consider EVs present on all nodes of the system collectively. On the other hand, decentralized strategies operate locally at the nodal level. This thesis covers the two approaches by contributing to the development of smart charging algorithms using centralized and decentralized strategies.

Charging of EVs involves many challenges for EV users by accomplishing their mobility energy requirement targets, minimizing the charging cost, reducing the charging time and maximizing the battery lifetime. On the other side, the power grid is impacted by the high penetration of EVs and aware of the potential benefits of the EVs to accomplish much more active role in the handling of existing challenges and avoiding future environmental problems. Charging EVs includes many nuanced considerations and subtleties to consider conflicting objectives of satisfying both EV user's requirement and the grid constraints.

From these perspectives, this PhD thesis, was carried out in the context of the chair between Centrale Nantes and Renault Group at Guyancourt about EV/HEV propulsion performances, addresses the problematic of optimized energy management of electric vehicles and infrastructure considering unidirectional and bidirectional charging of EVs. The main objective of this thesis is the development of EV smart charging algorithms that take into account the satisfaction of EV users and the grid infrastructure.

Nowadays, several EVs manufacturers and power grid operators give a big interest in smart charging strategies and the charging management of EV fleets. The optimal integration of EVs into a smart grid becomes one of the most challenging current topics for the industry. Nevertheless, it remains as even a virgin field which has a great potential to be developed in the

coming years by the industrial and the academic researchers in order to reduce the gap between the increase in the number of EVs and the available charging infrastructure.

This PhD thesis is part of the Renault Chair project for the improvement of EV/HEV storage performances. It will focus on the development of an innovative supervision strategies of EV charging allowing the reduction of financial cost of the EV charging using V2G technology on a decentralized framework. A particular interest is given to centralized charging strategies that can coordinate the charging of EV fleets on the charging stations and can provide services such as frequency regulation or spinning reserve to different actors in the grid.

1.2 Thesis Outline and the Main Contributions

In order to address the topics previously presented, this thesis is structured according to the following outline:

Chapter 2 presents the methodology of Li-ion battery modeling and gives an exhaustive review of the battery model such as electrochemical models, empirical models and equivalent circuit models. Given the importance of the thermal aspects of Li-ion batteries, some thermal models will be discussed. A combination of an equivalent circuit model and a thermal model is proposed. TFollowed by an proposition of an electro-thermal battery model that will be adopted afterwards in this work. The last section describes the parameters identification method for the used Li-ion thermal model.

Chapter 3 focuses on the development of smart charging strategies in a decentralized framework in order to reduce the charging cost. Two charging strategies are presented, both of them take into account the temperature of the battery and use the presented Li-ion electro-thermal model. The first strategy proposes a smart bidirectional charging algorithm that exploits the vehicle to grid (G2V) and V2G concepts using a constant time step. The second decentralized smart charging strategy takes into account the energy prices, EV's users needs, the outside air temperature and the temperature of the battery, in order to formulate and solve a non-linear constrained optimization problem. The second strategy is an updated version of the previous strategy with the use of an optimized dynamic time step.

Chapter 4 addresses the management of EV fleets charging by proposing two smart charging strategies in a centralized framework. While the first proposed strategy considers only unidirectional charging and grid infrastructure constraints, the second strategy outperforms the first one by proposing a bidirectional charging strategy with a frequency regulation service based on EVs V2G feature.

Chapter 5 is a general conclusion summarizing the work and proposing some queues for future research.

2

Lithium-ion Battery Modeling

2.1 Introduction

The Li-ion batteries are widely used as a storage technology in EVs (HEV, PHEV and BEV). Several different functions are assigned to the battery management system (BMS), but the most important one is the monitoring of battery states. In order to ensure the safety and the reliability of the Li-ion batteries, the supervision of the batteries is mainly based on an accurate battery modeling. The battery model is used in route planning, charging scheduling, range and SOC estimation, etc. All these tasks can not be done using sensors or measurements, therefore the battery modeling is a crucial topic in the design of an EV. Several battery modeling approaches are proposed in the literature, each model is designed for a specific application. The choose of the optimal battery model is a tradeoff between complexity and accuracy.

The next section explains the different modeling approaches of Li-ion batteries used in the electric vehicle field. Moreover, it reviews various battery modeling approaches including mathematical models, electrochemical models and electrical equivalent circuit models. It discusses also the different kinds and levels of battery modeling for each application.

2.2 Approach of Li-ion Battery Modeling

Several types of modeling exist, electrochemical models are the most accurate battery model because they describe the internal chemical behavior of the cell [27–31]. Based on the chemical process in the electrodes and electrolyte, the electrochemical models consist of a set of coupled partial differential equations that capture the chemical reactions taking place inside the cell [27]. In order to avoid the use of high complex model, the electrical modeling could be a good alternative in which there is a trade off between the high accuracy and the simplicity. The electrical models use a simplified electrical circuit to model the variables of the battery cell such as the voltage and the current. The accuracy can be achieved by adding more circuits that consider other internal phenomena of the battery. Significant temperature increases can develop when lithium-ion cells are assembled for EVs applications and, as a result, current and temperature distributions become more pronounced [29]. The thermal modeling provides essential information of the temperature distribution that can prevent the battery from a thermal runaway due to the heat generation. Another type of battery modeling consists of coupling

two physical domains in the same battery model such as electro-thermal models. This type of modeling can handle in the same model the electrical and the thermal behavior of the Li-ion batteries [32, 33].

2.2.1 Electrochemical models

The electrochemical models are based on the chemical processes that take place in the battery. These kind of models describe the different battery processes in great detail and considering the electrochemical phenomena that take place in the battery, such as diffusion and polarization [34]. As a result, this type of model becomes more complex.

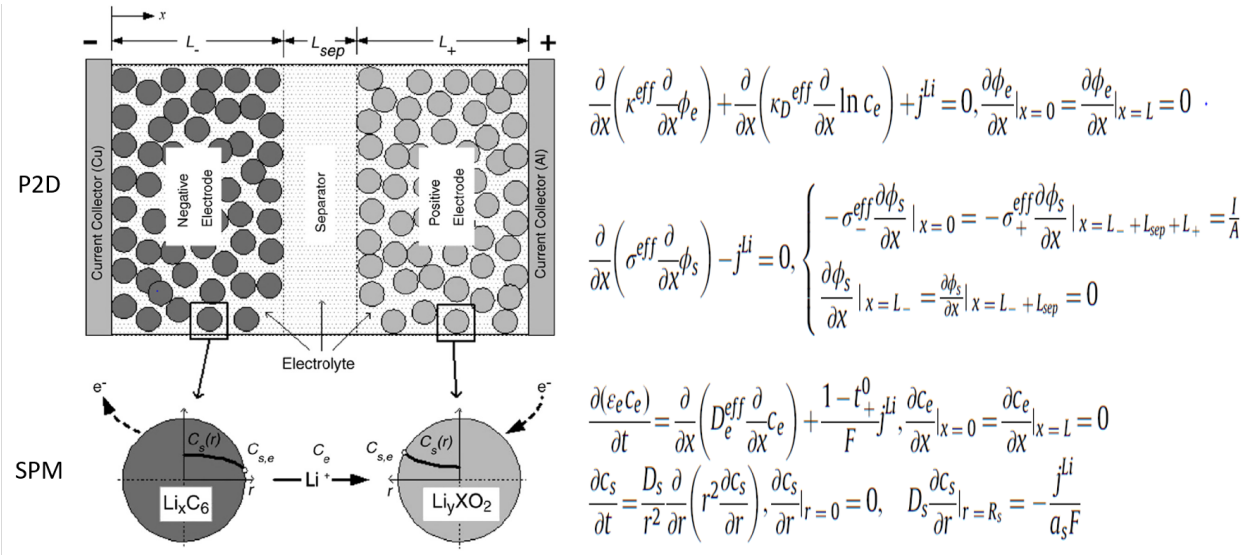

$$\frac{\partial}{\partial x}\left(\kappa^{eff}\frac{\partial}{\partial x}\phi_e\right)+\frac{\partial}{\partial x}\left(\kappa_D{}^{eff}\frac{\partial}{\partial x}\ln c_e\right)+j^{Li}=0,\ \frac{\partial\phi_e}{\partial x}|_{x=0}=\frac{\partial\phi_e}{\partial x}|_{x=L}=0$$

$$\frac{\partial}{\partial x}\left(\sigma^{eff}\frac{\partial}{\partial x}\phi_s\right)-j^{Li}=0,\ \begin{cases}-\sigma_-^{eff}\frac{\partial\phi_s}{\partial x}|_{x=0}=-\sigma_+^{eff}\frac{\partial\phi_s}{\partial x}|_{x=L_-+L_{sep}+L_+}=\frac{I}{A}\\ \frac{\partial\phi_s}{\partial x}|_{x=L_-}=\frac{\partial\phi_s}{\partial x}|_{x=L_-+L_{sep}}=0\end{cases}$$

$$\frac{\partial(\varepsilon_e c_e)}{\partial t}=\frac{\partial}{\partial x}\left(D_e^{eff}\frac{\partial}{\partial x}c_e\right)+\frac{1-t_+^0}{F}j^{Li},\ \frac{\partial c_e}{\partial x}|_{x=0}=\frac{\partial c_e}{\partial x}|_{x=L}=0$$

$$\frac{\partial c_s}{\partial t}=\frac{D_s}{r^2}\frac{\partial}{\partial r}\left(r^2\frac{\partial c_s}{\partial r}\right),\ \frac{\partial c_s}{\partial r}|_{r=0}=0,\quad D_s\frac{\partial c_s}{\partial r}|_{r=R_s}=-\frac{j^{Li}}{a_s F}$$

Figure 2.1 – Lithium cell electrochemical model [3]

There are two main types of electrochemical models used in the literature: the pseudo-two-dimensional model (P2D) and the single particle model (SP), as shown in Figure 2.1 [35, 36]. The P2D model [37, 38] is based on the concentrated solution theory and the porous electrode theory model. In this model the porous electrode structure increases the specific surface area, which adequately facilitates the diffusion of ions through the electrodes. The porous structure of the graphite and the lithium materials are able to provide sufficient contact with the electrolyte [39]. P2D models consider the active material in the electrode as spherical particles of equal size and volume [40].

The SP model [41, 42] is a simplification of the P2D model which considers the electrode as a unique particle. If the liquid phase concentration and the electrode potential are assumed constant, the reactions in the electrodes are assumed to be identical for different particles. Thus, the SP model does not consider of the distribution of the Li-ions concentration inside the electrolyte phase [43]. Compared to the P2D model, the description of the migration of Li ions inside a solid particle is much simpler for the SP model [40].

Generally, the electrochemical model consists of different mathematical models represented by partial differential equations difficult to solve because they require initial and boundary conditions. In addition to the high number of equations, the electrochemical models require several electrochemical parameters that are difficult to obtain directly. For this reason, optimization methods are often used for the parameters estimation [40].

Despite the complexity of an electrochemical model, there can be little doubt that electrochemical models are the most accurate among all battery models, as they explain the key

behaviors of the battery at the microscopic scale based on the chemical reactions occurring inside the electrodes and the electrolyte [27].

2.2.2 Empirical models

The computational cost of the electrochemical model (P2D and SP) make the integration of this kind of model difficult in the BMS. Considering the essential nonlinear characteristics of a battery, the empirical model avoids the coupled partial differential equations and uses only a reduced order polynomial expressions. There are different classical empirical models in the literature such as the Shepherd model, the Unnewehr Universal Model and the Nernst model. The three models can predict the terminal voltage of the cell based on the SOC and the current. These three empirical models are adapted from the reference [44].

— Shepherd model: The Equation (2.1) describes the electrochemical behavior of the battery directly in terms of voltage, SOC and current

$$U_t = K_0 - R_0 I_L + \frac{K_1}{z_s} \tag{2.1}$$

— Unnewehr Universal Model: The Equation (2.2) simplifies the Shepherd model and attempts to model the variation in resistance with respect to SOC

$$U_t = K_0 - R_0 I_L + K_2 z_s \tag{2.2}$$

— Nernst model : The Equation (2.3) can be viewed as a modifications to the Shepherd model and uses exponential function with respect to SOC

$$U_t = K_0 - R_0 I_L + K_3 \ln z_s + K_4 \ln(1 - z_s) \tag{2.3}$$

— Combined model: The Equation (2.4) can be viewed as a combination of the previous three models for better accuracy purpose

$$U_t = K_0 - R_0 I_L + \frac{K_1}{z_s} + K_2 z_s + K_3 \ln z_s + K_4 \ln(1 - z_s) \tag{2.4}$$

In these models, U_t is the terminal voltage; K_0, K_1, K_2, K_3, K_4 are constant parameters of the empirical models; I_L is the current; R_0 is the internal resistance; z_s is the abbreviation for SOC

The parameters in the empirical models could be estimated using a system identification procedure. These models have the advantage of being linear in term of the parameters. Using a set of empirical data (U_t,I_L,z_s), the parameters may be identified using least-squares estimation [44] or optimization methods [45].

Many Li-ion battery models are developed for vehicle power management control purpose and battery management system development. But it remains the most commonly used model is the equivalent circuit (EC) models.

2.2.3 Equivalent circuit models

The complexity of the electrochemical models, the low accuracy of the empirical models and limitations of the computers in the past, led researchers to investigate another modeling approach called EC model. Nowadays, for many applications, it is important to strike a balance between model complexity and accuracy so that models can be embedded in BMS microprocessors and provide accurate results in real-time [27, 40]. The EC models are formed by resistors, capacitors, Resistance-Capacitance (RC) networks, and voltage sources. Various EC Models such as the Rint model, the Thevenin model and DP model are now widely used in EV applications [4, 45].

The Rint Model

The simplest model is the internal resistance model Rint model. It consists of an ideal voltage sources U_{oc} representing the open circuit voltage, and a resistance R_0, as shown in Figure 2.2. Both R_0 and U_{oc} depend on SOC, SoH and temperature. U_L is the terminal voltage, and I_L is the current. The electrical equation of Rint model is expressed by Equation (2.5).

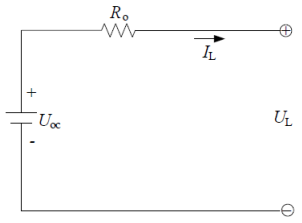

Figure 2.2 – Internal Resistance battery Model [4]

$$U_L = U_{oc} - R_0 I_L \tag{2.5}$$

The Thevenin Model

The Thevenin model adds a parallel RC network in series to the Rint model. The major added value is the dynamic behavior of the battery which was neglected in Rint Model. As shown in Figure 2.3, R_{Th} is the equivalent polarization resistance and C_{Th} is the equivalent polarization capacitance to model the battery relaxation effect during charging and discharging; U_{Th} is the voltages across C_{Th}. The electrical behaviour of the circuit can be expressed by Equation (2.6).

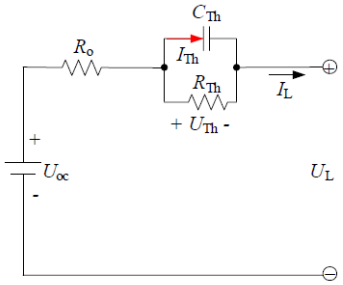

Figure 2.3 – Thevenin battery Model [4]

$$\begin{cases} \dot{U}_{Th} = -\frac{U_{Th}}{R_{Th}C_{Th}} + \frac{I_L}{C_{Th}} \\ U_L = U_{oc} - U_{Th} - R_0 I_L \end{cases} \tag{2.6}$$

The DP Model

The analysis of the power characteristics of Li-ion batteries at the end of charge or discharge, shows that there is an other phenomena that can be observed, is the polarization. The Thevenin model could simulate the polarization but in a small scale with inaccurate results. An improved

circuit model takes in consideration the two polarization effect: concentration polarization and electrochemical polarization, defined as dual polarization (DP) model is presented in Figure 2.4.

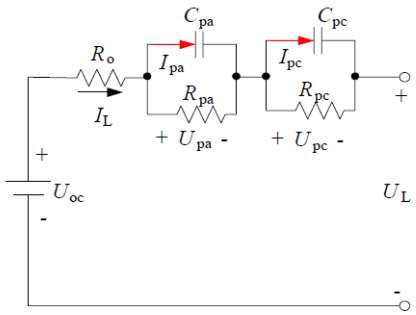

Figure 2.4 – DP battery Model [4]

The model connects a parallel RC network in series to the Thevenin model, in order to consider separately the concentration polarization and the electrochemical polarization. The consideration of the polarization characteristics may lead to more accuracy compared to Thevenin model. The electrical behavior of the circuit can be expressed by Equation (2.7)

$$\begin{cases} \dot{U}_{pa} = -\frac{U_{pa}}{R_{pa}C_{pa}} + \frac{I_L}{C_{pa}} \\ \dot{U}_{Th} = -\frac{U_{pc}}{R_{pc}C_{pc}} + \frac{I_L}{C_{pc}} \\ U_L = U_{oc} - U_{pa} - U_{pc} - R_0 I_L \end{cases} \tag{2.7}$$

where R_{pa} the effective resistance characterizing electrochemical polarization and R_{pc} the effective resistance characterizing concentration polarization. the capacitances C_{pa} and C_{pc}, which are used to characterize the transient response during transfer of power to/from the battery and to describe the electrochemical polarization and the concentration polarization separately. U_{pa} and U_{pc} are the voltages across C_{pa} and C_{pc} respectively. I_{pa} and I_{pc} are the current of C_{pa} and C_{pc} respectively.

2.2.4 Classification of battery models

The modeling approaches discussed in this section are summarized in Figure 2.5. Despite the difference between all proposed battery models, some essential connections remain between them. The empirical model simplify the electrochemical model by using mathematics and experience. Equivalent circuit model replace the chemical reaction by electric circuit components. Therefore the electrochemical model is the basis for other models.

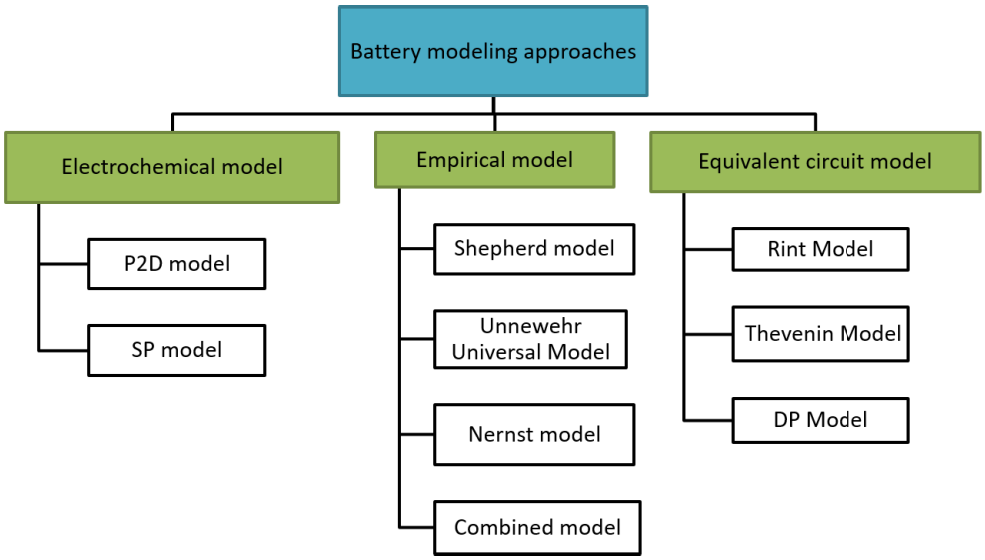

Figure 2.5 – The classification of battery modeling approaches

The sudy of the battery modeling methods leads us to conclude that the electrochemical models are highly accurate in terms of voltage. However, they require a prior knowledge of the battery internal characteristics and they are considered as high time consuming methods. This due to the coupled partial differential equations involved. In the one hand empirical model expressions are simple because of the linear equations that depend only on SOC and current. In the other hand, the limited capability of describing the variation of terminal voltage gives access to the development of equivalent circuit models, characterized by a high accuracy of voltage calculation, however, require a complex identification process.

Another topic that should be discussed in this section is the level of battery modeling. The battery modeling starts from material point of view to reach the battery system level as shown in the Figure 2.6. Battery modules consist of connecting cells in parallel and series to reach a high voltage and to ensure high operational current. When modules connected in series, the voltage of battery pack increases, while the parallel connection helps to achieve a higher capacity [46].

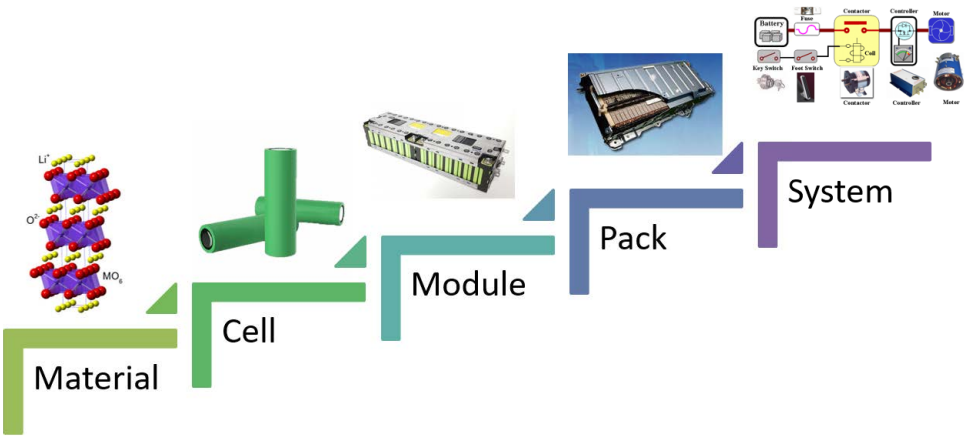

Figure 2.6 – Levels of battery modeling

A battery cell model is sufficiently representative of the dynamic behaviour of the battery module, and the battery module is the key requirement for a battery pack level simulation.

Various internal chemical processes occur on different time scales, battey modeling time scale is another important consideration in battery modeling. The short term battery modeling consist of modeling transient behavior of the battery resulting in a high accurate model for fast charge and discharge current. This kind of models can provide a very good estimation of the battery states like voltage. However, it remains limited in term of accuracy for SOC estimation. The solution is the use of medium term models that can provide knowledge about long time charge and discharge. In order to deliver accurate information about the battery age, long term models can estimate the battery SOH to evaluate the battery lifetime. In these models, capacity fade, resistance augmentation and loss of available peak power are model using ageing mechanism in anode and electrode.

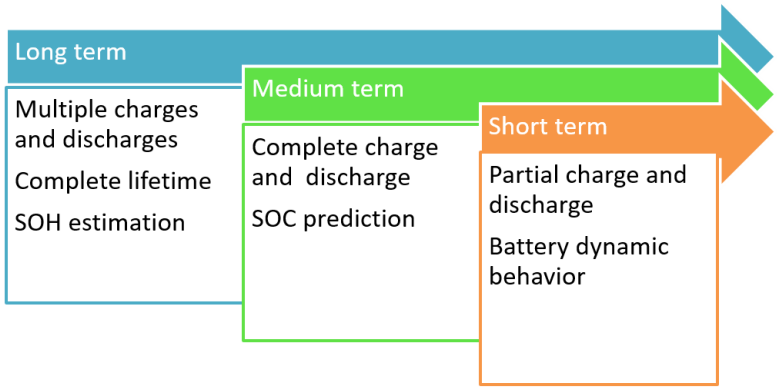

Figure 2.7 – Battery modeling times cale

2.3 Suggested Lithium-ion Model: Electro-thermal Battery Model

Particularly for EV manufacturers, modeling accurate lithium batteries is strategic for a better battery packs design and for estimating the battery lifetime. Further, battery lifespan models are crucial for vehicle manufacturers to manage their vehicle fleet warranties, and to predict failures in vehicles battery systems [33]. Lithium batteries performances highly depend on temperature [16, 17, 47]. Therefore, the thermal behavior of Li-ion battery must be taken as a serious matter. The temperature influence on Li-ion batteries affects the rated capacity and the internal resistance leading to reduction of performances and lifespan. In this context, in order to evaluate the thermal behavior of the Li-ion batteries, the development of a thermal model is a key element.

Various thermal models are being studied in the objective to overcome the weak point of temperature dependence in LiBs [47–56]. According to the heat transfer law [48, 54–56], the fundamental equation governing the heat transfer of LiBs is described in the Equation (2.8):

$$\rho C_p \left(\frac{\partial T}{\partial t} + v \cdot \nabla T \right) = \nabla \cdot \lambda \nabla T + \dot{q} \tag{2.8}$$

where ρ is the battery density, C_p is the specific heat capacity, v is the velocity of the electrolyte, λ is the thermal conductivity in x,y,z direction, $\dot{q}$ is the heat generation.

The Equation (2.8) that models the heat stored inside the battery could be simplified by assuming that the velocity of the electrolyte is almost zero [48, 54, 55], as shown in the Equation (2.9).

$$\rho C_p \left(\frac{\partial T}{\partial t} + v \cdot \nabla T \right) \approx \frac{\partial \left(\rho C_p T \right)}{\partial t} \approx \rho C_p \frac{\partial T}{\partial t} \tag{2.9}$$

The term $\nabla \cdot \lambda \nabla T$ in the Equation (2.10) is the three dimensional (3D) heat conduction term, and it can be one dimensional (1D), two dimensional (2D) or 3D in Cartesian or cylindrical coordinates. For simplification, we can assume that the air flow is a 1D conduction [48, 50].

$$\nabla \cdot \lambda \nabla T = -h(T - T_{out}) \tag{2.10}$$

where h is heat transfer coefficient, T is cell temperature, T_{out} is the outside temperature.

There are some commonly used expressions in the literature [47, 50, 52–54, 56] for heat generation. All these equations are deduced from the Bernardi thermal formula [48] presented in the Equation (2.11). The first term of the equation refers to Joule heat and the second one to the entropy change or the reversible heat, where U_{oc} is the open circuit voltage, U_L is the cell voltage, I_L is the cell current and T is the battery temperature.

$$\dot{q} = I_L(U_{oc} - U_L) - T I_L \frac{dU_{oc}}{dT} \tag{2.11}$$

In order to get a more accurate model that take into consideration the side reaction heat generation, a famous heat generation equation expressed by [57] in the Equation (2.12):

$$Q = Q_r + Q_p + Q_J = nFT \frac{\partial U_{oc}}{\partial T} + Q_p + Q_J \tag{2.12}$$

with Q_r is the reaction heat, Q_p is the polarization heat, Q_J is the Joule heat, F is the Faraday's constant, n is the number of charge involved in the battery reaction.

Reference [57] proposes a estimation of the three terms in the previous equation using Q_1 is the heat generated from positive and negative electrode, R_i is the internal resistance, and R_p is the polarization resistance as presented in the Equation (2.13):

$$\begin{cases} Q_r = -3.37 \times 10^{-2} Q_1 I_L \\ Q_p = 3.60 R_p I_L^2 \\ Q_J = 3.60 R_i I_L^2 \end{cases} \tag{2.13}$$

A rudimentary way of describing the heat transfer between a cell and its environment is with a 1D lumped-parameter (also known as lumped-capacitance) model. It considers the cell heat generation Q and the convective heat transfer between the cell surface. The surroundings are modeled with a convection resistance R_v. The rate of change of the cell temperature is represented in the thermal model with the heat capacity of the cell C_p. The equations governing heat transfer for the cell thermal model, can be expressed as shown in the following equation [58]:

$$mC_p \frac{dT}{dt} = Q - \frac{T - T_{out}}{R_v} = R_0 I_L^2 - \frac{T - T_{out}}{R_v} \tag{2.14}$$

Heat generation is approximated as a concentrated source of Joule loss in the battery core, computed as the product of the current I_L square and the internal resistance R_0. The internal resistance R_0 is considered as an unknown parameter to be identified. This simplification can lead to cycle-dependent values for the lumped resistance R_0, or even a non-constant resistance within a single cycle, because R_0 can vary with conditions, such as temperature, SOC and SOH [59].

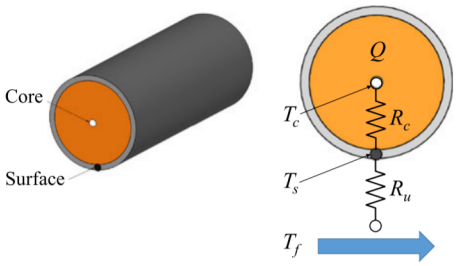

Figure 2.8 – Schematic of the thermal model [5].

Contrary to the previous model that considers a concentration of the heat in the core of the battery cell. The thermal model in Figure 2.8 describes the radial heat transfer dynamics of a cylindrical battery cell from the core to the surface. The two states are the core T_c and surface T_s temperatures are obtained Equations. (2.15) as follows [5, 59]:

$$\begin{aligned} C_c \frac{dT_c}{dt} &= \frac{T_s - T_c}{R_c} + R_e I_L^2 \\ C_s \frac{dT_s}{dt} &= \frac{T_{out} - T_s}{R_u} - \frac{T_s - T_c}{R_c} \end{aligned} \tag{2.15}$$

where the heat conduction resistance, the convection resistance, the internal resistance, the ambient temperature, the core temperature, the surface temperature, the core heat capacity, and the surface heat capacity are represented by R_c , R_u, R_e, T_{out}, T_c, T_s, C_c, and C_s, respectively.

The heat exchange between the core and the surface is modeled by heat conduction over a thermal resistance, R_c which is a lumped parameter aggregating the conduction and contact thermal resistance across the compact and inhomogeneous materials [60]. The convection resistance R_u is modeled between the surface and the surrounding coolant to account for convective cooling. The value of R_u is a function of the coolant flow rate, and in some vehicle battery systems, the coolant flow rate is adjustable to control the battery temperature. Here, it is modeled as a constant as if the coolant flow rate is fixed to accommodate the maximum required cooling capacity [59].

The internal resistance R_e is considered as an unknown parameter to be identified. This simplification can lead to cycle-dependent values for lumped resistance R_e,or even nonconstant resistance within a single cycle, because R_e can vary with conditions, such as temperature, and SOC [59]. The internal resistance dependence on SOC and temperature defines the Li-ion electro-thermal model.

Figure 2.9 shows the proposed electro-thermal model, which consists of three sub-system models: the electrical model, the SOC estimation model and the thermal model. The SOC estimation model is related to the electrical model by the battery current, which is the input of the SOC estimation model. The thermal model is linked to the electrical model by the generated heat, which is the quantity $R_0 I_L^2$. The output of the thermal model is the cell core temperature T which is a input for the electrical model.

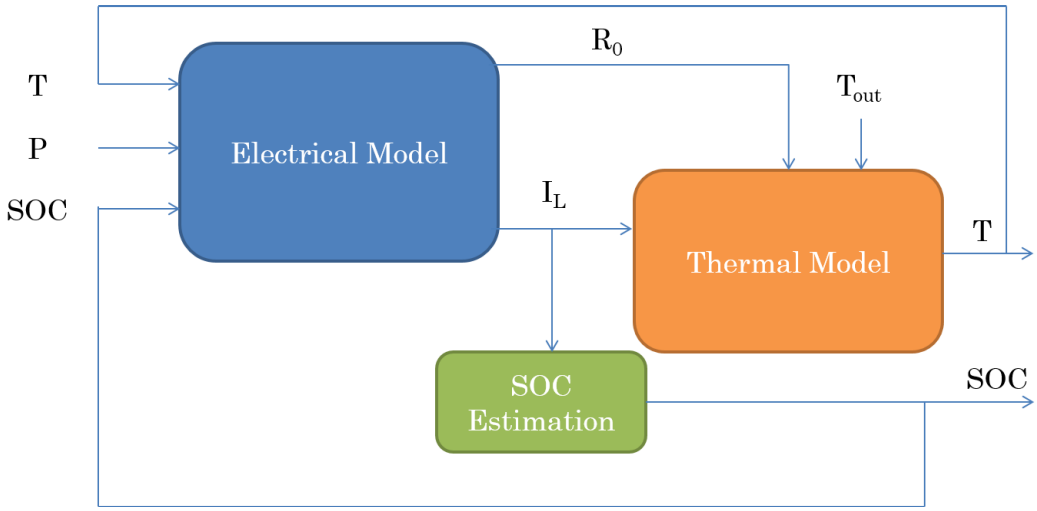

Figure 2.9 – The proposed electro-thermal model

The choice of the modeling approach for the electrical subsystem is turned towards the equivalent circuit model, specially the Rint model. This choice is based on the simplicity of the model and the possibility of integrating the dependency of the model parameters to the SOC and the temperature. Therefore, the internal resistance will depend on the SOC and the battery temperature as shown in the Figure 2.10.

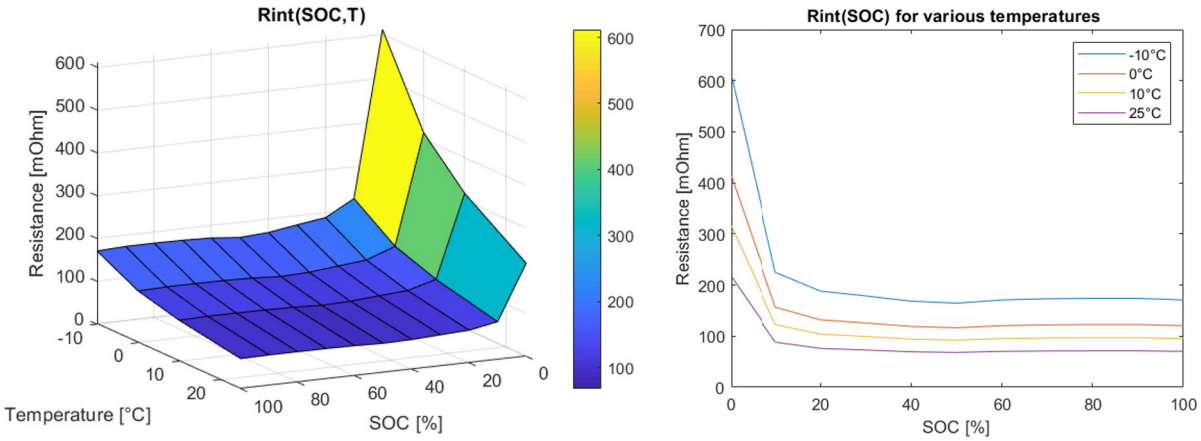

Figure 2.10 – The internal resistance value for various SOC and temperature

Several works [61, 62] have found that the open circuit voltage (OCV) curve OCV–SOC is not simply a one-to-one mapping but exhibits hysteresis (OCV differs at the same SOC value between charge and discharge), which impedes the developments of modeling or state estimations [63, 64]. Generally, this phenomenon can be neglected for some battery types such as lithium cobalt oxide ($LiCoO_2$), lithium manganese oxide ($LiMn_2O_4$) [62, 65], this is because the slopes of OCV–SOC curves are relatively steep for these battery types. Considering the low dependence of the OCV curve on temperature for lithium ion batteries, the influences of OCV deviations on the temperature are not immediately obvious and can be ignored for these battery types [66]. Thus, OCV will depend only on SOC as presented in the Figure 2.11.

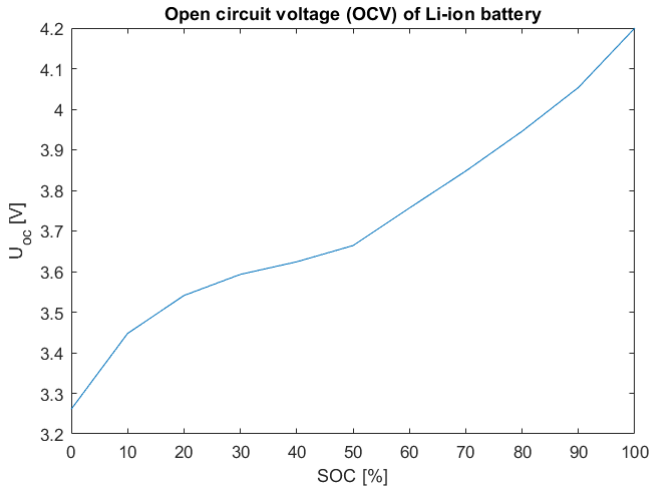

Figure 2.11 – The OCV of Li-ion battery cell

The battery model used for the electrical subsystem is a Rint model as shown in Figure 2.12.

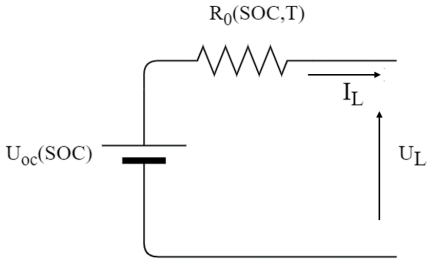

Figure 2.12 – The proposed Rint model

By neglecting the OCV dependency on temperature, the heat generated by the battery can be simplified to equal the Joule heat. Thus, the thermal subsystem model will be expressed as the Equation (2.14).

The SOC estimation subsystem calculates the ratio of the remaining capacity to the nominal capacity of the battery known as SOC and is computed by the Equation (2.16):

$$SOC(t) = SOC_i \pm \frac{1}{C_0} \int_0^t \eta I_L d\tau \tag{2.16}$$

where SOC_i is the initial value of the SOC, C_0 is the nominal capacity in Ah and η is the charging efficiency.

The state of energy (SOE) is an other method to estimate the SOC when the power is used instead of current [67–69]. The SOE is defined in the Equation (2.17):

$$SOE(t) = SOE_i \pm \frac{1}{Q_0} \int_0^t \eta P_L d\tau \tag{2.17}$$

where SOE_i is the initial value of the SOE, Q_0 is the nominal capacity in kWh and P_L is the charging power.

To sum up, the consideration of the Li-ion battery thermal behavior is carried out by adding the thermal model to the electrical model forming the battery electro-thermal model. In the next section, particular attention will be given to the identification of the battery thermal model parameters.

2.4 Identification Methodology of Battery's Parameters

This section will help understand how the parameters of the thermal model were identified. To identify the battery thermal parameters, the method of least squares is used [70–72]. Based on the temperature evolution of the battery and the Joules losses, the two parameters of the thermal model mC_p and R_v will be estimated. The Equation (2.18) shows the expression of the thermal model that will be used.

$$mC_p\frac{dT}{dt} = R_0 I_L^2 - \frac{T - T_{out}}{R_v} \tag{2.18}$$

By adjusting the thermal model to be useful for the estimation procedure, some simplifications could be done as expressed in the Equation (2.19):

$$R_0 I_L^2 = mC_p\frac{dT}{dt} + \frac{T - T_{out}}{R_v} \tag{2.19}$$

By defining $a = mC_p$ and $b = \frac{1}{R_v}$ the thermal model can be expressed as the Equation (2.20):

$$R_0 I_L^2 = a\frac{dT}{dt} + b(T - T_{out}) \tag{2.20}$$

The parameters in the thermal model could be estimated using a system identification procedure. This model has the advantage of being linear in terms of the parameters a and b as shown in the Equation (2.21):

$$y = ax + bz \tag{2.21}$$

Using a set of experimental data (x, y, z) defined in the Equation (2.22), the parameters may be identified using least-squares estimation.

$$\begin{cases} x = \frac{dT}{dt} \\ y = R_0 I_L^2 \\ z = T - T_{out} \end{cases} \tag{2.22}$$

A discretization transformation is employed to the continuous data (x, y, z) with a sampling time T_s to obtain a set of data of length N as presented in the Equation (2.23):

$$\{(x_i, y_i, z_i)/i = 1, 2, ..., N\} \tag{2.23}$$

Given data $\{(x_1, y_1, z_1), ..., (x_N, y_N, z_N)\}$, the error associated to the saying model $y = ax + bz$ can be defined by the Equation (2.24):

$$E(a, b) = \sum_{n=1}^{N} (y_n - (ax_n + bz_n))^2 \tag{2.24}$$

The goal is to find values of a and b that minimize the error. The method of least squares requires to find the values of (a, b) as expressed in the Equation (2.25):

$$\frac{\partial E}{\partial a} = 0 \quad ; \quad \frac{\partial E}{\partial b} = 0 \tag{2.25}$$

The differentiation of the error $E(a, b)$ yields the following expressions in the Equation (2.26):

$$\begin{aligned}\frac{\partial E}{\partial a} &= \sum_{n=1}^{N} 2(-x_n)(y_n - (ax_n + bz_n)) \\ \frac{\partial E}{\partial b} &= \sum_{n=1}^{N} 2(-z_n)(y_n - (ax_n + bz_n))\end{aligned} \tag{2.26}$$

Setting $\frac{\partial E}{\partial a} = \frac{\partial E}{\partial b} = 0$ gives the two simplified expressed in the Equation (2.27):

$$\begin{aligned}\sum_{n=1}^{N} (y_n - (ax_n + bz_n)) \cdot (x_n) = 0 \\ \sum_{n=1}^{N} (y_n - (ax_n + bz_n)) \cdot (z_n) = 0\end{aligned} \tag{2.27}$$

The simplification of the previous two equations gives the linear system to solve in the Equation (2.28):

$$\begin{aligned}\left(\sum_{n=1}^{N} x_n^2\right) a + \left(\sum_{n=1}^{N} x_n z_n\right) b = \sum_{n=1}^{N} y_n x_n \\ \left(\sum_{n=1}^{N} x_n z_n\right) a + \left(\sum_{n=1}^{N} z_n^2\right) b = \sum_{n=1}^{N} y_n z_n\end{aligned} \tag{2.28}$$

The linear system can be expressed in matrix form as presented in the Equation (2.29):

$$\begin{pmatrix} \sum_{n=1}^{N} x_n^2 & \sum_{n=1}^{N} x_n z_n \\ \sum_{n=1}^{N} x_n z_n & \sum_{n=1}^{N} z_n^2 \end{pmatrix} \begin{pmatrix} a \\ b \end{pmatrix} = \begin{pmatrix} \sum_{n=1}^{N} y_n x_n \\ \sum_{n=1}^{N} y_n z_n \end{pmatrix} \tag{2.29}$$

The values of a and b that minimize the error can be obtained if the matrix is invertible by the Equation (2.30):

$$\begin{pmatrix} a \\ b \end{pmatrix} = \begin{pmatrix} \sum_{n=1}^{N} x_n^2 & \sum_{n=1}^{N} x_n z_n \\ \sum_{n=1}^{N} x_n z_n & \sum_{n=1}^{N} z_n^2 \end{pmatrix}^{-1} \begin{pmatrix} \sum_{n=1}^{N} y_n x_n \\ \sum_{n=1}^{N} y_n z_n \end{pmatrix} \tag{2.30}$$

The solution of linear system that minimize the error is expressed in the Equation (2.31):

$$\begin{aligned} a &= \frac{\left[\sum_{n=1}^{N} x_n z_n\right]\left[\sum_{n=1}^{N} y_n z_n\right] - \left[\sum_{n=1}^{N} y_n x_n\right]\left[\sum_{n=1}^{N} z_n^2\right]}{\left[\sum_{n=1}^{N} x_n z_n\right]^2 - \left[\sum_{n=1}^{N} x_n^2\right]\left[\sum_{n=1}^{N} z_n^2\right]} \\ b &= \frac{\left[\sum_{n=1}^{N} x_n z_n\right]\left[\sum_{n=1}^{N} y_n x_n\right] - \left[\sum_{n=1}^{N} y_n z_n\right]\left[\sum_{n=1}^{N} x_n^2\right]}{\left[\sum_{n=1}^{N} x_n z_n\right]^2 - \left[\sum_{n=1}^{N} x_n^2\right]\left[\sum_{n=1}^{N} z_n^2\right]} \end{aligned} \tag{2.31}$$

Using temperature data from a charging case, the parameters of the thermal model can be estimated using the least square method.

$$\begin{pmatrix} 0.0035 & 5.0899 \\ 5.0899 & 50112.3248 \end{pmatrix} \begin{pmatrix} a \\ b \end{pmatrix} = \begin{pmatrix} 902.4746 \\ 1887482.6997 \end{pmatrix} \tag{2.32}$$

$$\begin{pmatrix} a \\ b \end{pmatrix} = \begin{pmatrix} 337.0396 & -0.0342 \\ -0.0342 & 0.0000 \end{pmatrix} \begin{pmatrix} 902.4746 \\ 1887482.6997 \end{pmatrix} \tag{2.33}$$

$$\begin{pmatrix} a \\ b \end{pmatrix} = \begin{pmatrix} 239555 \\ 13.3333 \end{pmatrix} \tag{2.34}$$

$$mC_p = a = 239555 \qquad R_v = \frac{1}{b} = 0.0750 \tag{2.35}$$

The obtained values are used as setting parameter for the thermal model. The plot of the temperature evolution curve is shown in the Figure 2.13:

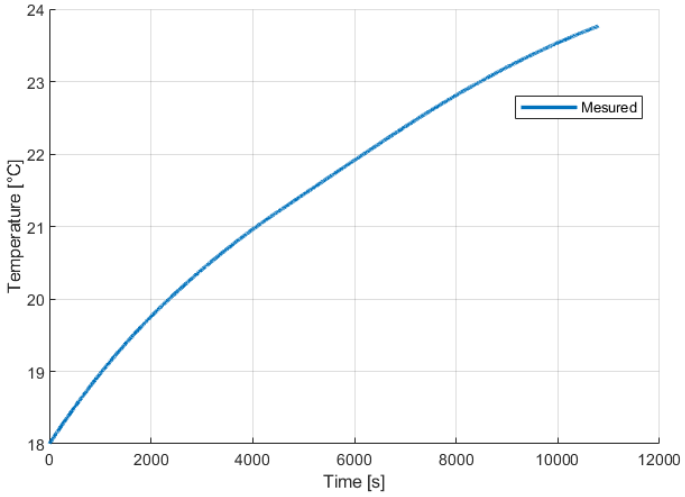

Figure 2.13 – The temperature evolution $mC_p = 239555 R_v = 0.075$

The comparison between the experimental used data and the thermal model temperature output is given in the Figure 2.14. The two curves are the same due to the large number of values used in the estimation method.

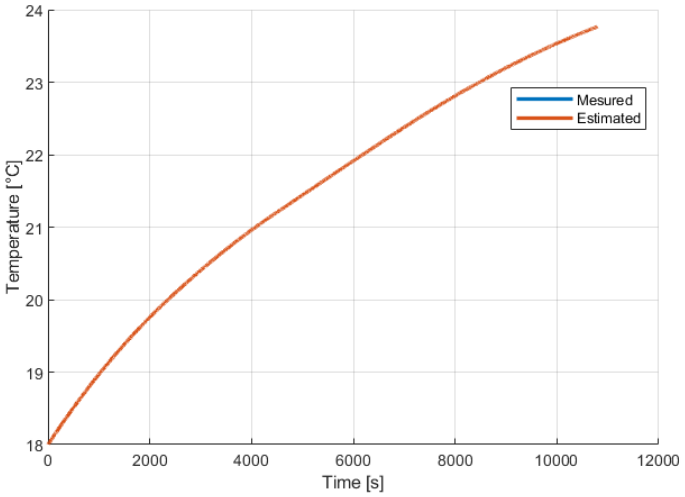

Figure 2.14 – The temperature evolution: measured and estimated

However, by choosing more than one sampling time, the size of the data set changes. Figure 2.15 shows four data sets that will be used in the least squares estimation for parameters identification.

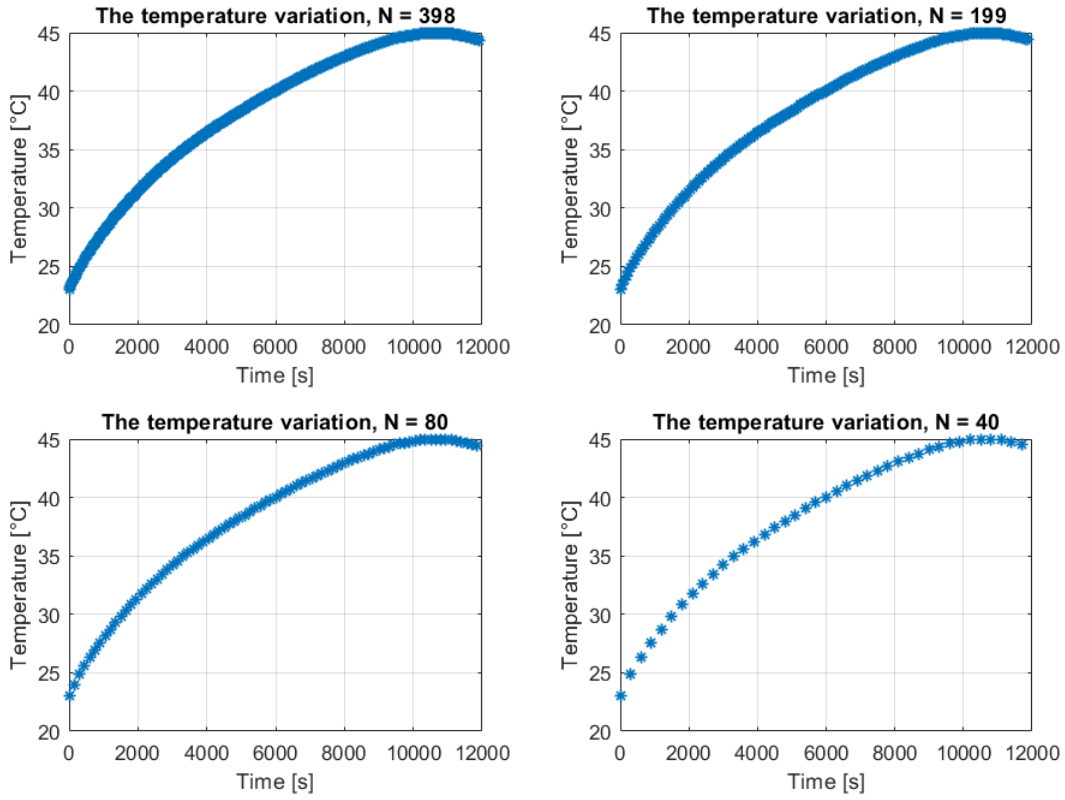

Figure 2.15 – The discretization of the temperature

The results of the least square estimation method show the impact of the number of samples on the accuracy. Using a big data set the estimated value converges to the real model value as shown in Table 2.1.

Table 2.1 – Least square estimation results

N	40	80	199	398	**Model value**
mC_p	173603	205171	226041	233413	**239555**
R_v	0.0573	0.0646	0.0703	0.0725	**0.075**

The Figure 2.16 presents the benchmarking between different temperature evolution curves depending on the used number of samples. A deviation between the estimated temperature curve and the measured temperature curve, caused by a difference in the values of the model's parameters. The impact of the number of samples, the sampling time and the accuracy of the estimation do not have a significant effect on temperature evolution curves. The small difference in the temperature curves does not influence the charging power limitation of the Li-ion battery.

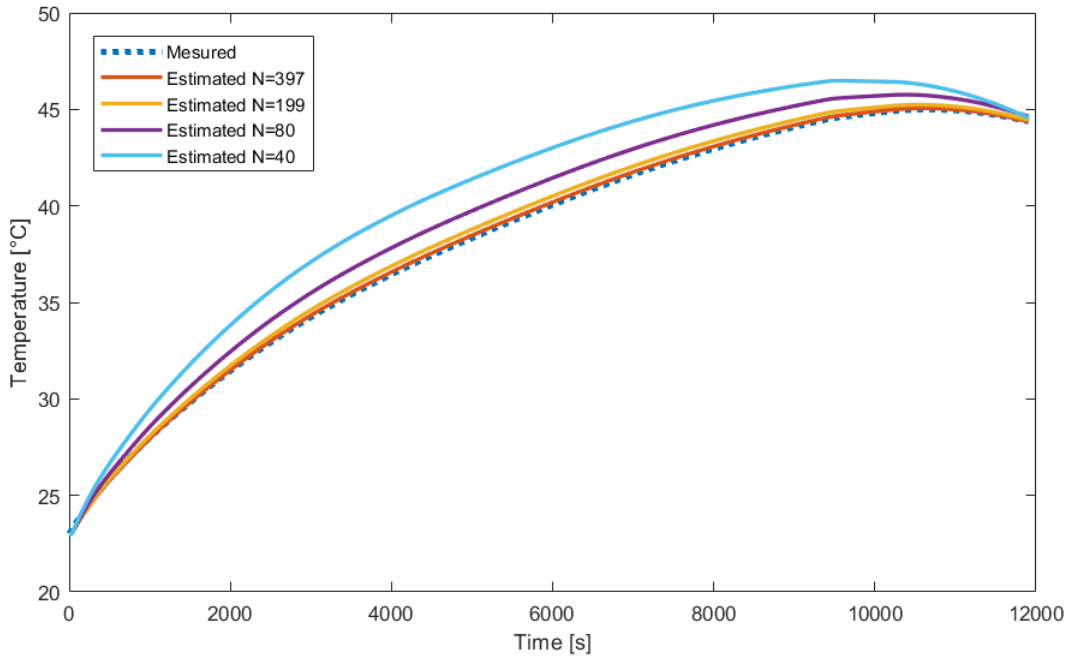

Figure 2.16 – The comparison of the temperature evolution for several used number of samples

2.5 Experimental tests on Zoé in Techenocentre of Renault Group

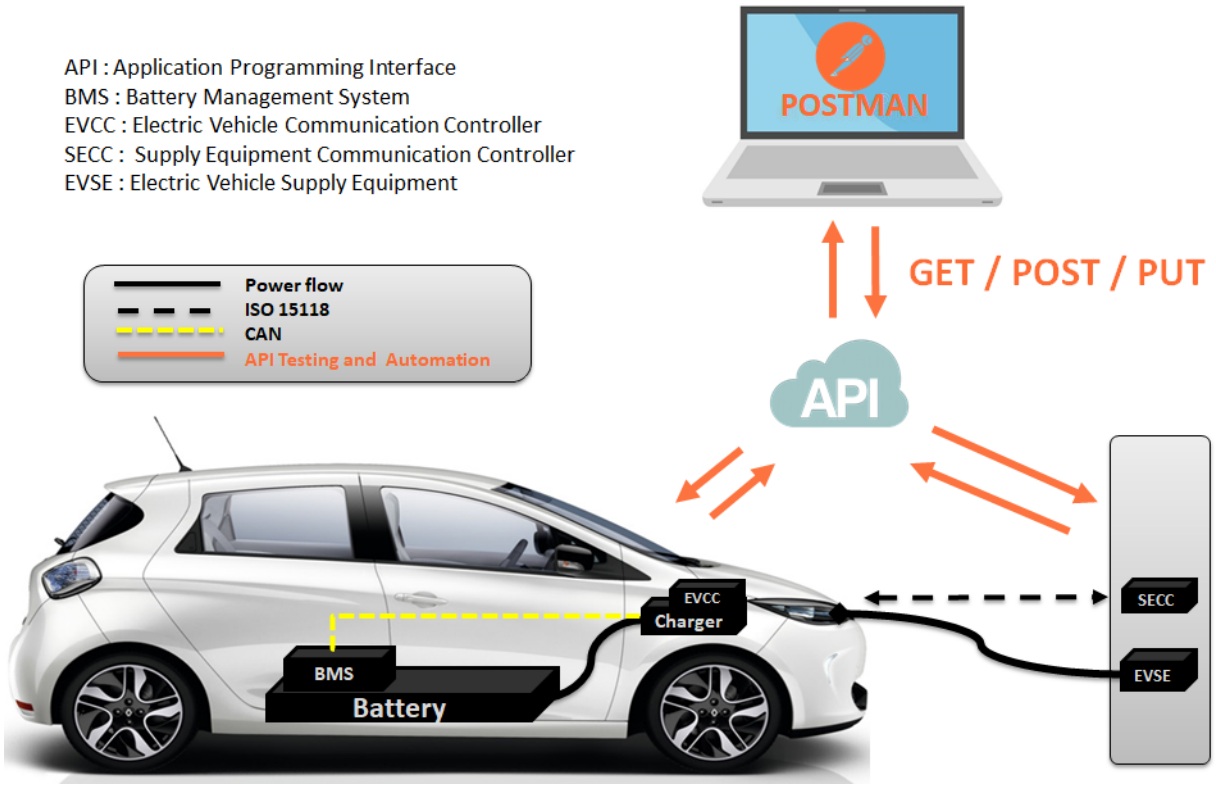

Figure 2.17 – The comparison of the temperature evolution

The work carried out in the SmartEVLab of Technocentre of Renault Group consists in :

— Getting to grips with the API Metier VOA

— Using the schedule mode

— Launch of the V2G algorithm to generate the power profile

— Sending a schedule on the terminal side with Postman

— Sending schedule on EV side with Postman

— Renegotiation of the EV side with Postman

The API Metier VOA is implemented by Trialog on the V2G proto (cars of the fleet included). Allows to send requests by being directly connected to the car via cable ethernet. The requests can be of type :

— GET : to retrieve information from the EV (batteryCapacity, SOC, Pcharge etc ...) or from the terminal if EV is connected (EVSE info, schedule of the terminal sent to the EV, etc ...).

— POST/PUT: to give a load instruction (Load Profile), to renegotiate the current schedule, etc...

2.5.1 Charging Session in G2V mode only: 1 hour 45 min

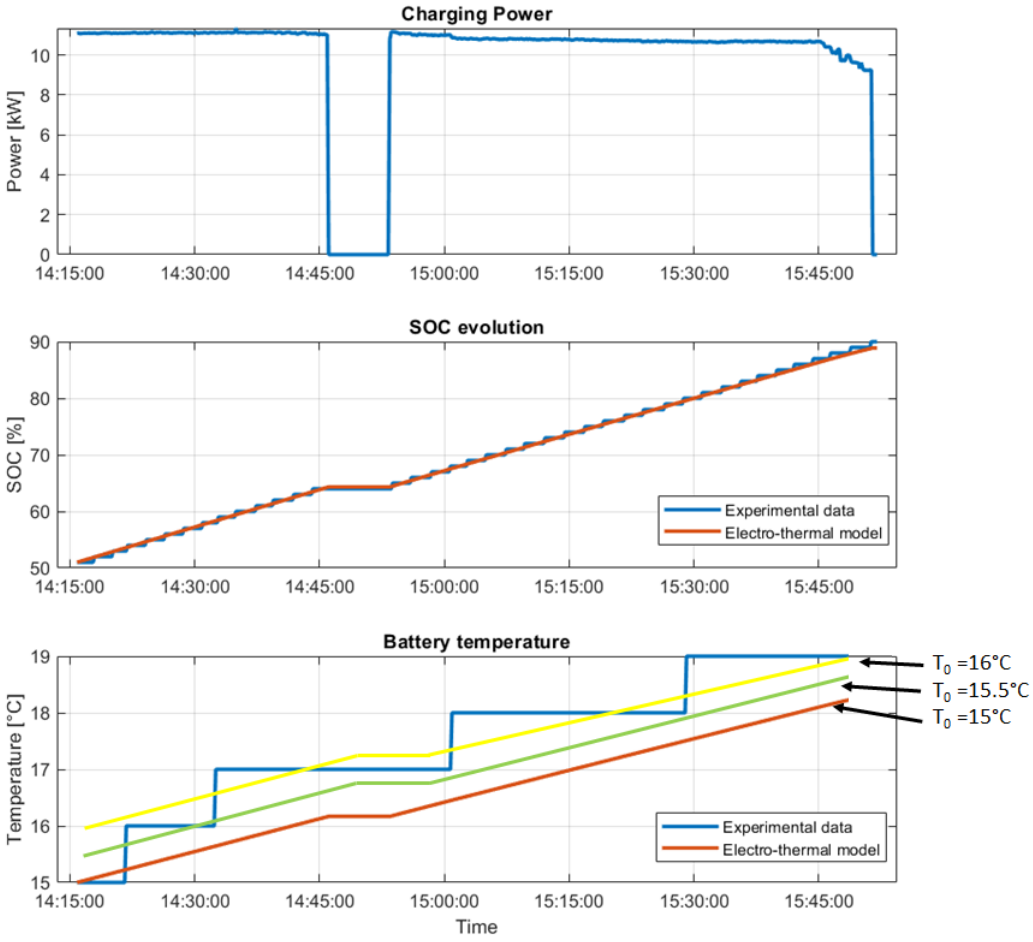

Figure 2.18 – The comparison of the temperature evolution

In this charging session, the EV will receive power from the grid (G2V mode) to reach a 90% SOC. For SOC estimation, It can be observed that the two curves of the estimated SOC by the electro-thermal model fits the curves of the SOC calculated by the EV (Experimental data). Concerning the temperature estimation, due to the decimal accuracy of experimental data, the received data from the EV are truncated to decimal value, therefore the number of digit (scale) is equal to zero. This problem affects the initial battery temperature, with the displayed value of $15°C$ three cases are possible is we consider a scale equal to 2: $T_0 = 15°C$, $15.01°C < T_0 < 15.99°C$ $T_0 = 15.99°C$.

Due to this problem three plots are used to estimate the evolution of the battery temperature considering three values of initial temperature: $T_0 = 15°C$, $T_0 = 15.5°C$ and $T_0 = 16°C$. It can be observed that the temperature evolution for the three estimated curves looks the same but they are different in the final value $T_f = 18.1°C$, $T_f = 18.5°C$ and $T_f = 19°C$ for $T_0 = 15°C$, $T_0 = 15.5°C$ and $T_0 = 16°C$ respectively. The estimation error depends on the used value of the initial temperature but the maximum estimation error that can be observed is $1°C$.

2.5.2 Charging Session in V2G and G2V modes: 1 hour

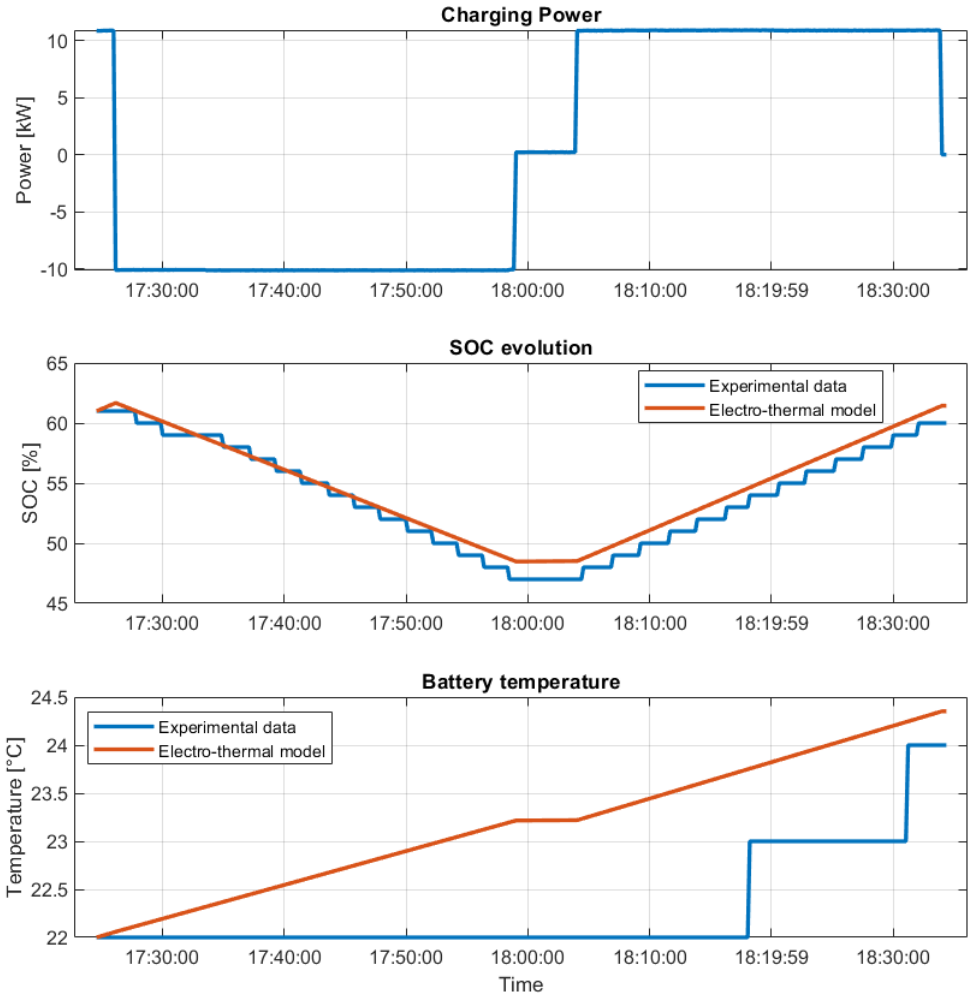

Figure 2.19 – The comparison of the temperature evolution

In this charging session, the EV will start by discharging the battery on the grid from 62% of SOC and after 30 minutes the EV will draw power from the grid (G2V mode) to return to its initial SOC value of 62%. For SOC estimation, it can be observed that the two curves of the estimated SOC by the electro-thermal model fits the curves of the SOC calculated by the EV (Experimental data) with a small error estimated to 1% of SOC.

Regarding the temperature estimation, it can be observed that the two curves of the estimated temerature by the electro-thermal model fits the curves of the mesured temperature of the battery by the EV (Experimental data)

To sum up, considering the application of the EV charging in meduim term time scale, the battery electro-thermal model can be considered as an adequate model for EV battery estimation with the consideration of the temperature.

The Renault SmartEVLab aims to provide a demonstration prototype of a bi-directional AC and DC charging services system, using the ISO 15118 standard. This prototype includes Renault Zoé modified for AC or DC support and ISO 15118, and modified EVTronic Charging Stations. The EVCC, also called Charge Manager, is the software installed in the Renault Zoé. It is responsible for :

- Monitoring and control of IEC 61861-1 parameters (PWM, Control Pilot, Proximity Signal, Locking cable)
- Control of the DC-Box relays
- Collaboration with Renault Zoé's EVC ECU through CAN communication for recharging management
- External AC charger control for EV (if applicable)
- ISO/IEC 15118 communication control by PLC
- Provide an HTTP/REST API for remote monitoring and control of recharging

2.6 Conclusion

The main points of Li-ion battery modeling approaches have been discussed in detail in this chapter. A particular focus on three modeling techniques: electrochemical models, empirical models, and equivalent circuit models. The electrochemical models can offer high accuracy due to their capacity to describe the chemical processes in the battery cell, however, they are not suitable for most real-time embedded applications. For EV application, two modeling approaches could be used. The first approach is the empirical models which are an approximation and a simplification of the electrochemical model, but the difficulty to understand the effect of ageing on the battery model parameters and their identification remain the main problems. The second approach is through the equivalent circuit models, the choice of a model from this category (Rint model, Thevenin model, and DP model) is a trade-off between precision and complexity. By assuming that the thermal behavior of Li-ion is crucial, several thermal models have been reviewed. Moreover, a thermal model has been proposed and added to the electrical model to form a electro-thermal model of the battery. Based on the temperature evolution data set, the parameters of the thermal model have been estimated using the least square method. The choice of the time step for the acquisition of temperature data has an impact on the accuracy of the estimation of the model parameters by the least-square estimation method. However, the impact of the estimation precision of the model parameters is less significant on the temperature evolution curves.

The electro-thermal model has been adopted for this work. In chapters 3 and 4, this model will be used in the proposed algorithms to evaluate the SOC and the temperature of the EVs during the scheduling of the charging.

3

Contribution to Smart Charging Algorithms For an Electric Vehicle

3.1 Introduction

Due to the diminution of fossil fuels and the increase of greenhouse gas emissions, researchers around the world are currently focused on finding an alternative, sustainable and smart transportation systems. EVs can take a big part of this change. Thanks to their high energy and high power density, Li-ion batteries provide enough range for the users of EVs and give the possibility of integrating EVs into the power grid. An EV can act as an energy source to support the grid during the peak hours using the V2G feature, and as a battery storage system at home by using the V2H functionality if available.

Today, most part of the charging of EVs is largely done in a simplistic way. As soon as a vehicle is connected to the grid, the battery is charged without any planning, until it reaches the desired SOC. This type of charging, called uncontrolled charging, is still widely applied today. This kind of strategies create high peaks of power demand when all EVs are plugged into the power grid at the same time such as an evening charging. Moreover, the users of EVs expect to start charging immediately, whereas in the majority of cases, the charging can be delayed. Using electricity prices as a lever to control the charging of EVs is a possible solution in a decentralized charging strategy. The user and the power network can directly obtain concrete benefits.

Controlling the charging of the EVs has become a particular interest to researchers in recent years because of the increasing levels of EV penetration and the impact of EVs on the power grid. The integration of EVs can accelerate the development of the smart grids, by enhancing the schedule and control of the charging that help to minimize the charging bill for customers, and at the same time, to support the power grid during the high power demand periods. Thus, the control of EV charging has a double impact on EV's customer daily use and a positive effect on the quality of service on the power grid.

The improvement of charging strategies for EVs is a challenge for the next decades. In order to maintain the EV purchase profitably, it is crucial for the EV users to properly schedule the charging taking into account the time of use (TOU) energy prices and the constraints of Li-ion batteries. Therefore, the EV charging scheduling strategies for the charging cost minimization is the primary focus for this chapter.

3.2 State of the Art and Work Statement

Several research studies have been conducted for developing new charging methods through centralized [19–22, 73–77] and decentralized [23–26, 78–80] strategies. The centralized charging strategies carry out the charging of EVs from a system level viewpoint and consider EVs present on all the nodes of the distribution system collectively as presented in Figure 3.1. Implementing the centralized charging strategy, the aggregator uses a central controller to coordinate the charging behavior of the EVs [73]. All decisions in this charging management strategy could be made based on the system level concerns such as the customer preferences, for example the permissible charging interval, final SOC, and charging cost, or also taking into account the request of transport system operator (TSO) such as frequency regulation, reducing total losses and feeder congestion [81].

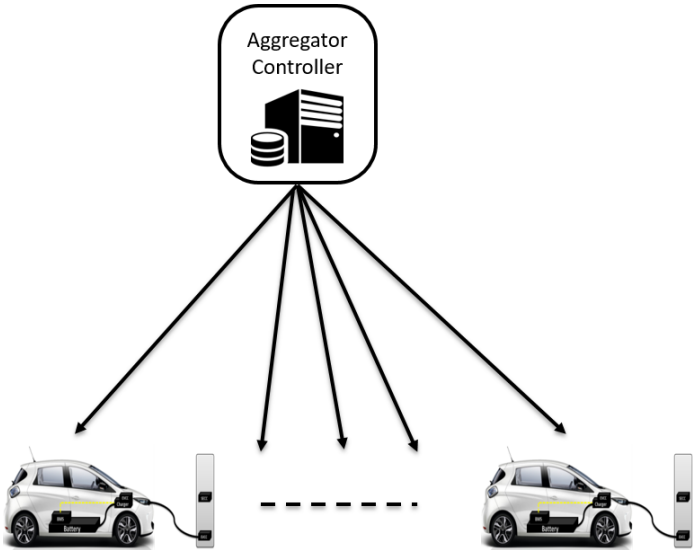

Figure 3.1 – Centralized charging architecture

In centralized strategies, the aggregator controls the time and the charging power rate of every EV to meet the commitments made in the electricity market between the aggregator and TSO. The drawbacks of centralized control is the updating of charging profile at any introduction of new EVs into the station or any demand from TSO. Thus, the aggregator may need restart again the optimization algorithm to update EV's control signal [82]. Compared to Decentralized strategies, centralized strategies need more information from every participating EV which describes their availability and willingness to respond to control actions [83]. These control strategies require extensive cyber-infrastructure, substantial communications, and processing resources. Moreover, the centralized algorithms are more sensitive to privacy problem, because all users' data is saved in servers for real-time optimization or in the system backup for data recovery in case of system failure. Moreover, the loss of communication with the central controller may cause a shutdown of the overall system. The major drawback of centralized architectures is the case of a potential failure, which makes the redundancy of the central controller inevitable, adding extra costs to the architecture. Finally, central systems are generally considered highly scalable and their maintenance requires a complete shutdown.

In the decentralized implementation, the strategies operate at the nodal level and perform the charging of EVs present on each node locally by a smart controller as shown in Figure 3.2. Decentralized or distributed strategies allow individual EVs to determine their own charging decisions. EV charging decisions could, for example, be made on the basis of TOU energy prices or EVs users preferences [79].

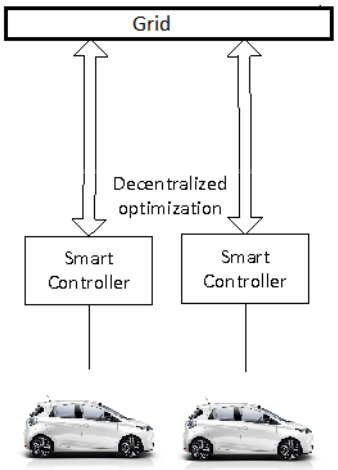

Figure 3.2 – Decentralized charging architecture

The result of a decentralized approach may be non-optimal, depending on the information and methods used to determine the charging power. There is no guarantee to reach optimal charging outcome employing decentralized approach from the system operator viewpoint. Anyhow, depending on the electricity tariff mechanism as well as the response behaviors of the electric vehicle owners, the total load of EVs may cover the power grid requirements [80].

The reactions of a large number of electric vehicles following a change in electricity prices could lead to a sudden change in the power demand, and could potentially destabilize the grid and do not respect the commitments made in the electricity market between the aggregator and TSO. Care must be taken to decentralized strategies cannot inadvertently synchronize this disturbance. More constraints should be added to the optimization strategies to overcome this disturbance [74].

To overcome these problems, distributed control architectures are currently in development, and are getting more interest from researchers and charging operators. EVs would require a charging application and an onboard controller installed on the vehicle. The adoption of a decentralized control strategy can be a solution to previous drawbacks of centralized strategies. It breaks the complexity of global optimization problem to local optimization problems at the EV level and it limits the communication between the aggregator and the EVs [75, 82]. However, a major disadvantage of the decentralized approach, in comparison to the centralized approach, is that the EVs on one node (of the distribution system) cannot supply energy to EVs on other nodes using vehicle to vehicle (V2V) feature. In general, the load demand on any node is greater than the V2G energy available from EVs on the same node. Therefore, in absence of a scenario where the V2G energy available from EVs on one node can be used to supply load demand on other nodes, the preferred way of implementing a charging strategy in a distribution system would be the decentralized approach [84]. To sum up, it should be noted that due to the centralized nature of the structure, the centralized control architectures presents several problems, such as the risk of a possible system failure, expensive communication infrastructure, access to transport habits of users. For all these reasons, it can be desirable to implement a decentralized control.

Different objectives have been used in charging scheduling problem [85]. Some works have focused on maximizing the benefits on the grid side, such as reducing the financial cost of power generation [86], optimizing grid operating costs, including the cost of renewable energies and the cost of availability for the provision of spinning reserves [87], minimizing the load on the distribution system variance [88], reducing losses in the distribution system [89, 90], and maximizing the benefits of thermal and wind power plants while minimizing the risks associated

with energy exchanges [91]. Some other work has focused on optimizing the benefits on the EV side, such as minimizing the charging costs [23, 25, 92], minimizing both CO2 emissions and charging costs [93], and maximizing the average SOC of electric vehicles [94]. However, another category of work focused on optimizing the benefits on the aggregator side, such as maximizing the benefits of the aggregator [95] and reducing imbalances resulting from the energy purchased by the aggregator on the day-ahead market and the actual energy consumed [96]. Several works have also attempted to jointly optimize grid side and EV side benefits [90, 97, 98].

In general, an EV charging scheduling from the customer's point of view is almost neglected, a few recent works studied the minimization of the EV owners charging cost [23, 25, 92, 94, 98, 99]. However, most of them focused on maximizing the aggregator profit without carefully addressing customers' needs [19–21, 24, 100–102]. The main drawbacks of this type of scheduling is that the SOC desired by the customer may not be reached at the departure time, therefore the customer would not have the required SOC to return home. The smart charging strategies developed in this chapter will consider EV users satisfaction as the main constraint, thus, the respect of the desired SOC of the EV users will be achieved.

Li-ion batteries are more sensitive to the temperature than other battery technologies. High operating temperatures increase power acceptance of the battery but rapidly decrease the battery lifetime, causing premature ageing and leakages on the Li-ion batteries [17]. On the other hand, subzero temperatures decrease the power acceptance, increasing the internal resistance of the Li-ion batteries, causing the raising of the Joules power losses, decreasing the efficiency of the charging, and affecting the State of Health (SOH) of the Li-ion batteries [16]. Controlling the temperature of the Li-ion batteries is a big challenge to make the EVs suitable to any climate condition and to extend the Li-ion batteries lifespan.

Despite the significant effect of temperature on the Li-ion batteries, almost all optimal charging strategies do not take into account the temperature effect on the charging scheduling. Due to the higher sensitivity to the temperature of the Li-ion batteries compared to other type of battery chemistry [103], extreme outside temperatures such as $40°C$ and over or $-20°C$ and lower, accelerate the ageing capacity loss [104]. High temperatures increase power acceptance of the battery but the battery lifetime decreases in a short time, causing premature ageing of the Li-ion batteries [17], [105]. On the other hand, subzero temperatures decrease the power acceptance, increasing the internal resistance of the Li-ion batteries, causing the raising of the Joules power losses, decreasing the efficiency of the charging, and affecting the state of health (SOH) of the Li-ion batteries [106] [16], [107]. In case of cold weather when the temperature is not considered, the final SOC estimation maybe false and the battery does not reach the SOC target desired by the customer [108]. Thus, charging the battery while considering temperature is a very important issue, to get a best estimation of SOC and to conserve the lifespan of EVs batteries. Considering the outside temperature and temperature of the Li-ion batteries is a big challenge to make the EVs suitable to any climate condition and to extend the batteries lifespan.

3.3 Smart Charging Algorithm Considering the Temperature

The objective of this algorithm is to minimize the charging cost of the EVs by giving the scheduled optimal power flow that satisfies the customer energy need. This contribution corresponds to the content of my first conference paper [108] presented in the section 5. The minimization of EV' cost charging, takes into account the variation on the TOU price based on the transmitted information from the TSO. Thus, the TOU prices is defined as an input of the optimization system.

An example of TOU price is given in the Figure 3.3. The TOU price profile is a typical one, it allows to evaluate the charging cost with the current energy market. On the one hand, the G2V

energy price refers to the charging price for each period, on the other hand, it can describe the power demand from the grid. For example, between 6 PM (18h00) and 12 AM (00h00), the price is the highest one because of the high power demand on the grid. So, during this period the remuneration for V2G action is very attractive compared to other periods. In order to limit the charging of the EV during peak hours, and to prevent the grid from high voltage drop and frequency deviation, the TSO increases the price of the energy for charging but increases the remuneration to participate on grid support by using V2G feature.

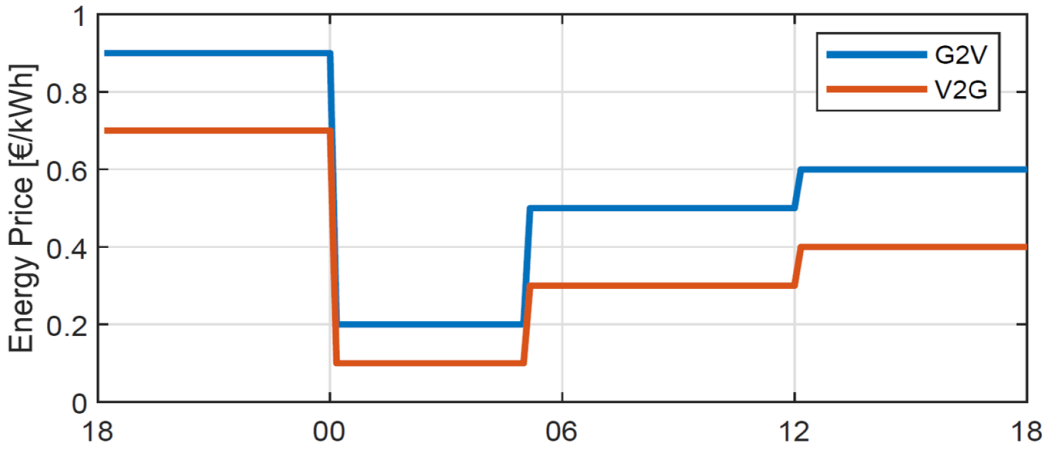

Figure 3.3 – Electricity price for G2V and V2G

The EV users will plug the EV and start the charging after work, at home or in the nearest charging station. The objective of the smart charging algorithm is to explore the economical benefit of charging in a real case by using the information of TOU energy prices (see Figure 3.3).

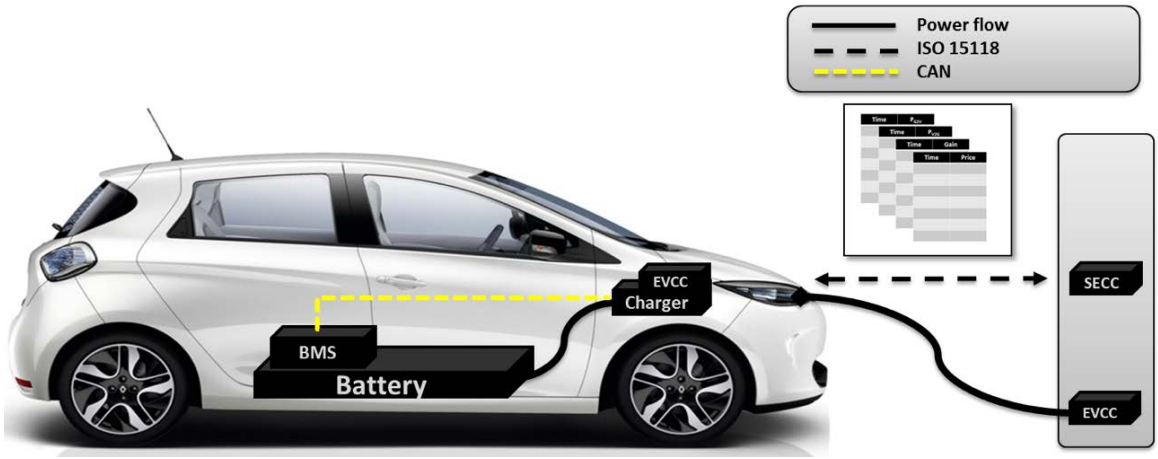

Figure 3.4 – Synoptic of EV charging

In this section a new decentralized algorithm for optimal EV charging considering temperature is proposed. It carries out the optimization from EV users perspective in order to minimize the charging cost. The consideration on bidirectional charging through the V2G feature can provide more profit to the users of EVs. Regarding the problem of sensitivity of Li-ion batteries to the temperature, the power limitation of Li-ion batteries is formulated and a electro-thermal model of Li-ion is used for SOC evaluation. As a consequence, the estimation of the SOC target is more accurate specially in cold temperature conditions such as night charging.

3.3.1 Mathematical formulation of the optimization problem

The vector of decision variables can be divided in two subsets: P_{G2V} which represents the power from the grid to the battery and P_{V2G} which is the power from the battery to the grid. The size of these vectors depends on the sampling time.

The objective function is composed of two objectives, a positive one J_1 and a negative one J_2. The optimization leads to minimize J_1 that refers to the EV charging cost and maximize J_2 corresponding to the EV discharging remuneration or the economic profit of discharging EV's battery on the grid, the two objectives are expressed in Equation (3.1), and Equation (3.2):

$$J_1 = \sum_{t=1}^{T} DEP_{G2V}(t) \cdot P_{G2V}(t) \cdot \Delta t \tag{3.1}$$

$$J_2 = \sum_{t=1}^{T} DEP_{V2G}(t) \cdot P_{V2G}(t) \cdot \Delta t \tag{3.2}$$

where DEP_{G2V} is the charging electricity price of the day, DEP_{V2G} is the the discharging electricity remuneration of the day, P_{G2V}, P_{V2G} is the charging and the discharging power respectively, Δt is the sampling period, and t the time. The proposed optimization approach is formulated to select the optimum charging power P_{G2V}, and the discharging power P_{V2G} that minimize the weighted sum of the two criteria. The proposed formulation of the objective function to be minimized is given in Equation (3.3):

$$J(x) = \alpha_1 J_1(x) + \alpha_2 J_2(x) \tag{3.3}$$

where α_1, α_2 are constant positive values, given the weight for each criterion: α_1 enforces charging operation mode, α_2 leads the system to discharge the EV using the available battery power to support the grid.

The setting of the parameters α_1 and α_2 depends on the choice of the customer to use the smart charging with V2G feature or non. The definition of the value of α_1 and α_2 is given in the Equation (3.4):

$$\begin{cases} \alpha_1 = 100; \alpha_2 = 0, & \text{Smart charging algorithm without V2G (only G2V)} \\ \alpha_1 = 100; \alpha_2 = 100, & \text{Smart charging algorithm with V2G} \end{cases} \tag{3.4}$$

The optimization problem includes linear and nonlinear constraints resulting from EV technical constraints and customer needs.

The charging power constraint related to the daily available power on the grid and the discharging power constraint related to the daily required power by the grid are expressed in Equation (3.5):

$$\begin{aligned} 0 \leq P_{G2V}(t) \leq P_{G2V-Max} \\ -P_{V2G-Max} \leq P_{V2G}(t) \leq 0 \end{aligned} \tag{3.5}$$

where $P_{G2V-Max}$, $P_{V2G-Max}$ are the maximum available power on the grid and the maximum required power by the grid.

The maximum power that can be accepted or delivered by the battery depends on the relation between the battery' SOC and the battery's temperature. This power is set by the values obtained in the Powermap function presented in the Figure 3.5. The expression of the power limitation constraint is presented in Equation (3.6):

$$\begin{aligned} P_{G2V}(t) \leq Powermap(SOC, T)(t) \\ P_{V2G}(t) \geq -Powermap(SOC, T)(t) \end{aligned} \tag{3.6}$$

Where *Powermap* represents the dependence of battery acceptance on the SOC and the temperature.

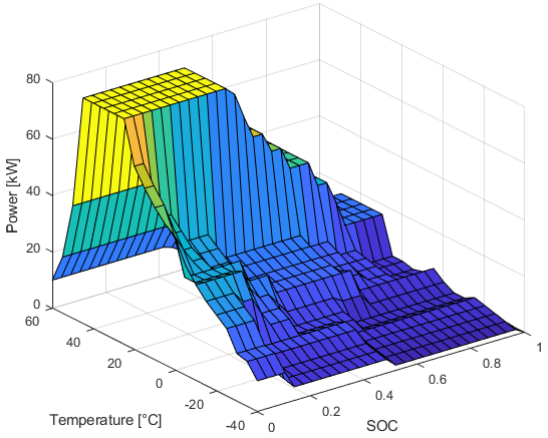

Figure 3.5 – Lithium-ion battery power map

The global constraints related to the upper and the lower bound of the SOC are expressed in Equation (3.7):

$$SOC(t) \leq SOC_{maxi} \tag{3.7}$$

where SOC_{maxi} is the maximum value of the SOC expected by the user.

In order to limit the battery cycling degradation in discharging mode and to avoid customer's range anxiety in case of an emergency use of the EV, we add a SOC constraint presented in Equation (3.8):

$$SOC(t) \geq SOC_{mini} \tag{3.8}$$

where SOC_{mini} is the minimum value of the SOC expected by the user, avoiding high battery DOD during V2G mode.

The calculation of the required energy $E_{required}$ to reach the SOC desired by the costumer is expressed in the Equation (3.9):

$$E_{required} = (SOC(t_f) - SOC(t_i)) \times E_0 \tag{3.9}$$

The initial and the final time labeled t_i, and t_f respectively. $SOC(t_i)$ is SOC of the EV in the beginning of the charging, $SOC(t_f)$ is the SOC desired by the customer, and E_0 is the capacity of the battery in kWh.

The constraint related to the final energy of the battery is presented in Equation (3.10) and Equation (3.11):

$$E_{final} = SOC(t_i) \times E_0 + (P_{G2V} + P_{V2G}) \cdot \Delta t \tag{3.10}$$

$$E_{required} \leq E_{final} \leq E_0 \tag{3.11}$$

To limit the use of the battery in V2G mode for better battery lifespan, the constraint is expressed in Equation (3.12) and Equation (3.13):

$$E_{V2G} = -P_{V2G} \cdot \Delta t \tag{3.12}$$

$$E_{V2G} \leq p \times E_0 \tag{3.13}$$

where p is a parameter to specify the proportion of the battery capacity shared with the grid.

The most important constraint that does not allow to charge and discharge in the same time slot is presented in Equation (3.14):

$$\begin{aligned} P_{G2V}(t) \neq 0 \Rightarrow P_{V2G}(t) = 0 \\ P_{V2G}(t) \neq 0 \Rightarrow P_{G2V}(t) = 0 \end{aligned} \tag{3.14}$$

This nonlinear constraint can be expressed by one mathematical condition in Equation (3.15):

$$P_{G2V}(t) \times P_{V2G}(t) = 0 \tag{3.15}$$

The battery' SOC is estimated using the SOE as explained in Equation (2.17). The dynamic monitoring of the battery SOC is given by the Equation (3.16):

$$\begin{cases} SOC(t+1) = SOC(t) + \frac{E(t)}{E_0} \\ E(t) = \eta_{charger}(P_{G2V}(t) + P_{V2G}(t)) \cdot \Delta t \end{cases} \tag{3.16}$$

where $\eta_{charger}$ is the charger efficiency.

The temperature calculation is a first order model expressed in Equation (3.17):

$$mC_p \frac{dT}{dt} = P_{Joule} + P_{convective} \tag{3.17}$$

$$T(t+1) = T(t) + \frac{\Delta t}{mC_p} \cdot (P_{Joule}(t) + P_{convective}(t))$$

The convective power is modeled by the Newton law showed in Equation (3.18):

$$P_{convective} = -\frac{T - T_{out}}{R_v} \tag{3.18}$$

The Joule power is formulated as linear model in terms of charging and discharging power as shown in Equation (3.19):

$$P_{Joule} = k \times P \tag{3.19}$$

with P is P_{G2V} or $-P_{V2G}$ depending the charging or discharging mode, and k is a thermal factor depending on the thermal inertia of the battery.

The modeled problem under the constraints is represented by a linear and non-linear equation. Therefore, a generic solver that uses Non-Linear Programming (NLP) with constraints was used to solve the optimization problem. The sampling period Δt = 10 minutes is a parameter of the optimization problem, the choice of this value defines the trade-off between precision and calculation time. The maximum number of the sampling time step is 144, corresponding to the simulation of one day and the decision variables are two vectors of 144-element.

3.3.2 Results of the proposed smart charging algorithm

Below the simulation results for the proposed smart charging algorithm are presented. The algorithm has been tested for several scenarios to validate its performance. A real French energy price profile was chosen to illustrate the user charging case. The results present two cases, the first case is a charging under an outside temperature of $20°C$, and the second case is a charge under an extreme outside temperature of $-20°C$.

In the first case, a smart charging with just G2V considered as unidirectional charging (Figure 3.8) and smart charging with V2G feature considered as bidirectional charging (Figure 3.9)

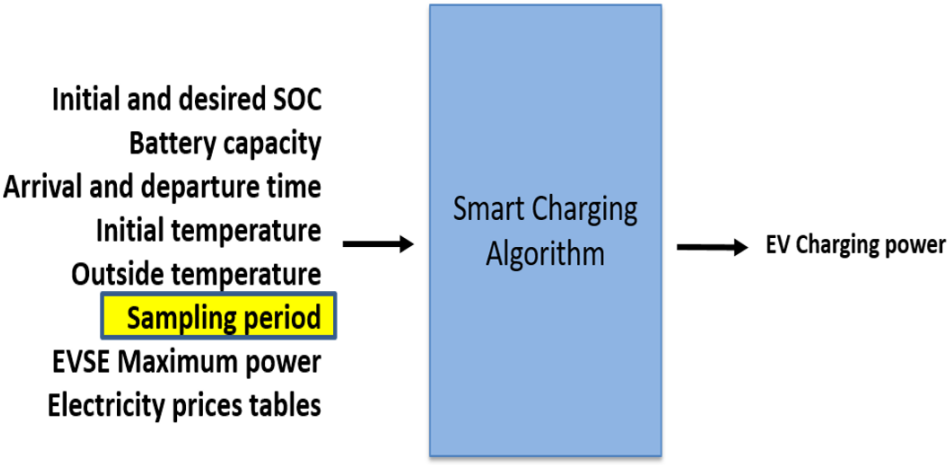

Figure 3.6 – Black box implementation of the smart charging algorithm with fixed time step

are compared to the traditional charging known as uncontrolled charging or plug and charge (Figure 3.7), to estimate the economical gain of the smart charging algorithms compared to the classical method. In the second case, a smart charging with V2G feature considering the effect of temperature on lithium batteries compared to a classical smart charging algorithm without temperature consideration.

The initial conditions are $SOC(t_i) = 0.35$, $SOC(t_f) = 0.7$, $SOC_{mini} = 0.1$, $E_0 = 60kWh$, $\eta_{charger} = 0.9$, $p = 0.5$, $P_{G2V-Max} = 7kW$, $P_{V2G-Max} = -7kW$ and $\Delta t = 10$ min. The initial battery temperature is fixed to $20°C$.

For the first case, $T_{out} = 20°C$, the arrival time is 6 PM and the departure time is 8 AM of the next day.

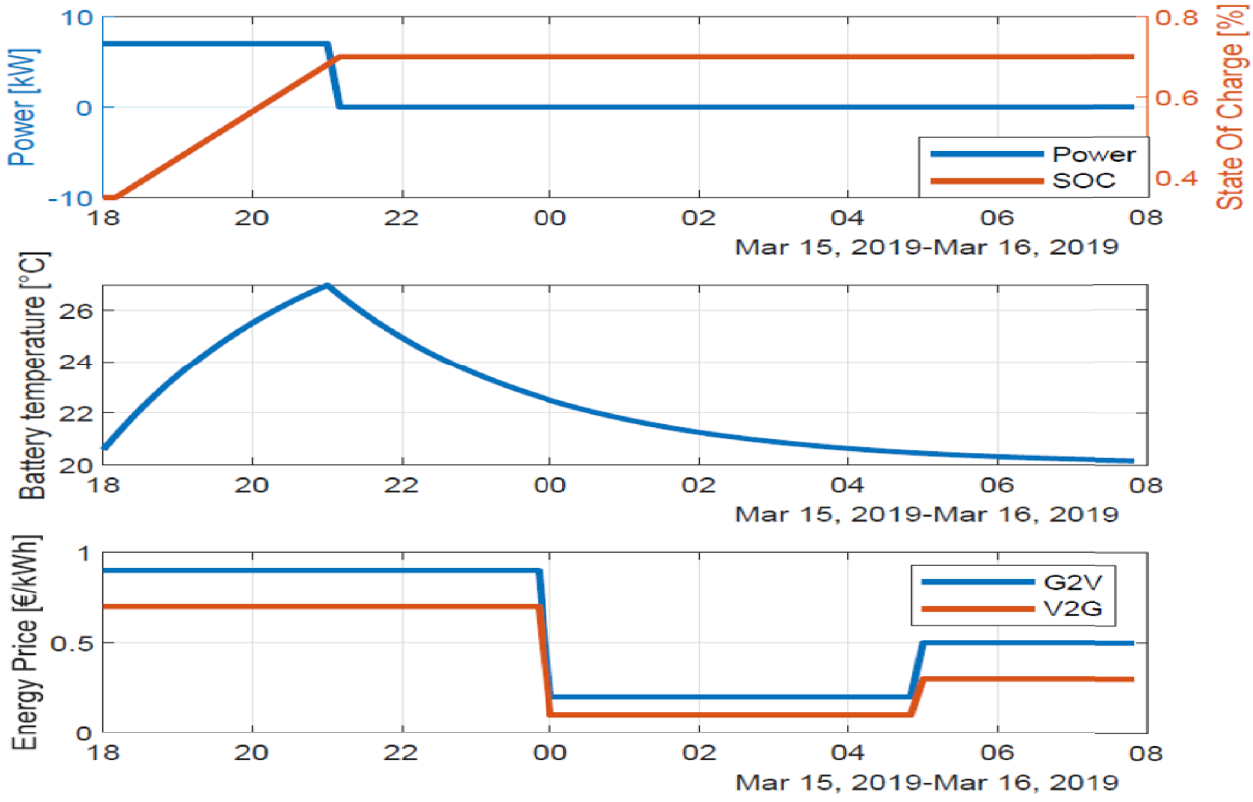

Figure 3.7 – Uncontrolled charging, $T_{out} = 20°C$.

With the uncontrolled charging presented in Figure 3.7, the EV starts the charging the moment it plugs-in, neglecting the high energy prices, so the charging cost will be high too. The estimated cost of charging for this first scenario is 19.95€. Without a smart charging algorithm, the charging power is fixed to the maximum power accepted by the battery. Moreover, the temperature increases very fast, in case of a high desired SOC, at a fast charging station and without cooling, the battery lifespan can decrease rapidly. In case of high penetration level of EVs in the grid, the plug and charge method leads to grid overloading, voltage drop, and frequency deviation.

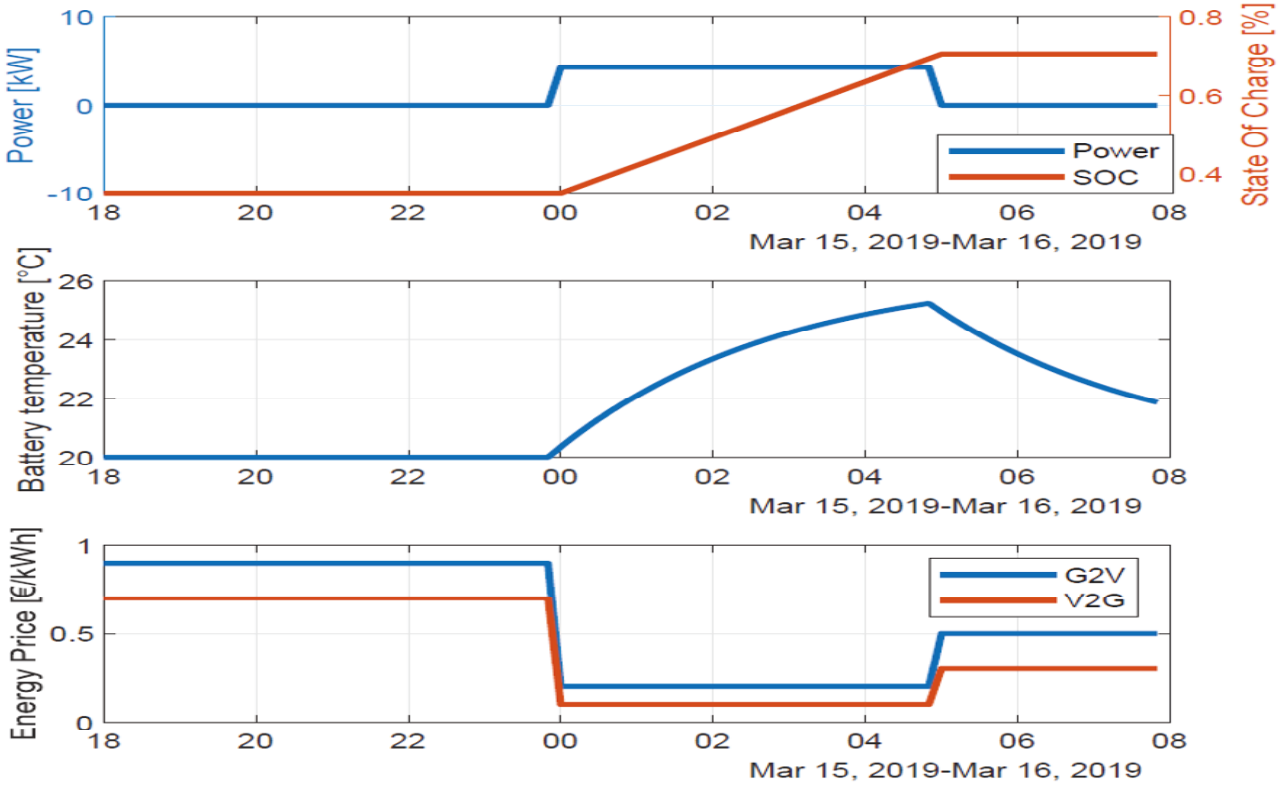

Figure 3.8 – Smart charging with G2V and without V2G, $T_{out} = 20°C$.

However, with smart charging algorithm, the EV is plugged-in at 6 PM, but the charging effectively starts until midnight when the electricity price is lower. The algorithm can shift the charge to the period when the electricity price is more attractive corresponding to the less period used on the night. Figure 3.8 shows that the temperature increases slowly, compared to the fast temperature evolution in the uncontrolled charging case.

The desired SOC is reached before the departure time. Using the smart charging algorithm, the power is distributed along the charging period to avoid the overload in the high EV penetration level. The smart charging algorithm can perform the charging of a fleet of EVs with normalized distribution of the power in the whole charging station. The estimated cost of charging for this simulation is 4.25€. The charging bill is lower than the uncontrolled charging showed in Figure 3.7.

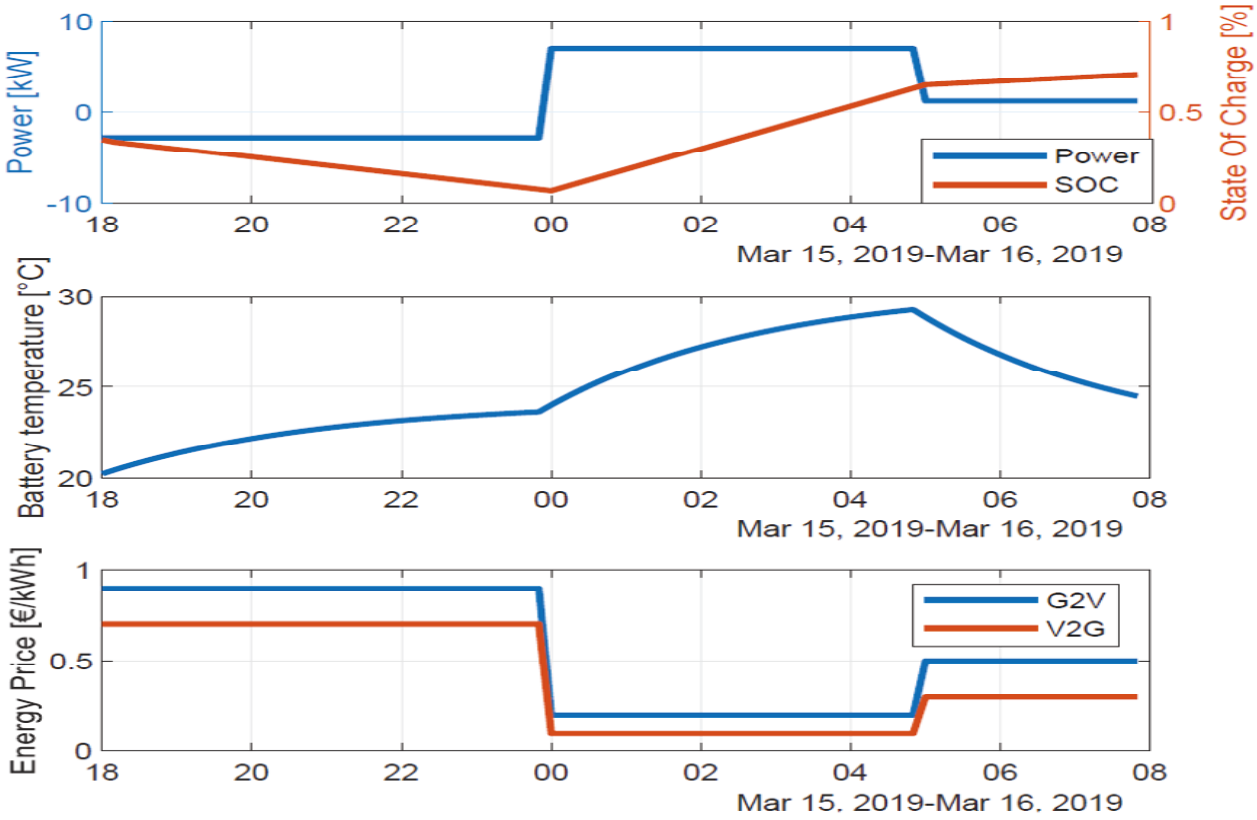

Figure 3.9 – Smart charging with G2V and V2G, $T_{out} = 20°C$.

Figure 3.9 presents the charging power, SOC, battery's temperature evolution and energy prices. Using the V2G feature, the smart charging algorithm, begins the discharging in the period of high V2G remuneration to maximize the profit while the SOC decreases until it reaches the minimal value SOC_{mini}. At the same moment, the energy price becomes cheaper so the G2V charge begins to realize the desired SOC. It can be observed that the smart charging algorithm distributes power throughout the period in such a way that the battery SOC decreases and converges to the minimal value SOC_{mini}, as opposed to uncontrolled charging or smart charging algorithm without V2G feature, where the battery SOC increases continuously until it reaches the SOC_{target}. With this decentralized algorithm, the estimated profit of charging for this simulation is 2.83€. Thus the cost improvement compared to the smart charging without V2G feature is 7.08€, and 22.78€ in comparison to uncontrolled charging.

Setting SOC_{mini} to 0.05 in order to maximize the reward, may have an impact on battery lifespan. However, setting the SOC_{mini} at a value greater than 0.2 to extend the battery lifetime, makes the EV's customer miss out a significant profit. The SOC_{mini} is a trade off between the economical profit and battery degradation. The SOC_{mini} value could be setup between 0.1 and 0.2 for optimal performances. Moreover, high temperatures increase significantly the internal resistance and the capacity loss compared to medium ambient temperatures. Therefore, strong capacity fading is usually reported for storage and/or cycling at high important temperatures, due to the degradation of active materiel causing a reduction of Li-ion batteries lifetime.

For the second case, $T_{out} = -20°C$, the arrival time is 12 AM and the departure time is 8 AM.

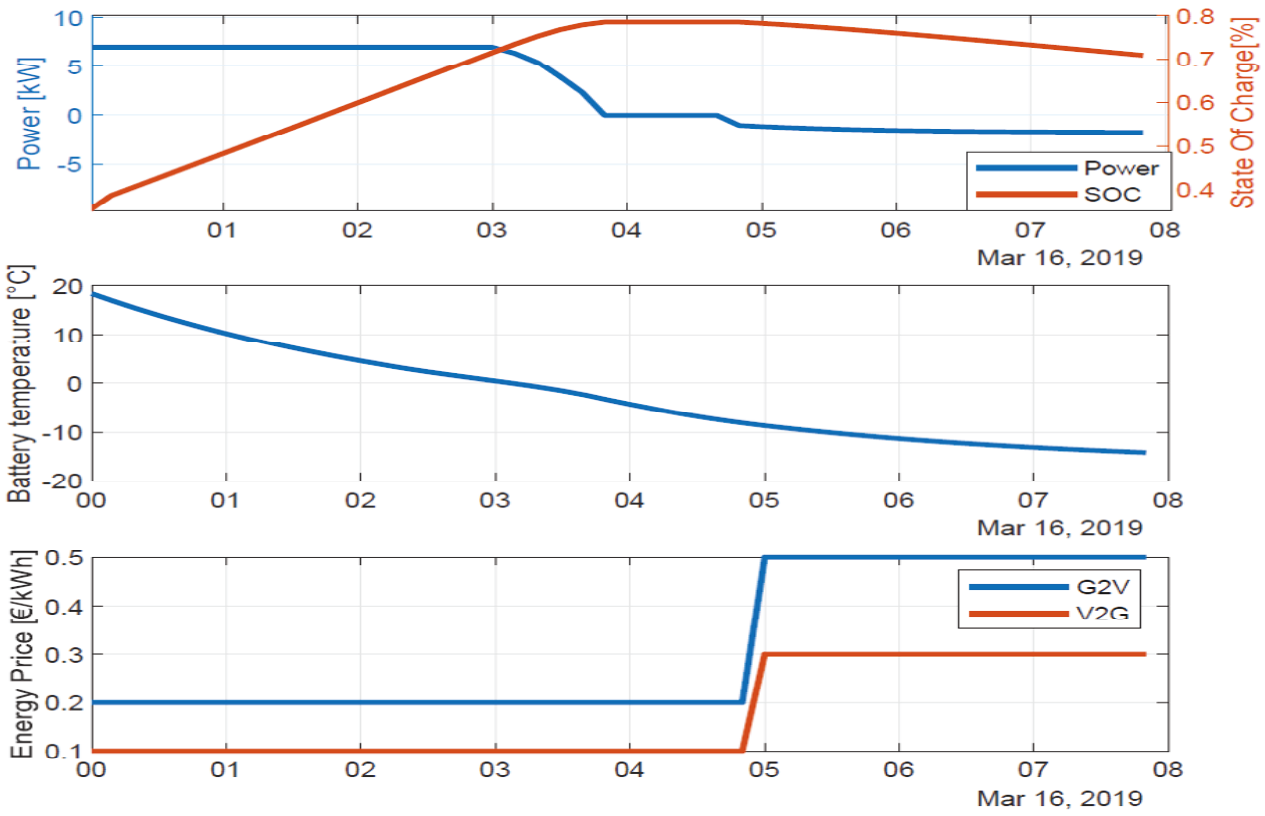

Figure 3.10 – Smart charging with G2V and V2G considering the external and battery temperature, $T_{out} = -20°C$.

In Figure 3.10, the algorithm begins charging immediately to exploit the period of time when the temperature is above $0°C$, to benefit from the low G2V energy prices and to maximize the energy stored in the battery. As the battery temperature decreases, the acceptance of battery power also decreases. This property is directly related to the poor performance of lithium batteries in subzero temperatures. When the price of V2G energy is more attractive, the battery discharge begins to reach the desired SOC and minimize the total cost of charging. The estimated charging cost is 3.62€.

Figure 3.11 presents a classical smart charging algorithm without considering temperature. This algorithm takes advantage of the low G2V energy prices to charge the battery and benefits from high V2G remuneration to discharge the battery while neglects the outside temperature and the battery temperature. The estimated charging cost is 2.5€. In low temperatures, lithium batteries limit the charging power, so the profile of the charging power in the first sub-figure of Figure 3.11 is not realistic. Therefore, the estimated value of the final SOC of 0.7 is false. Considering the outside and battery temperatures and the same power profile, the realistic value of the final estimated SOC is 0.57. To achieve the desired SOC of 0.7, the battery needs to keep on charging for a longer period of time. Consequently, the charging cost is estimated at 4.41€. The smart charging algorithm performs the charging, reaches the desired SOC and saves 0.79€, compared to a smart charging algorithm without considering temperature. Without considering the outside temperature and the battery temperature, the charging power profile could be unrealistic and the estimated value of final SOC can be false.

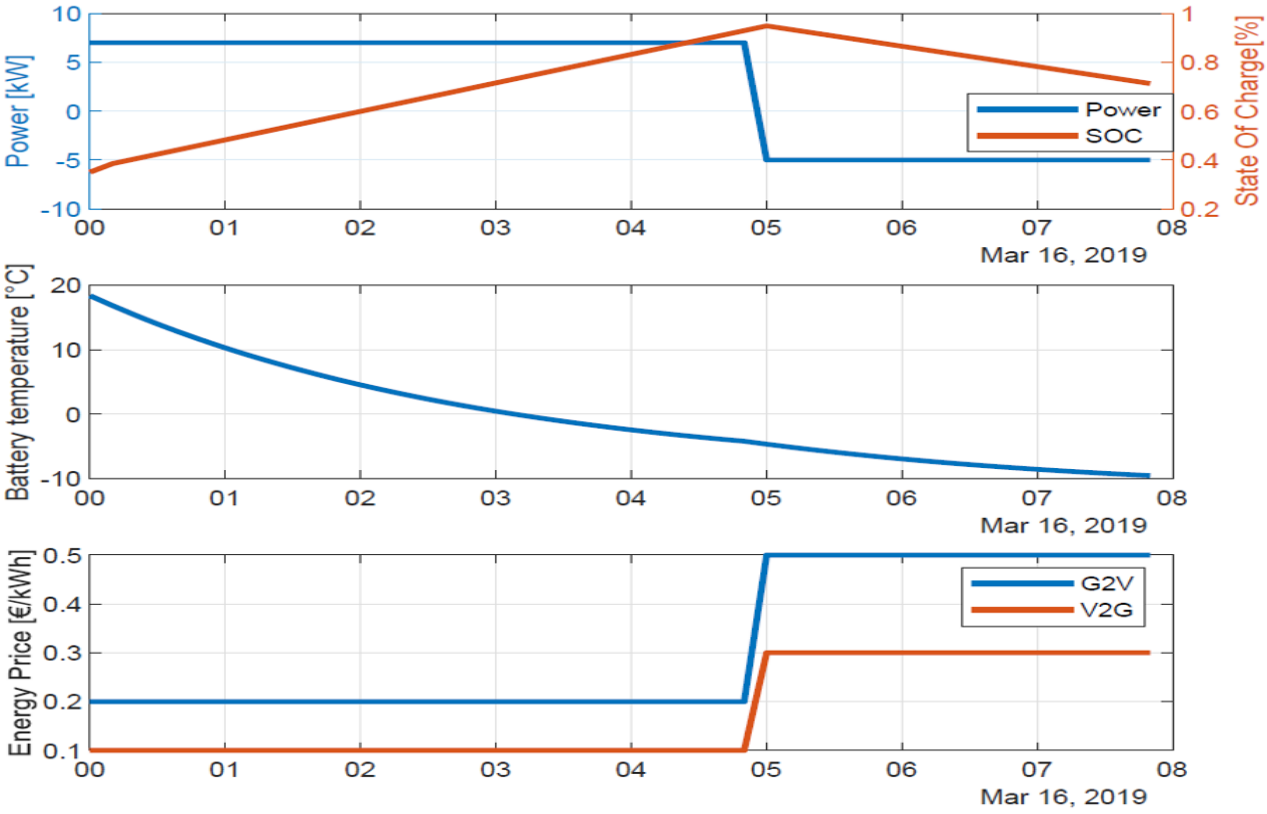

Figure 3.11 – Smart charging with G2V and V2G without considering the external and battery temperature, $T_{out} = -20°C$.

3.4 Smart Charging Algorithm with Dynamic Time Step Considering the Temperature

In addition to the studies mentioned in Section 3.2, many other optimal algorithms and strategies are available in the literature to solve the cost minimization problem. Nevertheless, all of them use a constant sampling period or fixed calculation step defined at the beginning or before starting the optimization [22, 26, 100, 108, 109]. In the event of a fluctuation of energy prices of a few seconds within a long planning optimization window, the charging scheduling will cause an important issue with a huge number of steps.

Indeed, the calculation step is defined by the minimal duration between two changes of energy price. Therefore, the size of the decision variable vector becomes very significant, so the computation time and the complexity of the problem increase. The classical embedded scheduling algorithms with constant calculation steps may not be able to carry out this optimization task because of the large number of decision variables involved in this optimization.

To overcome this issue, a smart charging algorithm with dynamic time step is proposed. The charging strategy uses the time step as decision variable in the optimization problem. The sampling time Δt will be removed from the input parameters' list (see Figure 3.12) compared to the previous algorithm with fixed sampling period presented in Figure 3.6. The contribution corresponds to the content of my first article presented in the section 5. The proposed strategy consists of three steps: pre-processing, optimization, and post-processing.

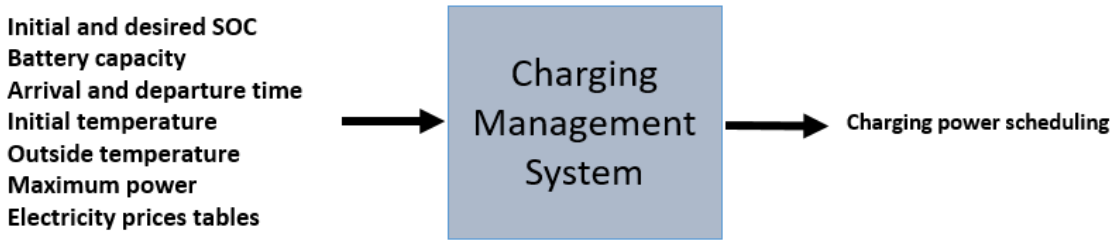

Figure 3.12 – Charging management system black box of the smart charging algorithm with dynamic time step

3.4.1 Pre-processing

The pre-processing step allows, before starting the scheduling, to provide the essential data for the optimization step, namely the data collection, the subdivision of the time interval into time slots, the size of the decision vectors, as well as the determination of the upper bounds of the optimized time step. The data collection operation consists in receiving the data and parameters of the optimization problem to initiate the planning, either of the Battery Management System (BMS) or the charging station.

Figure 3.13 presents the context of the contribution and the elements interacting with the Charging Management System (CMS). The device receives from the BMS the measurement of the initial temperature, the outdoor temperature, the initial SOC, and the battery capacity.

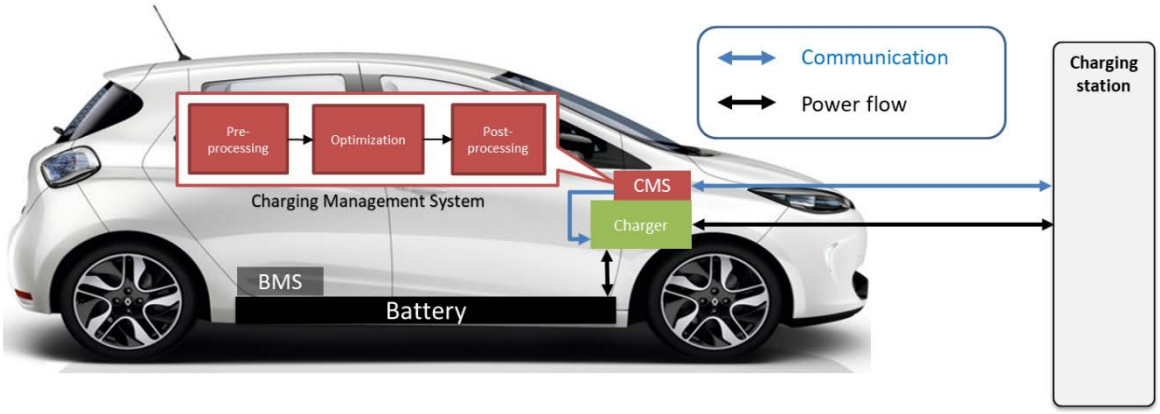

Figure 3.13 – Charging system synoptic

The charging station sends the data over a maximum availability period of 24 hours. The device receives from the charging station the following information shown in Figure 3.14:

— The charging energy price for the next 24 hours: $price_{G2V}$
— The maximum charging power for the next 24 hours: $Pmax_{G2V}$
— The discharging fees from V2G for the next 24 hours: $price_{V2G}$
— The maximum discharging power for the next 24 hours: $Pmax_{V2G}$

In this step, the pre-processing algorithm restricts the time base to the actual availability period of the EV on the charging station i.e. between the arrival time and departure time of the EV.

The next step is to subdivide the horizon time into a sequence of time slots. In each defined time slot, the four variables $price_{G2V}$, $Pmax_{G2V}$, $price_{V2G}$, and $Pmax_{V2G}$ have a constant value. The subdivision to time slots is the conversion of data from time scale in Figure 3.14 to slot scale in Table 3.1.

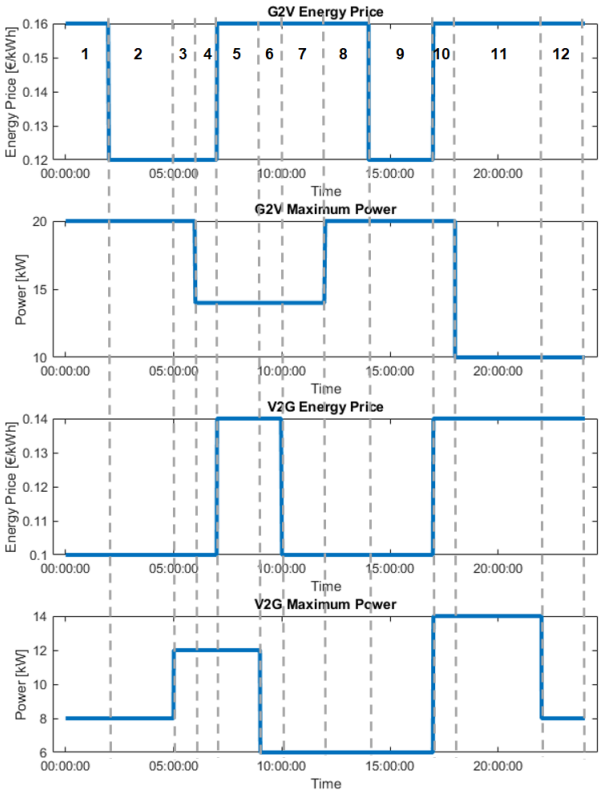

Figure 3.14 – Subdivision on time slots (case 1)

Thus, we can conclude the number of time slots corresponding to the size of the decision vectors $N = 12$ and the duration of each time slot $dmax$ shown in Figure 3.15. The subdivision on time slots of the $price_{G2V}$, $Pmax_{G2V}$, $price_{V2G}$, and $Pmax_{V2G}$, can be observed in figures 3.14-3.15 and in Table 3.1.

For current data with a constant time step for scheduling, the maximal sampling time that can be used with optimal charging strategies is $\Delta t = 1$ hour corresponding to the minimal duration of d_{max}. Thus the size of decision vector is 24. For our strategy, the size of decision vector is 12. The difference between these two numbers mainly depends on the minimal duration that can be smaller than 1 hour in many real cases.

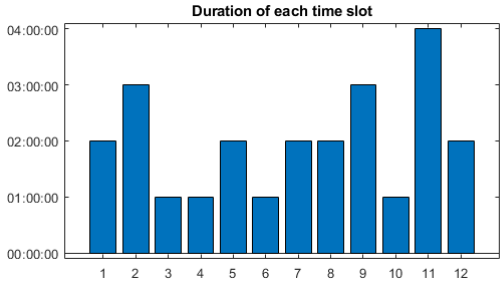

Figure 3.15 – Duration of time slot: d_{max}

In case of a small variation of G2V energy prices, due to an extra event such as the half-time of important sporting events such as the Euro or the world cup. A rise in power demand at half-time of the matches is observed at the national level due to the use of ovens and microwaves in this period. An example of a small variation of 10 minutes between 8 PM and 8:10 PM is shown in Figure 3.16. The maximal sampling time that can be used with optimal charging

Table 3.1 – Subdivision results to slot scale

Slot	$price_{G2V}$	$P_{max_{G2V}}$	$price_{V2G}$	$P_{max_{V2G}}$	d_{max}
1	0.16	20	0.10	8	2
2	0.12	20	0.10	8	3
3	0.12	20	0.10	12	1
4	0.12	14	0.10	12	1
5	0.16	14	0.14	12	2
6	0.16	14	0.14	6	1
7	0.16	14	0.10	6	2
8	0.16	20	0.10	6	2
9	0.12	20	0.10	6	3
10	0.16	20	0.14	14	1
11	0.16	10	0.14	14	4
12	0.16	10	0.14	8	2

strategies with constant time step is $\Delta t = 10$ minutes corresponding to a size of 144 for the decision vector. For the proposed strategy, the size of decision vector is 14.

A single event of a few minutes duration can penalize the whole optimization problem. To sum up, a short fluctuation of prices or maximal power can make the optimization task very difficult and even impossible (time and memory constraints) for an embedded charging scheduling system.

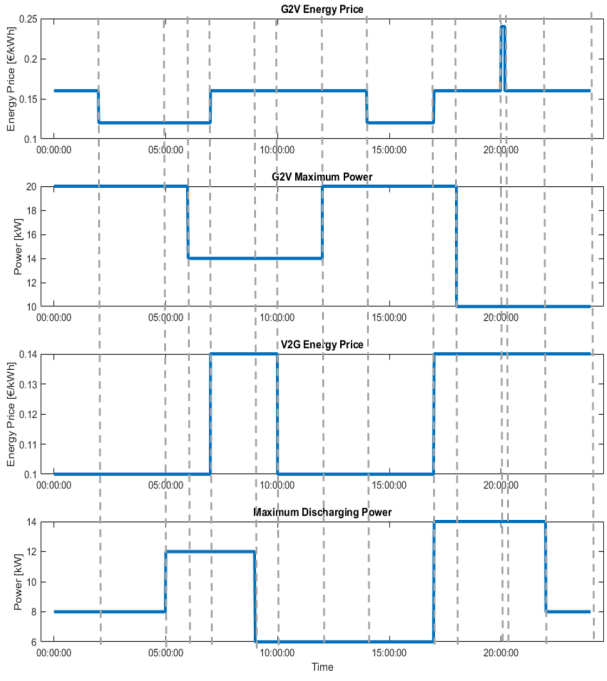

Figure 3.16 – Subdivision on time slots (case 2)

3.4.2 Optimization

This section is devoted to modeling the EV charging problem with cost minimization and temperature consideration. The modeling is done as follows:

The time horizon vector is described by $S = [1,...,i,...,N]$ and it contains N non equal

duration time slots as defined in the previous subsection and in Figure 3.15. The charging and the discharging of the EV can be expressed by four decision vectors as expressed in Equation (3.20).

$$X = \begin{bmatrix} P_{G2V} & P_{V2G} & d_{G2V} & d_{V2G} \end{bmatrix} \tag{3.20}$$

With

$$\begin{aligned} P_{G2V} &= \left[P_{G2V_1}, ..., P_{G2V_i}, ..., P_{G2V_N}\right] \\ P_{V2G} &= \left[P_{V2G_1}, ..., P_{V2G_i}, ..., P_{V2G_N}\right] \\ d_{G2V} &= \left[d_{G2V_1}, ..., d_{G2V_i}, ..., d_{G2V_N}\right] \\ d_{V2G} &= \left[d_{V2G_1}, ..., d_{V2G_i}, ..., d_{V2G_N}\right] \end{aligned} \tag{3.21}$$

For the i^{th} time slot the vector X_i can be defined as shown in Equation (3.22):

$$X_i = \begin{bmatrix} P_{G2V_i} & P_{V2G_i} & d_{G2V_i} & d_{V2G_i} \end{bmatrix} \tag{3.22}$$

This algorithm have two aims:

— Minimize the vehicle's charging cost through optimal grid to vehicle power flow taking into account G2V energy prices.

— To maximize the profit from selling energy from vehicle to grid considering V2G energy prices.

The objective function is composed of two objectives, a positive one C_1 and a negative one C_2. The optimization leads to minimize C_1 that refers to the EV charging cost and to maximize C_2 corresponding to the EV discharging remuneration or the economic profit of discharging EV's battery on the grid. The two objectives are expressed in Equation (3.23), Equation (3.24):

$$C_1 = \sum_{i=1}^{N} price_{G2V_i} \cdot P_{G2V_i} \cdot d_{G2V_i} \tag{3.23}$$

$$C_2 = \sum_{i=1}^{N} price_{V2G_i} \cdot P_{V2G_i} \cdot d_{V2G_i} \tag{3.24}$$

Where $price_{G2V_i}$ is the charging electricity price of the i^{th} time slot in €/kWh, $price_{V2G_i}$ is the discharging electricity remuneration of the i^{th} time slot in €/kWh, P_{G2V_i}, P_{V2G_i} is the charging and the discharging power of the i^{th} time slot in kW respectively, d_{G2V_i}, d_{V2G_i} are the calculation step in hours, and i the time slot index.

The proposed optimization approach is formulated to select the optimum charging power P_{G2V} for the period of time d_{G2V}, and the discharging power P_{V2G} for the period of time d_{V2G} that minimize the weighted sum of the two criteria. The proposed formulation of the objective function to be minimized is given as follows:

$$F(X) = \alpha_1 C_1(X) + \alpha_2 C_2(X) \tag{3.25}$$

where X is the decision variable, α_1, α_2 are constant positive values, given the weight for each criterion: α_1 enforces charging operation mode, α_2 leads the system to discharge the EV using the available battery power to support the grid.

The setting of the parameters α_1 and α_2 depends on the choice of the customer to use the smart charging with V2G feature or non. The definition of the value of α_1 and α_2 is given in the Equation (3.4).

The optimization problem includes linear and nonlinear constraints resulting from EV technical constraints and customer needs.

The charging power constraint related to the daily available power on the grid and the discharging power constraint related to the daily required power by the grid are expressed in Equation (3.26):

$$\begin{aligned} 0 \leq P_{G2V_i} \leq Pmax_{G2V_i} \qquad & i = 1,...,N \\ -Pmax_{V2G_i} \leq P_{V2G_i} \leq 0 \qquad & i = 1,...,N \end{aligned} \tag{3.26}$$

where $Pmax_{G2V_i}$, $Pmax_{V2G_i}$ are the maximum available power on the grid and the maximum required power by the grid in the i^{th} time slot respectively.

The maximum duration of use for charging and discharging in the i^{th} time slot is formulated in Equation (3.27):

$$\begin{aligned} 0 \leq d_{G2V_i} \leq dmax_i \qquad & i = 1,...,N \\ 0 \leq d_{V2G_i} \leq dmax_i \qquad & i = 1,...,N \end{aligned} \tag{3.27}$$

where $dmax_i$ is the maximum duration of the i^{th} slot.

To allow the charging and discharging operation in the same time slot, a constraint is expressed in Equation (3.28):

$$d_{G2V_i} + d_{V2G_i} \leq dmax_i \qquad i = 1,...,N \tag{3.28}$$

The maximum power that can be accepted or delivered by the battery depends on the relation between the SOC and the battery's temperature. This power is set by the values obtained in the Powermap function:

$$\begin{aligned} P_{G2V_i} \leq Powermap(SOC_i, T_i) \qquad & i = 1,...,N \\ P_{V2G_i} \geq -Powermap(SOC_i, T_i) \qquad & i = 1,...,N \end{aligned} \tag{3.29}$$

The Powermap function is the internal dependence of battery power on temperature T_i of the i^{th} slot and SOC of the i^{th} slot SOC_i. It provides information on the maximum power that can be accepted by the battery or delivered to the battery. An example of Powermap is shown in Figure 3.5.

The global constraints related to the upper and the lower bound of the SOC are expressed in Equation (3.30) and Equation (3.31).

In order to limit the battery cycling degradation in discharging mode and to avoid customer's range anxiety in case of an emergency use of the EV, we add a SOC constraint expressed as follows:

$$SOC_i \geq SOC_{mini} \qquad i = 1,...,N \tag{3.30}$$

Where SOC_{mini} is the minimum value of the SOC expected by the user, avoiding high battery DOD during V2G mode.

The case of overcharging is taken into account because it affects the lifetime of Li-ion batteries. Despite the fact that EV owners tend to prefer autonomy over battery life, because of the anxiety related to autonomy, which is considered one of the main obstacles to the large-scale adoption of EVs.

$$SOC_i \leq SOC_{maxi} \qquad i = 1,...,N \tag{3.31}$$

The calculation of the required energy $E_{required}$ to reach the SOC desired by the costumer is expressed as follows:

$$E_{required} = (SOC_{target} - SOC_0) \times E_0 \tag{3.32}$$

SOC_0 is the initial SOC of the EV, SOC_{target} is the SOC desired by the customer, and E_0 is the capacity of the battery in kWh.

The constraint related to the final energy of the battery is:

$$E_{required} \leq E_{final} \leq E_0 \tag{3.33}$$

The evaluation of the energy variation of the battery at each time step can be computed as follows:

$$E_i = \eta_{charger}(P_{G2V_i} \cdot d_{G2V_i} + P_{V2G_i} \cdot d_{V2G_i}) \quad i = 1,...,N \tag{3.34}$$

Where $\eta_{charger}$ is the charger efficiency. Then, the final energy quantity in the battery can be expressed as:

$$E_{final} = SOC_0 \times E_0 + \sum_{i=1}^{N} E_i \tag{3.35}$$

The dynamic monitoring of the SOC is given by Equation (3.36):

$$SOC_{i+1} = SOC_i + \frac{E_i}{E_0} \qquad i = 1,...,N \tag{3.36}$$

The temperature calculation is a first order model expressed in Equation (3.17). The convective power is modeled by the Newton law showed in Equation (3.18).

The Joule power is formulated as a linear model in terms of charging and discharging power:

$$P_{Joule_i} = k \times P_{G2V_i} + k \times (-P_{V2G_i}) \quad i = 1,...,N \tag{3.37}$$

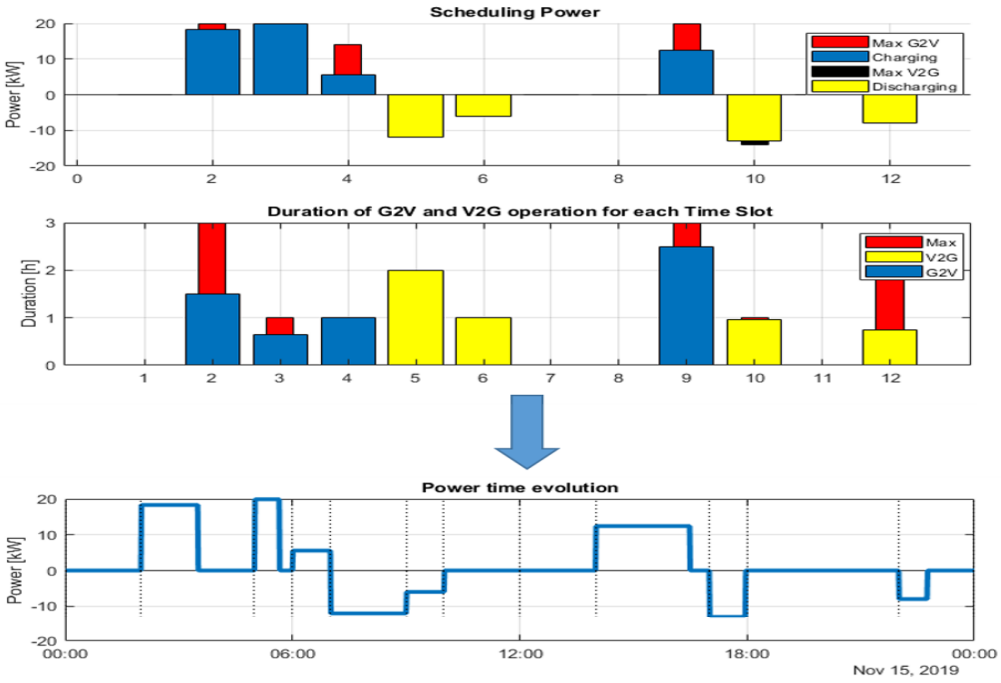

Figure 3.17 – Data conversion to time scale

3.4.3 Post-processing

This step is used to generate the order for the charger to control the charging and discharging of the EV, respecting the scheduling carried out in the optimization stage. It consists in generating the control signal of the charge/discharge to charger by choosing a time step adapted to the communication between the CMS and the charger. In addition, at this stage the battery SOC and battery temperature is estimated over the entire period of the EV availability. To summarize, the conversion of the optimization results from slot scale to time scale is done in the post-processing step as shown in Figure 3.17 using the Algorithm 1.

Algorithm 1 Transforming data from time slot to time scale

$d_{G2Vm} \leftarrow round(d_{G2V} \times 60)$
$d_{V2Gm} \leftarrow round(d_{V2G} \times 60)$
$d_{maxm} \leftarrow round(d_{max} \times 60)$
$t_{maxm} \leftarrow \sum_{i=1}^{N} d_{G2Vm_i} + \sum_{i=1}^{N} d_{V2Gm_i}$
$P(1) \leftarrow P_{G2V}(1)$
while $t \leq t_{maxm}$ **do**
  for $i \leftarrow 1, N$ **do**
    for $j \leftarrow 1, d_{G2Vm}(i)$ **do**
      $P(t) \leftarrow P_{G2V}(i)$
      $t = t + 1$
    end for
    for $j \leftarrow 1, d_{V2Gm}(i)$ **do**
      $P(t) \leftarrow P_{V2G}(i)$
      $t = t + 1$
    end for
    $R = d_{maxm}(i) - d_{G2Vm}(i) - d_{V2Gm}(i)$
    for $j \leftarrow 1, R$ **do**
      $P(t) \leftarrow 0$
      $t = t + 1$
    end for
  end for
end while

3.4.4 Results of the proposed smart charging algorithm with dynamic time step

The purpose of this section is to demonstrate the effectiveness of the proposed strategy. On the one hand, the results of the proposed strategy with an optimized time step have been compared to the classical approach using a fixed time step. On the other hand, the proposed strategy will be tested under an extreme outside temperature to show the effect of the temperature on the power scheduling and the final SOC. Finally, the optimized time step strategy will be tested on several daily energy price profiles to prove the effectiveness of the proposed strategy compared to the fixed time step strategy, in term of running time, the number of decision variables and the number of constraints. The initial conditions are $SOC_0 = 0.35$, $SOC_{target} = 0.7$, $SOC_{mini} = 0.1$, $E_0 = 60kWh$, $\eta_{charger} = 0.9$, $P_{G2V\_Max} = 7kW$, and $P_{V2G\_Max} = -7kW$. The initial battery temperature is fixed to $20°C$.

The simulation results for the proposed scheduling strategy are presented below. The algorithm has been tested for several scenarios to validate its performance. A real French energy price profile was chosen to illustrate the charging cases. The results show two cases, the first case is the charging under an outside temperature of $20°C$, and the second case is a charging under an extreme outside temperature of $-20°C$.

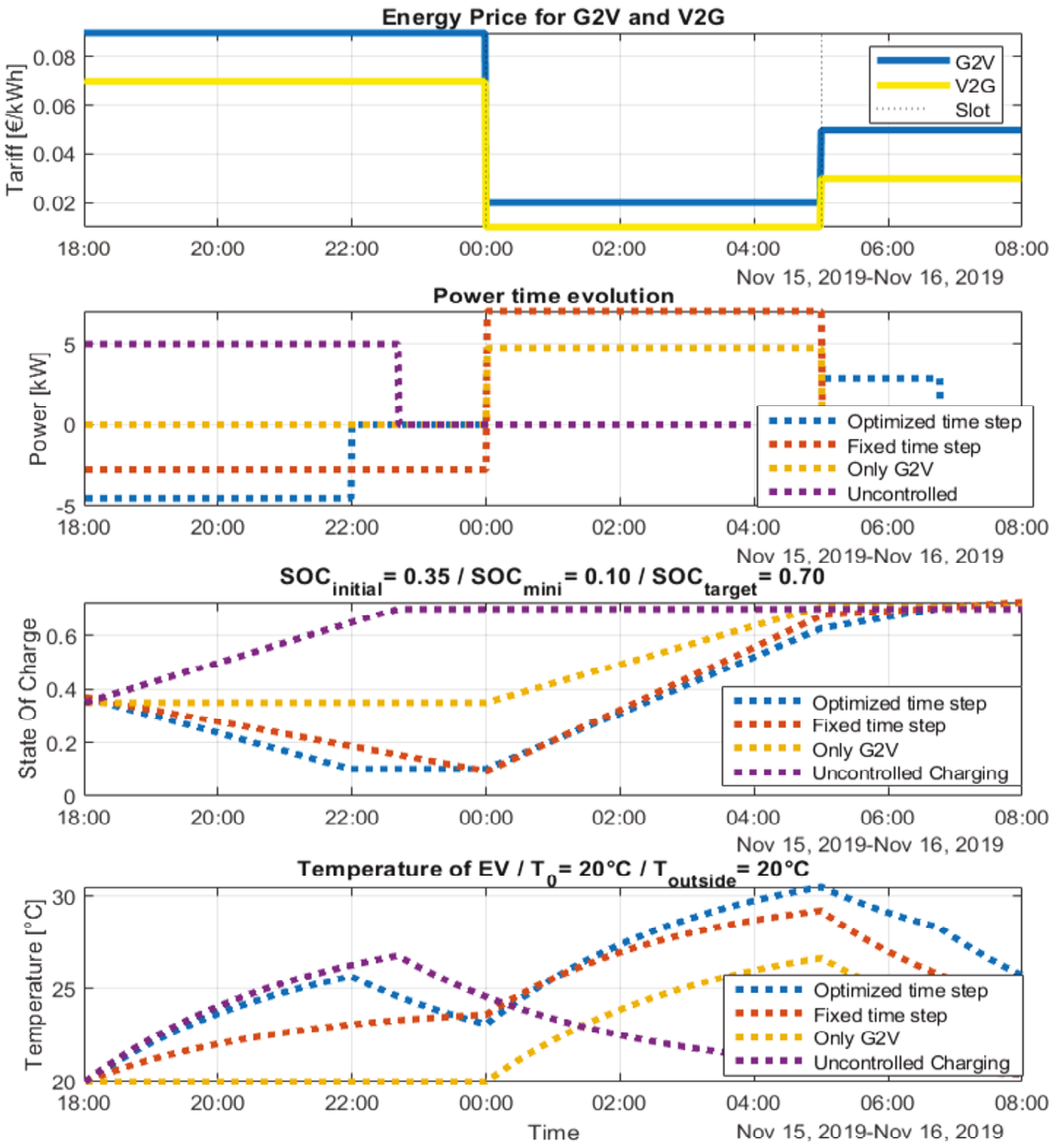

Figure 3.18 – Charging strategies comparison under $T_{out} = 20°C$.

For the first case, which implies a charging of the EV at night under an outside temperature of $20°C$. The Figure 3.18 shows the comparison between several charging strategies. The SOC_{target} is achieved by all strategies, however, the charging cost is different from one strategy to another. Using the uncontrolled charging, the charging starts at the moment of plug-in, neglecting the high energy prices, so the charging cost will be high and it is estimated to 2.1€. Smart charging algorithm with only G2V can shift the charging to midnight, the EV is plugged-in at 6 PM, but the charging effectively starts until midnight when the electricity price is more attractive so the estimated charging cost is 0.47€. Using the V2G feature, the scheduling strategy, begins the discharging in the period of high V2G remuneration to maximize the profit while the SOC decreases until it reaches the minimal value of 0.1 corresponding to the SOC_{mini}. When the G2V energy price becomes cheaper, the charging begins to reach the desired SOC. The two strategies with optimized time step and fixed time step use the V2G feature, but with the proposed strategy the charging profit is 0.31€ and the executing time is 0.25 second se compared to 0.28€ and

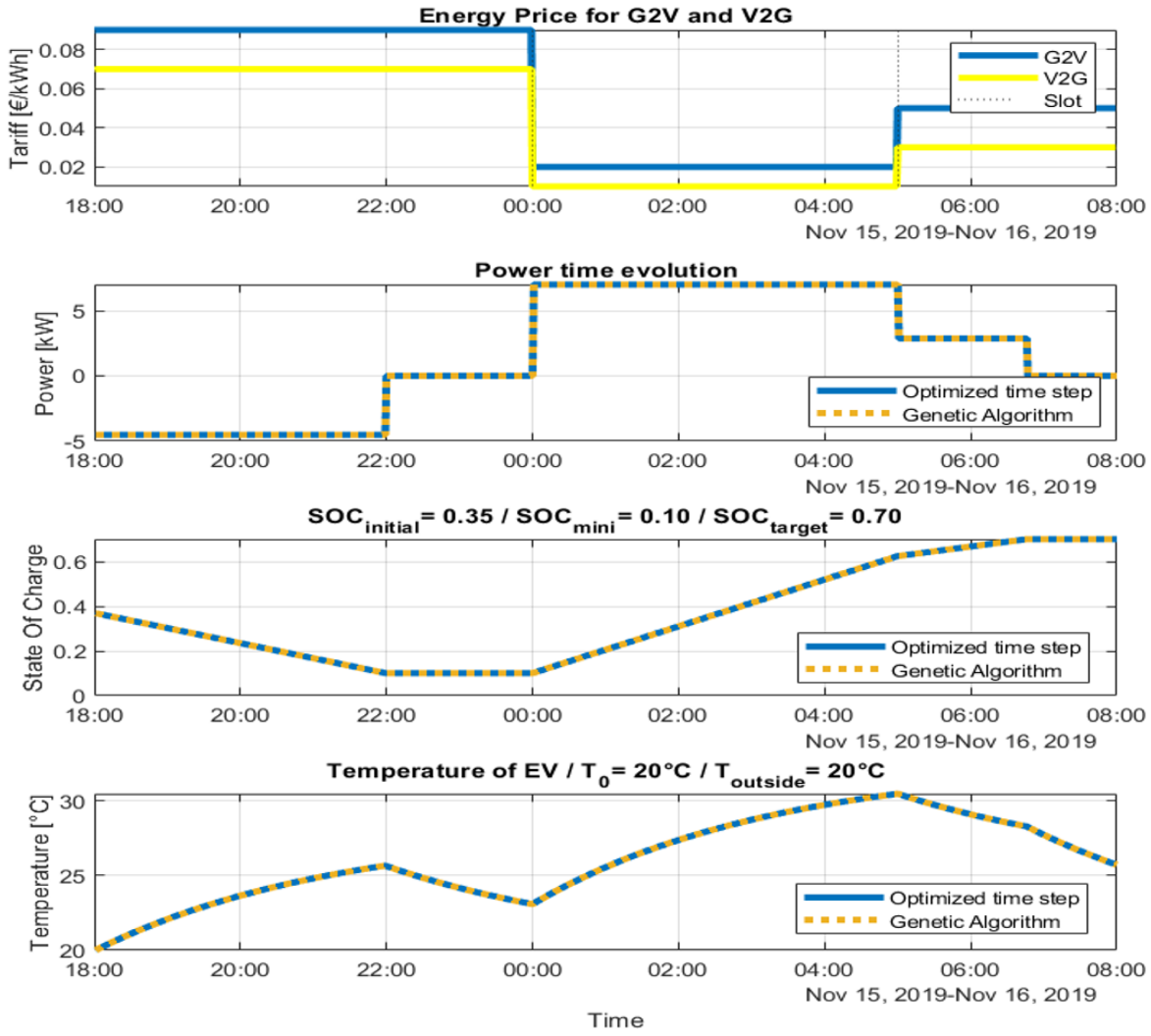

Figure 3.19 – The impact of optimization algorithm

1.95 second for the classical strategy with fixed time step.

For the strategy using optimized time step, the number of decision variables is 12 and the number of constraint is 21. However, for the classical strategy using fixed time step of 10 minutes, the number of decision variables is 84 and the number of constraint is 420.

In brief, the classical strategy with fixed time step requires higher computing capacity because of the high number of decision variable and constraints compared to the proposed strategy with optimized time step that could be integrated easily to EV onboard embedded system.

Figure 3.19 illustrates the impact of optimization method on convergence to the optimal solution. The two charging profiles reached the targeted SOC before the departure time. Although the difference between the global methods such as genetic algorithm and the locally method based on the gradient, the two charging power profiles are the same corresponding to the optimal solution presented in Fig. 3.18 with the blue color. Because of the low number of decision variables and constraints (12 decision variables and 18 constraints) the genetic algorithm and the gradient method converge to the same optimal solution. In brief, the proposed method does not require the use of an advanced optimization method to converge to the optimal solution. A local optimization method may be sufficient to solve the optimization problem.

Figure 3.20 shows the impact of an extra event such as a football match. The energy prices are directly impacted by this extra event. In order to demonstrate the advantage of the proposed

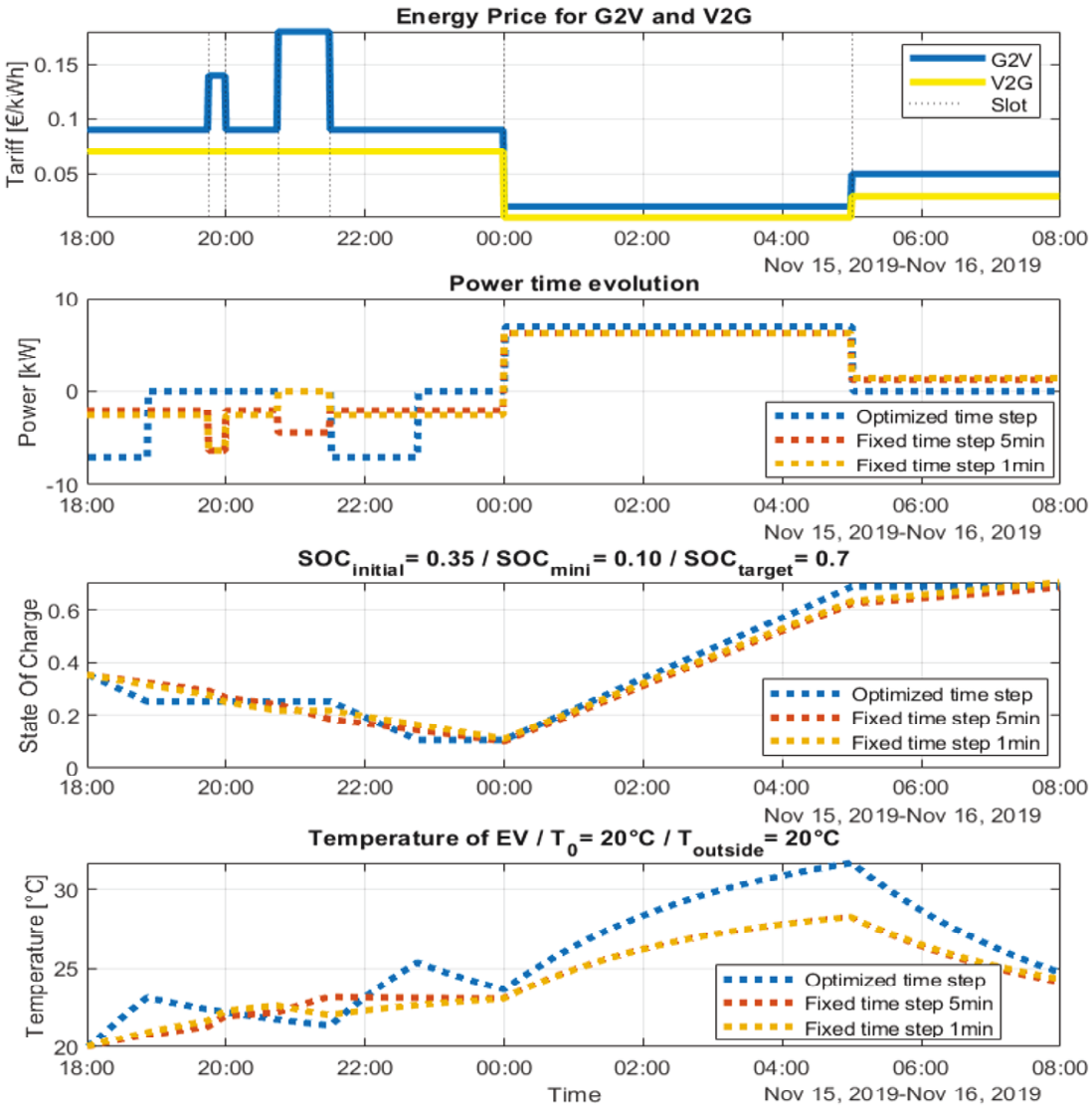

Figure 3.20 – The impact of an extra event on power scheduling power

optimized time step strategy and the inconvenient of the use of fixed time step, a scenario of two perturbations of 15 minutes and 45 minutes in G2V prices is used. For the fixed time step strategy, the time step should be adapted for each use case. For fixed time step strategy, the time step could be 15min or 5min or 1min. By decreasing the time step the execution time becomes greater and convergence to the optimal solution is more complicated. The main reason is the increasing of the number of decision variables from 84 for 10min to 168 for 5 minutes fixed time step and to 840 for 1 minute fixed time step. The number of constraints has been increased from 420 for 10min to 840 for 5 minutes fixed time step and to 4200 for 1 minute fixed time step. However, for the optimized time step strategy the number of constraints has been increased from 12 to 28 and the number of constraints from 21 to 49. Moreover, the execution time of the optimization problem increases as the size and complexity of the problem increases. For this case, it can be noted that the solving time is 72 seconds for 1 minute fixed time step, 2.4 seconds for the 5 minutes fixed time step, and 0.24 second for the optimized time step strategy. Furthermore, the charging profit is different for each power profile, it is estimated to 0.225€ for 1 minute fixed time step strategy, to 0.24€ for 5 minutes fixed time step strategy, 0.31€ for optimized time step strategy. To sum up, the optimized time step strategy ensures high speed

convergence to optimal solution and needs low computing capacity compared to fixed time step strategies.

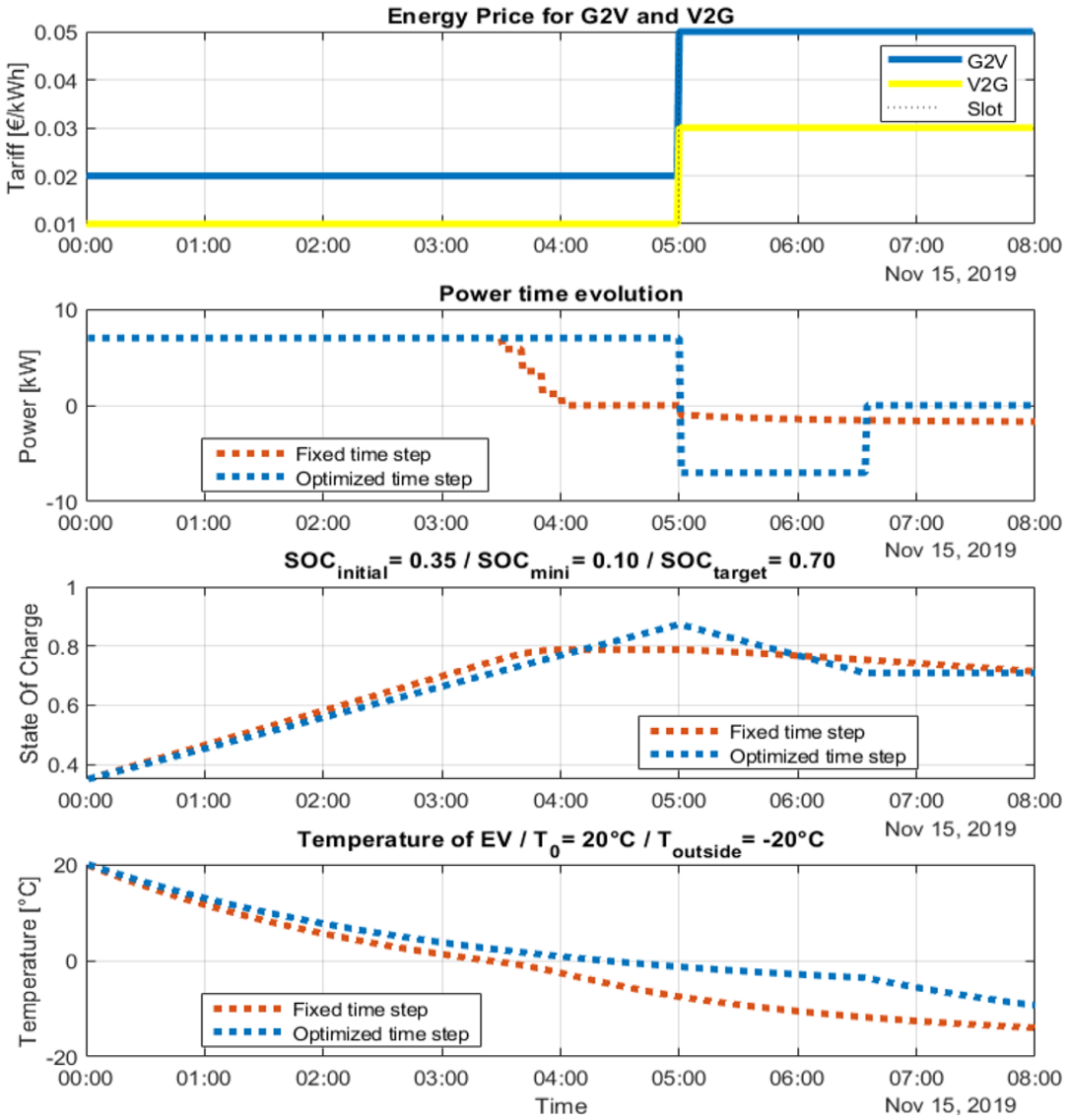

Figure 3.21 – Charging strategies comparison under $T_{out} = -20°C$.

For the second case presented in Figure 3.21, the charging is done under an outside temperature of $-20°C$. The comparison between the fixed time step strategy and optimized time step strategy shows the advantage of fixed time step to follow the temperature constraint. However, it highlights the fact that the constraint evaluating process in the scheduling process is done 48 times for the fixed time step against 2 times for the optimized time step. Thus, convergence to the optimal solution is 24 times faster with the optimized time step strategy. In the case of significant variations of system inputs (energy prices and maximum powers) and long planning period the most important thing is to find a sub optimal solution in the feasible area that satisfies the constraints as quickly as possible. Therefore, the proposed strategy with optimized time step performs perfectly this task.

By applying the two power profiles defined above to the battery model, the results show a slight error between the final SOC and the SOC target. Despite the consideration of temperature in the scheduling strategy, it remains important to note that the scheduling power profiles in Figure 3.21 are distinct from the effective charging power profile in Figure 3.22. Due to the rapid

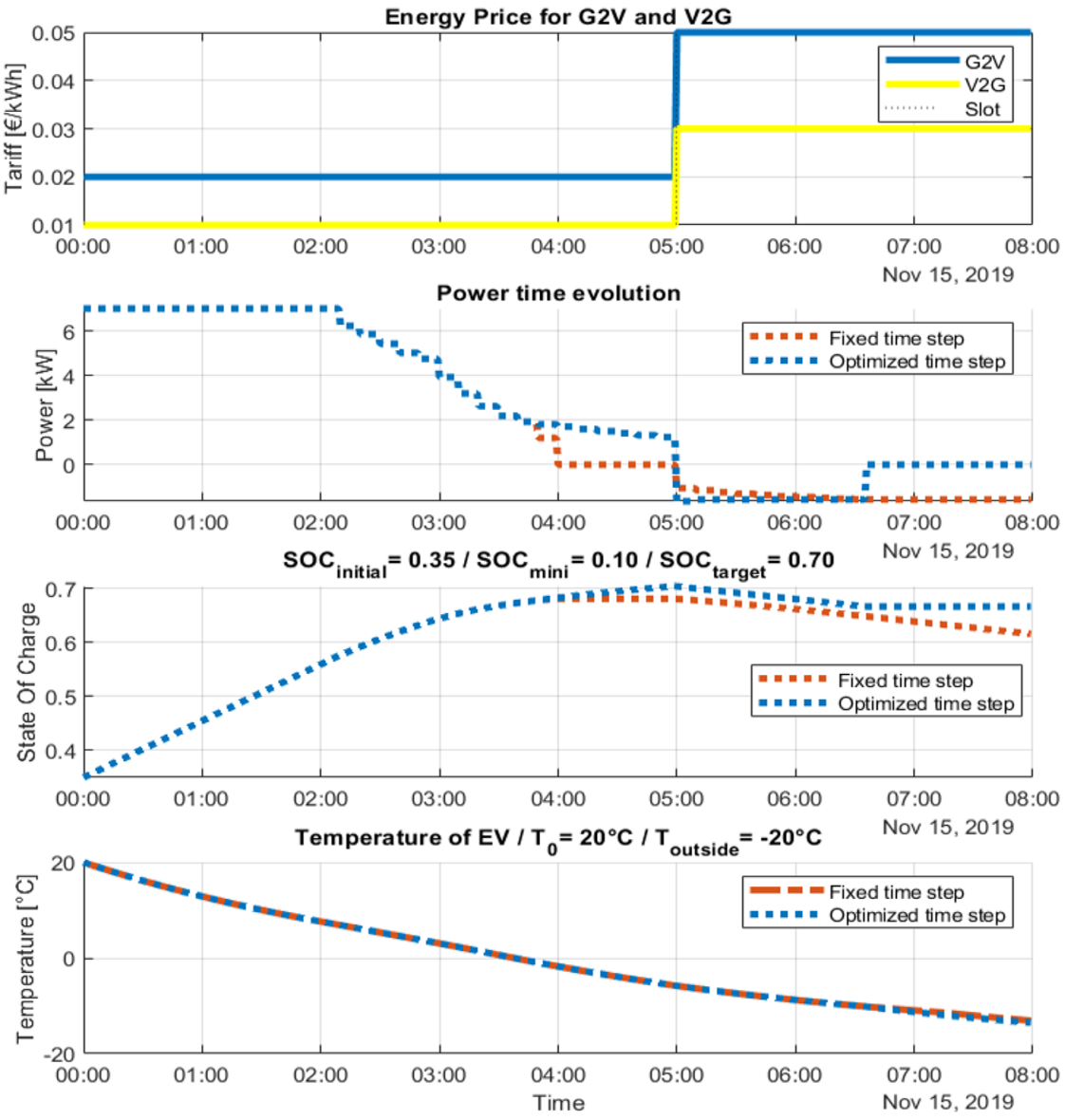

Figure 3.22 – The simulation of battery charging with the obtained scheduling power, $T_{out} = -20°C$.

decrease of the battery power acceptance caused by the fast drop of the battery temperatures, the power profile is limited by the battery power restriction given by the powermap updated every minute. It is possible to overestimate the energy requirement by 5% to 15% to overcome this problem in extreme temperature.

Moreover, the proposed algorithm with optimized time step has been tested on five daily energy prices profiles and the results were compared to classical algorithms with 10 minutes and 1 minute fixed time step. The comparison has been done on several levels such as the number of the decision variables, the number of constraints, the running time and the charging cost/profit. The results of the case study are presented in Table 3.2.

According to the results presented in Table 3.2, the algorithm with optimized time step performs the charging scheduling by using a minimal number of decision variables and the number of constraints. By subdividing the energy price profiles on optimal time slot the number of decision variables is minimized compared to the classical strategies with fixed time step. For an optimization window of 14 hours, the number of decision variables is 840, 84, for 1 minute

Table 3.2 – The result of the case study

Profile	Strategy	N^o Var	N^o const	Running time	Cost
1	1min	14x60	5x14x60	188	-0.47
	10min	14x6	5x14x6	2.7	-0.41
	Optimized	4x4	7x4	0.3	-0.41
2	1min	14x60	5x14x60	112	0.15
	10min	14x6	5x14x6	1.6	0.26
	Optimized	4x11	7x11	0.8	0.41
3	1min	14x60	5x14x60	187	-1.7
	10min	14x6	5x14x6	2.5	-1.69
	Optimized	4x14	7x14	1.4	-1.63
4	1min	14x60	5x14x60	138	-1.29
	10min	14x6	5x14x6	1.85	-1.23
	Optimized	4x5	7x5	0.37	-1.22
5	1min	14x60	5x14x60	167	0.92
	10min	—	—	—	—
	Optimized	4x16	7x16	0.40	1.89

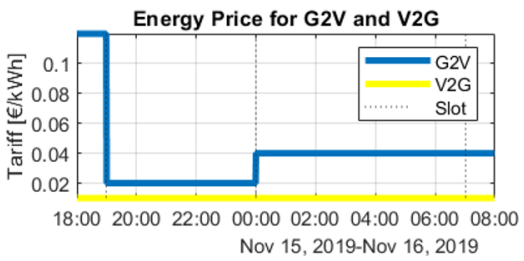

Profile 1

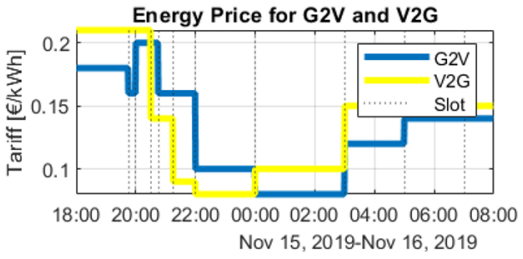

Profile 2

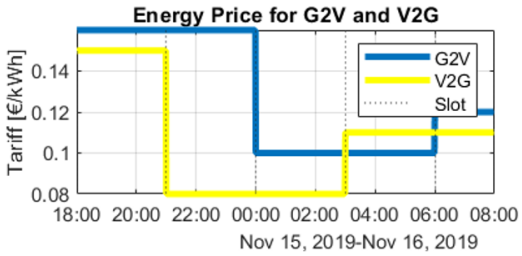

Profile 3

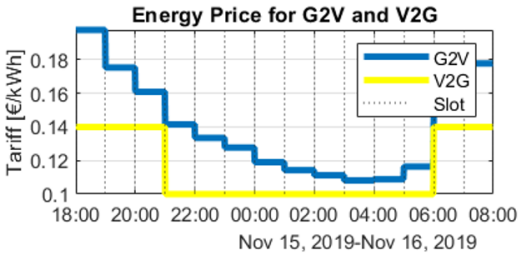

Profile 4

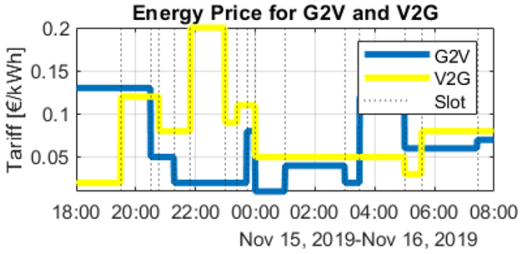

Profile 5

Figure 3.23 – The used energy price' profiles

and 10 minutes fixed time step respectively. Therefore, the executing time is very small for the proposed strategy with optimized time step compared to the strategies with fixed time step.

Moreover, the last column shows the charging cost (negative number) or the charging profit (positive number). The charging cost/profit value gives the information about the convergence to the optimal solution. According to Table 3.2, the strategy with optimized time step outperformed the charging compared to other strategies. In case of many variations in the energy price profile (profile 2 and 5) presented in Figure 3.23, the charging profit of the optimized time step strategy is almost double compared to the classical strategies with fixed time step. In conclusion, the optimized time step strategy converges to the optimal solution quickly and performs the charging cost minimization despite the many variations in the energy price profile.

3.5 Conclusion

This chapter presented two smart charging algorithms for EVs in a decentralized framework. The proposed strategies are based on the minimization of the charging cost and maximize the customer profit from customer perspective. The two scheduling strategies takes into consideration: the time of arrival and time departure of the EV, the TOU energy prices, the initial SOC, the final SOC desired by the customer, the power limitations by the grid, the charging station and the battery, the initial battery temperature and the outside air temperature.

The first smart charging strategy aim to schedule the EV charging while considering the V2G feature and the temperature. The proposed algorithm calculates the optimal scheduling power to reach the SOC target desired by the customer without neglecting the outside temperature and the battery temperature. The results show that with the use of the V2G feature, the EV's users can earn money by charging his EV, and supporting the grid, while respecting the SOC_{mini} limits, thus, extending battery lifetime. The right choice of SOC_{mini} limits the degradation of the battery and maximizes the economic profit offsetting the degradation of the battery caused by the high DOD as well as related to the charging.

Considering the poor performances of the lithium-ion batteries in cold weather, the estimation of the final SOC is more accurate and the charging power profile will be achievable by the Li-ion battery in such condition. Taking into account the outside temperature and the battery temperature specially in cold weather can make the night charging profitable for the EVs owners and ensuring the reaching of the desired final SOC before the morning departing time.

While the first strategy uses a constant sampling period, the second smart charging strategy considers a optimized dynamic time step. The proposed strategy can deal with small variations of the TOU energy prices (V2G and G2V) compared to others algorithms with fixed time step. The time to reach the global optimum is reduced by the second smart charging strategy due to the low number of decision variables compared to the first one with constant time step.

On one hand, the smart charging algorithm outperforms uncontrolled charging, achieves the desired SOC by the EV customer, and supports the grid with V2G feature. On the other hand, the smart charging algorithm performs charging at low temperatures and saves money regardless of weather conditions. The results show the effectiveness of the smart charging algorithm in high and low battery operating temperature. On the one hand, the V2G feature can reduce the charging bill for the EV users due to the remuneration of the discharging of the battery into the grid. On the other hand, the V2G operations can participate in the ageing of the Li-ion batteries and accelerate the need for the battery replacement before the manufacturer estimated replacement date. The V2G feature can provide an economic reward, which does not just compensate the battery degradation but can decrease the total cost of owning if the V2G energy prices are more attractive. To conclude, the decentralized charging strategies only require that each EV solves

its optimization problem locally, therefore, its deployment requires a low computing capacity compared to centralized algorithms that will be discussed in the next chapter.

4

Contribution to Electric Vehicle Fleet Charging Management

4.1 Introduction

The increasing of the penetration level of EVs in the grid will generate an additional load caused by the charging of the EVs. In addition to this, EV manufacturers are continuing to increase the capacity of the batteries of BEV to overcome the social fear of range anxiety. Moreover, the uncoordinated charging of EVs may cause many problems such as power transformer lifespan drop, power system losses and peak load increase [110].

The major constraint in public charging station is the limitation of transformer power in EV charging stations, where the installed power is generally 1.5 to 2 times greater than the nominal transformer power. For all these reasons, the charging station transformer power would be insufficient, thus the charging management can perform the EV fleet charging in real-time to avoid an important increment of grid investment.

Furthermore, the charging of EVs can help to improve the quality of power grid by participating in the ancillary services such as valley filling, reactive power compensation, voltage drop and frequency regulation. The fast dynamic of EV batteries and high power density of the lithium batteries and the massive integration of the V2G feature in the EVs' chargers will make the EVs a flexible connected energy storage system. Therefore, EVs can be suitable for frequency control. [111].

In order to keep the power grid in a proper functioning level, the coordination of EV charging is a major concern for the years to come. This chapter will presents the main contributions of this thesis from the side of the EV fleet charging management. The Section 4.2 presents the state of the art of the coordination of EVs' charging in the unidirectional mode and the bidirectional mode. The proposed coordinated charging strategy for a large number of EVs in unidirectional mode pased on a priority criterion is introduced in Section 4.3. In Section 4.4, a new bidirectional charging strategy with frequency regulation is proposed based on V2G technology with the consideration of a variable the charger efficiency.

4.2 State of the Art and Work Statement

The existing EV fleet charging management strategies is classified into two categories, centralized approaches and decentralized ones as presented in Section 3.2 of the Chapter 3. Moreover, the EV fleet charging management can be divided also into two types, namely time coordinated charging (TCC) and power coordinated charging (PCC) [112]. In TCC, the number of EVs allowed to charge at a given time is controlled to ensure that the total EV load demand is within the total power available for EV charging. The control of the charging power is done by a binary variable as shown in the Equation (4.1).

$$x_i^j = \begin{cases} 0, & \text{not charging} \\ 1, & \text{charging} \end{cases} \quad \text{and} \quad \sum_{j=1}^{N} x_i^j \cdot P^{EV} \leq P_{total} \tag{4.1}$$

where x_i^j is the binary control variable, P_{total} is the maximum available power, and P^{EV} is the rated power.

However, in PCC, the charging power of each EV is controlled to ensure that the total EV power demand is within the total power available for EV charging as presented in Equation (4.2).

$$P_{min} \leq P_i^j \leq P_{max} \quad \text{and} \quad \sum_{j=1}^{N} P_i^j \leq P_{total} \tag{4.2}$$

where P_i^j is the controlled charging power, and P_{min} and P_{max} are the maximum and minimum power, respectively.

The study [113] uses a centralized TCC approach to achieve several optimization objectives with different constraints considered. The charging strategy is based on an economic and a technical objective, namely minimization of total daily cost and minimization of peak-to-average ratio. The purpose of the study is to evaluate the impact of a high penetration level of EVs in distribution system and to propose an adapted smart charging strategy to the existing distribution infrastructure. In [114] a PCC strategy for EVs based on multi-objective optimization is presented. Through electricity price signal control and two-stage optimization, the adjustment of EV charging power is done. In decentralized strategies, each EV can update its charging rate according to the control signal transmitted by the utility grid. In [115], decentralized PCC strategies are performed to achieve valley-filling objective in the context of residential distribution network. The control problem is formulated as an optimization problem subjected to local constraints and strongly coupled linear inequality network constraints. A decentralized control scheme allows all EVs to update their charging rates in a parallel way and no communication network is needed among EVs.

In the one hand, various coordinated charging strategies, considering only unidirectional charging, have been proposed in the literature [23, 24, 89, 100, 116–121]. The unidirectional coordination charging G2V remains the first step towards a full V2G implementation because it requires no hardware other than the standard EV charging point. The unidirectional charging contributes to make EV a flexible load that can reduce uncertainty in power demand [91].

In the other hand, the EVs coordinated charging approaches is often based on scheduling or EV load shifting which can discourage EV users to use smart charging. In this type of strategies, the grid performance is considered as the priority and the customer's constraints are neglected, thus some EVs could be not fully charged or reach their requested SOC by the time of departure from the charging point [122]. Moreover, when the number of EVs is large and the computation time step has to be very small, the real-time optimization problem solving becomes too costly. What makes the iterative coordinated charging algorithm attractive and gives more flexibility to

quickly achieve EVs power coordination [123]. Another alternative to handle the topic of EV fleet power management is the use of priority criteria in iterative coordinated charging algorithm.

In [124], the EVs are classified into two categories low priority (LP) EVs and high priority EVs. Three classic priority criterion presented in the Equation (4.3) developed by [112]. The first one α^1 based only on the SOC of the EV, the second α^2 one based on slack time available for charging and the third one α^3 based on time/energy already allotted for the EV.

$$\begin{aligned} \alpha^1 &= 1 - \left(\frac{SOC}{100}\right) \\ \alpha^2 &= 1 - \left(\frac{N_{dep} - N_{req}}{N_{total}}\right) \\ \alpha^3 &= \quad 1 - \left(\frac{N_{com}}{N_{total}}\right) \end{aligned} \tag{4.3}$$

where N_{dep} is the number of half-hour time intervals from current time to departure time for the EV. N_{req} is the minimum number of half-hour time intervals required for charging the EV up to the desired SOC. N_{total} is the equivalent number of half-hour time intervals required for charging EV from initial to desired SOC. Slack time is the difference between the time available before departure and time required to complete charging. With higher the value of slack time, the feasibility of charging the EV to desired SOC is higher, thus the priority value will decrease with increase in slack time. N_{com} is the equivalent number of half-hour time intervals used for charging the EV.

In [118], the coordinated charging of a large scale of EVs in the framework of smart grid is carried out in order to fill the valley of the conventional power load curve. The proposed algorithm uses a dynamic charging priority factor expressed in the Equation (4.4).

$$Pri = \frac{E_n}{(Time_n \cdot \Delta t) \cdot P^n_{Max}} \tag{4.4}$$

E_n indicates the remaining electric energy needed to be charged for the n-th EV (in kilowatt-hours). $Time_n$ indicates the remaining time slots of the n-th EV connected to the grid. P^n_{Max} indicates the maximum operating power of the n-th charger (in kilowatts). Δt indicates the length of the time slot (in hour).

The California Institute of Technology (Caltech) has developed Adaptive Charging Network Simulator (ACN-Sim) [125], a data-driven, open-source simulator based on their experience building and operating real-world charging systems. ACN-Sim integrates with a larger ecosystem of research tools for EV charging, including ACN-Data [126], an open dataset of EV charging sessions to provide realistic simulation scenarios, and ACN-Live, a framework for field-testing charging algorithms.

Caltech regrouped a collection of open-source tools in the Adaptive Charging Network Research Portal (ACN-Portal) [127], to help researchers and other stakeholders understand the challenges of large-scale EV charging and develop practical solutions to those challenges.

ACN-Sim provides researchers who do not have access to real EV charging systems a realistic environment to evaluate their algorithms and test their assumptions. It also provides a common platform on which algorithms can be evaluated head-to-head, allowing researchers to better understand and articulate how their work fits into the existing literature.

ACN-Sim includes many common online charging algorithms which can be used as references benchmarks presented in [125]:

1. Uncontrolled Charging is the most common algorithm used in charging systems today. It allows each Electric Vehicle Supply Equipment (EVSE) to charge at its maximum allowable rate. This algorithm does not factor in infrastructure constraints.

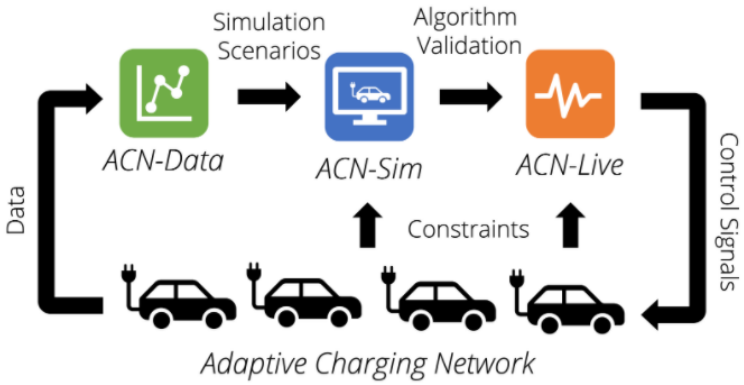

Figure 4.1 – The ACN Research Portal

2. Round Robin (RR) is a simple algorithm which attempts to equally share charging capacity among all active EVs. To do this, it first creates a queue of all active EVs then iterates over this queue. It first checks if it is feasible to increment the rate of the current EV by one unit. If it is, the rate is incremented and the EV is added back to the end of the queue. If not, the charging rate of the EV is fixed, and it is not returned to the queue. This continues until the queue of EVs is empty. In this context a feasible charging rate is one which does not cause to an infrastructure constraint to be violated and is less than the maximum charging rate of the EVSE.
3. Sorting Based Algorithms: There are three sorting based algorithms included in ACN-Sim: First-Come First-Served (FCFS), Earliest-Deadline First (EDF), and Least-Laxity First (LLF). Sorting based algorithms are commonly used in other deadline scheduling tasks such as job scheduling in servers due to their simplicity [128]. The first algorithm FCFS is an operating system scheduling algorithm that automatically executes queued requests and processes in order of their arrival. The second algorithm EDF is a dynamic priority scheduling algorithm used in real-time operating systems to place processes in a priority queue. Whenever a scheduling event occurs (task finishes, new task released, etc.) the queue will be searched for the process closest to its deadline. The third algorithm LST is a scheduling algorithm that assigns priority based on the slack time of a process. Slack time is the amount of time left after a job if the job was started now. These algorithms work by first sorting the active EVs by the given metric then processing them in order. Each EV is assigned its maximum feasible charging rate given that the assignments to all previous EVs are fixed. This process continues until all EVs have been processed.

The charging priority models defined above consider the remaining charging time, the remaining energy needed to reach the desired SOC and the maximum operating power of the charger. However, all presented priority criterion do not take into account the effect of temperature, the state of health of the Li-ion batteries *SOH*, and the charging efficiency. To overcome these issues, the contribution in Section 4.3 proposes a new priority criteria that take into account all neglected aspects.

One other promising solution for optimal integration of EVs into smart grids is the implementation of V2G technology for PHEVs and EVs. The objective of using V2G feature is the provision of energy and ancillary services to the power grid from EVs. Due to the Li-ion batteries power and energy density characteristics, Li-ion batteries fast response, and high battery capacities of EVs, several potential grid services can be provided by EVs [120, 129, 130] such as valley filling [131–134], peak load shaving [131, 135–137], voltage regulation [138, 139], reactive power

compensation [140–143], renewable energy support [144–147], spinning reserve [148–151], frequency regulation (primary control, secondary control, tertiary control) [6, 111, 119, 152–165]. The problem of EV charging with frequency regulation service has been addressed in several researches. [6, 154–157] deal with the problem of EV charging considering frequency regulation using the theory of control. Others such as [111, 158–162, 166] use the optimization approach to find the optimal charging power. Other methods have been used in [163–165] like the fuzzy logic, deep reinforcement learning, and priority model.

To address the problem of EV charging with frequency regulation, there are several considerations to take into account. The objective of maintaining the operational capacity limit within the optimal region - where regulation up power is maximal and regulation down power is maximal - is considered in [160, 162], whereas [159, 161] did not take into account this problem. Moreover, [160, 161] consider a constant value of regulation up power and regulation down power of the EV. Therefore, these papers ignore the dependence of the capacity of regulation up and down on the battery's SOC. Furthermore, the consideration of EV owners expectation is a big challenge in this topic. In [159, 160, 162, 167], the EV's users satisfaction has been considered, whereas this point has been totally ignored in [7], [168]. Ignoring this aspect could discourage the EV's owners to participate in ancillary services. Many studies have also focused on investigating the benefits and challenges involved in implementing V2G technology. In Many studies consider a high number of EVs participating in the ancillary services. In [160], the study has been conducted under a large number of EVs equal to 100000, [111] assumes the use of 1000 EVs in the simulation and [6] sets the total number of EVs participation in the simulation of the frequency regulation algorithm to 500. This paper focuses on studying the possibility of offering a frequency regulation services with a low number of EVs. Therefore, in all simulations the maximum number of EVs is 20. Moreover, [160], [162], use a symmetrical assigned perturbation signal, that simplify the problem of the SOC target's achievement and the problem of maintaining regulation's capacity. Furthermore, [6] and [160] consider an equally likely distribution of the number of EVs in each SOC category (low, medium, and high).

Most of the research that uses the optimization approach [160], [162], puts a hard strict equality constraint in their optimization models. Equalities are more difficult to satisfies and not compatible with all solvers. One modeling trick consists in reformulating each equality as two inequalities. This increases the number of inequality constraints and therefore the size of the problem [169]. Accordingly, the proposed optimization model will only use the inequality constraints.

With the control theory, the perturbation is divided between the EVs in an equal way. In case of a small disturbance and a high number of controlled EVs, each EV will participate with small power variations in frequency regulation to maintain the SOC without considering the poor efficiency of the charger in low power regions. However, according to [7], the charger is designed to operate more efficiently closer to the maximum power values. In the same context, [159] and [7] study the effect of the charger's efficiency on the accuracy tracking of the perturbation signal, and assume that without considering the dependence of charger's efficiency on power the tracking error increases.

To the best of our knowledge, none of the existing works take into account the dependence of the charger's efficiency on power. Almost all researches consider a constant charger's efficiency in the range $[0.8, 1]$. Some of them do not use a discharging efficiency or use a perfect charger with unit efficiency.

When managing the EV charging, the energy available provides information on the accumulation of charging power for the EV. So, the energy gives a kind of future possibilities of the power's use, such as the maximum charging and discharging rates and the energy remaining to reach full capacity or full discharge. However, power cannot convey long term knowledge

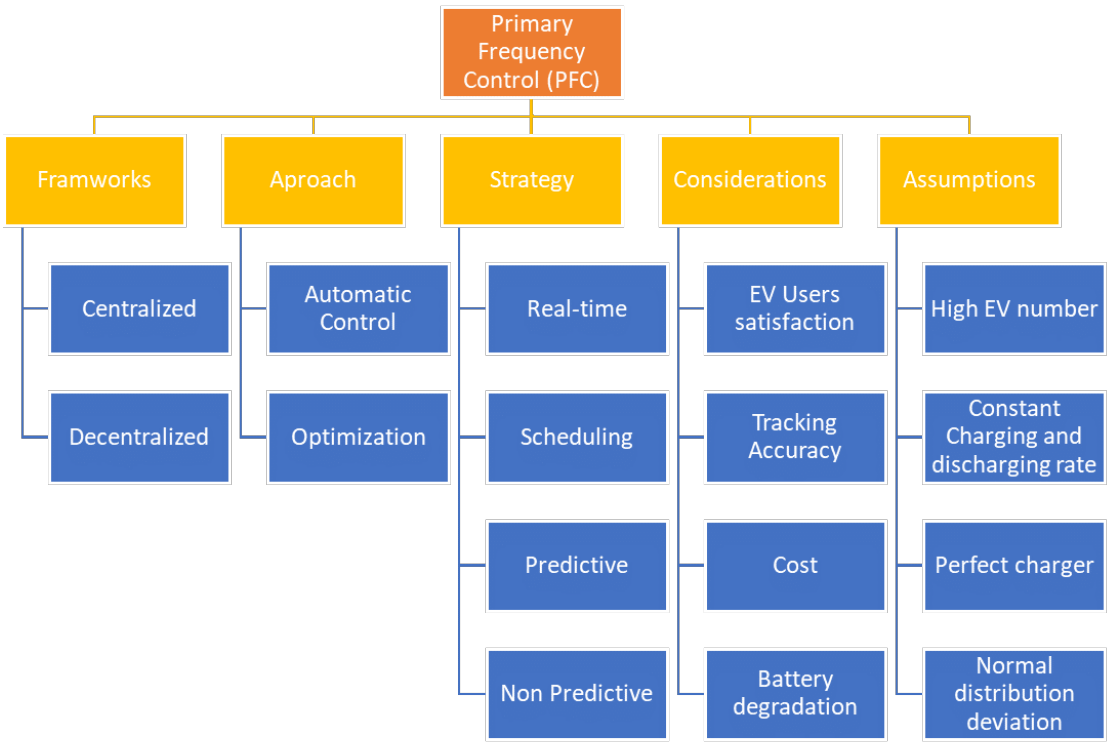

Figure 4.2 – The review of frequency regulation strategies in EV fleet charging management

about the state of the EV or its history, but it gives a short term information. Combining two heterogeneous physical quantities such as the energy and the power in the same objective function, gives a global vision on the charging management of an EV fleet both on the long term and on the short term, in the past, in the present and in the future. The proposed bidirectional charging strategy presented in Section 4.4 allows to solve a scheduling optimization problem as an instantaneous problem. Thus, the scheduling problem whose resolution is heavy in computing time and memory consumption will be replaced by an instantaneous dispatch problem whose resolution is simple and fast. The added value in this model allows us to reduce the execution time, thus to deal with real-time problems such as frequency regulation for coordinated EV charging and to reduce the time step as small as the desired precision.

4.3 Centralized Electric Vehicle Fleet Unidirectional Charging Coordination Algorithm

This contribution focuses on centralized unidirectional charging strategy, in which EV charging point operator (CPO) is able to control the EV charging directly. Most of the mathematical models are nonlinear programming for the centralized charging strategies in pervious literatures. Their computational complexities will growth nonlinearly. It means that they have to spend quite a long time if the input variables become large. However, it should be pointed out that the calculating time is a key factor to schedule the charging strategy for large scale EVs [22] or get real time solutions [31]. Therefore, it is worthwhile to put forward a new algorithm whose computational complexity is near-linear. The contributions corresponds to the content of my second conference paper [167] presented in the section 5, the proposed strategy are highlighted as follows:

— A centralized charging control algorithm of a large number of EVs is proposed based on EV priority considering both EV users' satisfaction and grid power constraints.
— The proposed priority model considers several factors such as the EV initial SOC, the EV user desired final SOC, the capacity the EV battery, the arrival time of the EV user and the departure time of the EV user.
— The proposed strategy takes into consideration transformer maximal power, charging system limitation, and the effect of temperature on the LiBs using a thermal LiBs model in conjunction with a battery powermap.
— An analytical study is presented to assess the maximum possible number of EVs that can be integrated into the grid without any reinforcement of the charging infrastructure.

In this study, the focus of study are commercial EV charging parks where the charging station is highly solicited and has limited power at the transformer. The purpose of this study is to evaluate the maximum number of EVs that can be integrated into the distribution grid without any reinforcement of the charging infrastructure (upgrading the transformer power). Therefore, it is assumed to have unlimited charging points for all EVs but a limited total power at the transformer. EVs can be parked daily during working hours. All EVs parked at a commercial charging area are assumed to be taken in charge by a CPO or aggregator which implements the proposed coordinated charging control strategy to charge the EVs. Figure 4.3 displays a diagram of the system composed of the parking spot associated to a charging point connected to the same transformer and managed by the aggregator.

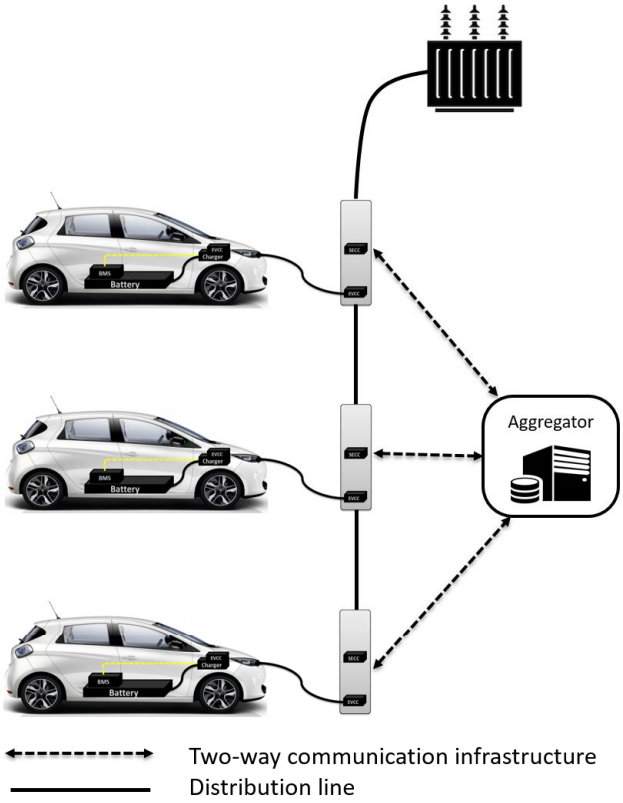

Figure 4.3 – Charging system overview

When an EV arrives at the car park, the charging point directly collects all required information such as the initial SOC, battery capacity, the SOH of the LiB, the maximum power available at the charging point, the arrival time and the outside temperature. Then, the EV owner submits the desired final SOC and the departure time. Based on the collected information, the aggregator

calculates the priority of the EVs and performs the coordinated charging control. The above tasks are achieved at each time step by the aggregator, so that incoming EVs are included to the algorithm in the next time step. It is crucial to keep in mind that the EV owner is responsible for the submitted information and it is possible to modify the departure time and the desired SOC at any time through the EV owner's connected phone app. In some cases, it is possible to have unfeasible scenarios for which the final desired SOC can not be reached because of the high value of the desired SOC or the short duration of EV plug-in time at the charging station or the low power of the charging point. These scenarios are expressed by a priority factor higher than 1. Unfeasible cases have an impact on the effectiveness of the coordinated charging control algorithm, but in anyway, all charging algorithms will be affected and cannot perform this unfeasible charging task

4.3.1 The proposed Priority Criterion and the Coordinated Charging Approach

The proposed charging strategy is focused on charging coordination of a large EV fleet with a limited total power of the charging station without neglecting the EV owners satisfaction. EV user satisfaction can be characterized by reaching the final SOC before departure time. In order to achieve this goal, a priority model is proposed to evaluate the energy requirement of each EV. For example, if an EV has a low initial SOC coupled with a high final SOC requested and a short period of time to complete the task, then the EV will get a higher charging priority and it should take the utmost charging point power available. Therefore, the priority factor is expressed as shown in Equation (4.5):

$$prio_i^j = \frac{(SOC_{target}^j - SOC_i^j) \cdot E_{batt}^j \cdot SOH^j}{P_{max}^j \cdot (t_{departure}^j - t_{arrival}^j) \cdot \eta \cdot \alpha(T_{out})} \tag{4.5}$$

where SOC_i^j is the SOC of the j-th EV during the time step i, SOC_{target}^j is the desired SOC value by the j-th EV at the departure time, E_{batt}^j is the initial battery capacity in kWh of the j-th EV, SOH^j is the SOH of the LiBs of the j-th EV, P_{max}^j is the maximum power allowed by the charging point of the j-th EV in kW, $t_{departure}^j$ is the departure time of the j-th EV in hour (h), $t_{arrival}^j$ is the arrival time of the j-th EV in h, η is the charger efficiency, and α as the LiBs temperature effect factor defined in Figure 4.4 with $\alpha(-40°C) = 0.02$.

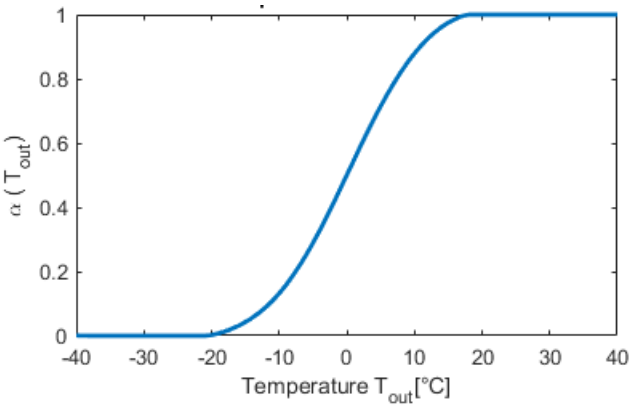

Figure 4.4 – Temperature effect factor of LiBs

In very cold weather $T_{out} < -20°C$, the internal resistance of the LiBs increases significantly, so most of the charging power is dissipated as heat to warm the battery. As the temperature rises

$T_{out} \in]-20,20[^{\circ}C$, the internal resistance of the LiBs decreases, so the impact of the outside temperature decreases. When the outdoor temperature exceeds $20^{\circ}C$, the internal resistance becomes stable at its lowest nominal value, so the effect of the outdoor temperature is eliminated. To sum up, the temperature effect factor α affects the charging time, since α appears in the denominator of the Equation (4.9).

The priority criterion is a non-dimensional factor, that can be calculated using collected information to: sort EVs based on their priority and to determine the feasibility of charging. To decide on the charging power for each EV in a rational way, it is necessary to find an appropriate approach to sort EVs from the highest to the lowest priority. The charging priority of an EV at the charging point will be affected by several factors:

— Energy requirement: The energy that the customer wishes to acquire during his stay at the charging station. This is the difference between the desired SOC and the initial SOC, times the real battery capacity.

— The real battery capacity: LiBs capacity varies from one EV to another depending on the initial capacity and battery ageing condition

— Available charging time which is the time the user wishes to spend at the station.

— The temperature effect: The power acceptance of LiBs decreases in cold temperature and affects the charging speed.

— The maximum power of the charging point: The power available at the charging point is not the same at any charging point. We consider fast, normal and slow charging points, where the power available will affect the charging speed.

Some examples of charging scenarios could clarify the purpose and utility of the priority factor. If an EV owner arrives with an EV of $60kWh$ LiB battery capacity at $08h00$ with an initial SOC of 30% and wants to leave the charging station at $12h00$ with 80% of SOC using a power of $7kW$, then the calculation of the priority factor is presented in the Equation(4.6):

$$prio_0^1 = \frac{(0.8-0.3)\cdot 60\cdot 1}{7\cdot(12-8)\cdot 0.8\cdot 1} = 1.34 \tag{4.6}$$

With a priority value of 1.34 the desired SOC cannot be achieved before the departure time due to the low charging speed of the charging point. Any other charging algorithm can not accomplish this charging tasks. Whereas, if the EV owner had chosen a charging point with higher charging speed such as $P_{max}^1 = 22kW$ the EV would have reached the desired SOC of 0.8 before the departure time as explained in the Equation (4.7) and the Equation (4.8).

$$prio_0^1 = \frac{(0.8-0.3)\cdot 60\cdot 1}{22\cdot(12-8)\cdot 0.8\cdot 1} = 0.43 \tag{4.7}$$

$$\begin{cases} \text{if } prio_j^i \leq 0 & \Rightarrow SOC_{target}^j \text{ has been reached} \\ \text{if } prio_j^i \in]0,1] & \Rightarrow SOC_{target}^j \text{ will be reached} \\ \text{if } prio_j^i > 1 & \Rightarrow SOC_{target}^j \text{ can not be reached} \end{cases} \tag{4.8}$$

To summarize, there is a twofold benefit from the priority factor. The first is to make it possible to compare EVs and distinguish which EV needs the most power at a given moment to complete its energy requirement. The higher the "Prio" factor of an EV, the higher charging power. The second benefit, is the information given by the obtained value, which indicates the feasibility of the charging where a priority factor greater than 1 means that the EV will not be able to reach the desired SOC within the time window provided. Either because of a high energy demand, a low charging speed of the charging point or a low availability at the charging station.

4.3.2 Charging Constraints

This section describes the physical aspects limiting the charging power that shall be taken into consideration by the coordinated charging control algorithm.

The powermap function determines the power that the battery can accept depending on the SOC and battery temperature overtime. This behavior is recorded in the powermap of each battery model (see Figure 4.5). This 3D surface defines, for a given SOC and a given temperature, the maximum power that the battery can accept.

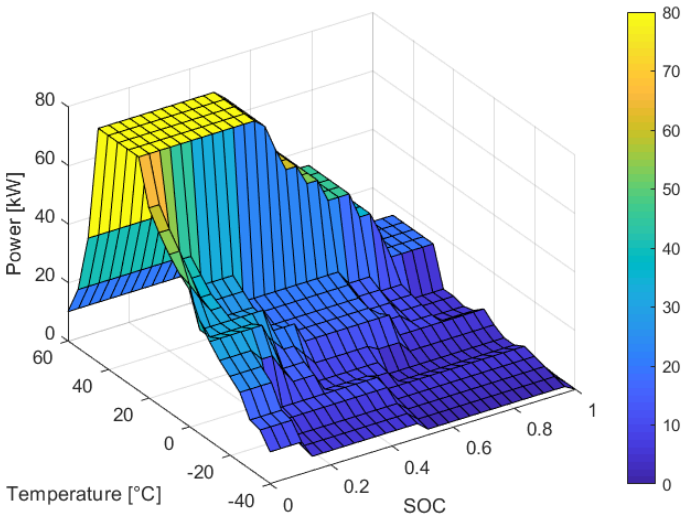

Figure 4.5 – Lithium-ion battery power map

The maximum charging point power depends on the selected charging mode. A charging mode refers to the power level that rates a charger and its connectors. Several charging modes can be used, mode 1 as the slowest, mode 2 is an upgraded version of mode 1, in the middle, mode 3 with a power level between 11kW and 55kW and mode 4 a super charging mode with 400V DC or higher as the fastest. Using the information of the power level of the charging point given in Table 4.1, the charging time can be calculated using the Equation (4.9):

$$t_{charg\_time} = \frac{(SOC^j_{target} - SOC^j_i) \cdot E^j_{batt} \cdot SOH^j}{P^j_{max} \cdot \eta \cdot \alpha(T_{out})} \tag{4.9}$$

If the priority factor has already been calculated, the charging time can be easily deduced from the Equation (4.10):

$$t_{charg\_time} = prio^j_i \cdot (t^j_{departure} - t^j_{arrival}) \tag{4.10}$$

Table 4.1 – Charging modes of supply equipment [8], [9]

Mode	Power	Power supply	Voltage	Max. current
Mode 1	3.7 kW	Single phase	230 V AC	16 A
Mode 2	7.4 kW	Single phase	230 V AC	32 A
Mode 3	11 kW	Three phase	400 V AC	16 A
Mode 3	22 kW	Three phase	400 V AC	32 A
Mode 3	43 kW	Three phase	400 V AC	63 A
Mode 4	160 kW	Direct current	400 V DC	400 A

The coordinated charging power can be calculated by dispatching the maximum transformer's power for the whole EV fleet according to priority level. Once the priority factor of the EVs have been evaluated according to their energy needs, the aim is to distribute the power in an optimized way. The priority factor serves to intelligently distribute the power available. The weighting factor is calculated as shown in the Equation (4.11):

$$w_i^j = \frac{prio_i^j}{\sum_{j=1}^{N_i} prio_i^j} \qquad \forall i \forall j \tag{4.11}$$

where N_i is the number of available EVs in the charging station in the time step i.

The coordinated charging power can be expressed as shown in the Equation (4.12):

$$P^j_{coordinated,i} = w_i^j \times S_i^j \times P_0 \qquad \forall i \forall j \tag{4.12}$$

where $P^j_{coordinated,i}$ is the calculated power based on priority factor of the j-th EV during the time step i, S_i^j is the charging status of the j-th EV during the time step i, and P_0 is the maximum transformer power.

The charging status of EVs can be described as presented in Equation (4.13):

$$S_i^j = \begin{cases} 0, & \text{idle} \\ 1, & \text{charging} \end{cases} \tag{4.13}$$

The idle status, has three different interpretations: the charging has been successfully completed, the departure time has been reached and the EV has not yet been unplugged.

The power withdrawn from the grid is calculated by finding the minimum of power in Equation (4.14):

$$P_i^j = min(P^j_{max}, P^j_{coordinated,i}, P^j_{maxBattery,i}) \tag{4.14}$$

where P^j_{max} is the maximum power allowed by the charging point of the j-th EV, $P^j_{maxBattery,i}$ is the battery maximum power from the powermap of the j-th EV during the time step i.

Depending on the element of the system that is limiting the maximum power (the charging point, the coordinated charging or the battery constraints), the power absorbed by the battery can take different values.

Depending the number of available EVs required to charge at the parking spaces, the total power distributed for all EVs could be less than the maximum power of the transformer as a result, top priority EVs can take advantage of this remaining power to match their requirement.

In algorithm 2, x_i^j is defined as follows:

$$x_i^j = \begin{cases} 0, & \text{if } P_i^j \neq P^j_{max} \\ 1, & \text{if } P_i^j = P^j_{max} \end{cases} \tag{4.15}$$

4.3.3 Battery monitoring

The dynamic monitoring of the battery SOC is given by the Equation (4.16):

$$SOC^j_{i+1} = SOC^j_i + \frac{\eta P_i^j \cdot \Delta t}{E^j_{batt} \cdot SOH^j} \tag{4.16}$$

where SOC_i^j is the SOC of the j-th EV during the time step i, SOC^j_{i+1} is the SOC of the j-th EV during the time step $i+1$, P_i^j is the charging power of the j-th EV at the time i in kWh, η is the

Algorithm 2 Distributing the remaining power

if $\sum_{j=1}^{N} S_i^j P_{max}^j > P_0$ **then**
  $P_0^{'} \leftarrow P_0$
else
  $P_0^{'} \leftarrow \sum_{j=1}^{N} S_i^j P_{max}^j$
end if
$P_{used} \leftarrow 0$
while $P_{used} \neq P_0^{'}$ **do**
  $P_{available} \leftarrow P_0^{'} - \sum_{j=1}^{N} x_i^j P_i^j$
  $W_i^j \leftarrow x_i^j \cdot prio_i^j$
  $W_i^j \leftarrow \frac{W_i^j}{\sum_{j=1}^{N} W_i^j}$
  $P_{new,i}^j \leftarrow min(P_{max}^j, w_i^j \cdot P_{available}, P_{maxBattery,i}^j)$
  $P_{used} \leftarrow \sum_{j=1}^{N} P_{new,i}^j$
end while

charger efficiency, Δt is the time step in h, E_{batt}^j is the initial battery capacity in kWh of the j-th EV, SOH^j is the SOH of the LiB of the j-th EV.

For simplification purposes, this works considers an evenly distributed joule heat generation, and a temperature of the battery cell uniformly distributed. Thus, the temperature estimation is a first order model expressed as shown in Equation (3.17).

The temperature first model is linearized for each time step to get the expression given by the Equation (4.17):

$$T_{i+1}^j = T_i^j + \frac{\Delta t}{m^j C_p^j}(P_{joule,i}^j + P_{convective,i}^j) \tag{4.17}$$

where m^j is the mass of the j-th EV battery, C_p^j is the specific heat coefficient of the j-th EV battery, T_i^j is the temperature of the j-th EV battery at the time i, T_{i+1}^j is the temperature of the j-th EV battery in the next time step $i+1$, $P_{joule,i}^j$ is the power dissipated by joule effect of the j-th EV battery in the time step i, $P_{convective,i}^j$ is the power heat transfer between the battery and the outside.

The joule power is formulated in Equation (4.18) as a linear model in terms of charging and discharging power:

$$P_{joule,i}^j = k^j \times P_i^j \quad \forall i, \forall j \tag{4.18}$$

where k^j is a thermal factor depending on the thermal inertia of the j-th EV battery.

The convective power is modeled by the Newton law showed in Equation (4.19):

$$P_{convective,i}^j = -\frac{T_i^j - T_{out}}{R_v^j} \qquad i = 1, ..., N \tag{4.19}$$

where T_{out} is the outside temperature and R_v^j is the heat convection coefficient transfer between the j-th EV battery and the outside.

4.3.4 Control flow of coordinated charging strategy

The problem of coordinated charging is a real-time control algorithm, working during opening hours of a commercial area. The algorithm aims to fulfill the stability requirement of distribution

power system infrastructure by respecting maximum power limit of the transformer. Moreover, the algorithm tries to respect the EV users' satisfaction as much as possible, interpreted by respecting the final desired SOC before the departure time. The algorithm stops if all EVs are charged or there is no EV in the commercial charging car park.

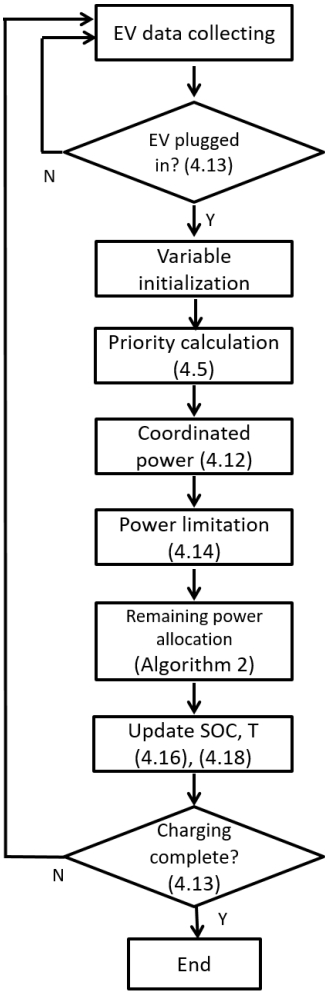

Figure 4.6 – Coordinated charging flowchart

When an EV is plugged to a charging point, it will be detected immediately and added to the EV charging pile. Considering the ISO 15118 standard, the system will automatically get the EV information through the communication infrastructure between the charging points and the aggregator. However, two requests remain to be submitted by the EV owner: the final desired SOC and the departure time.

If the EV is connected to the charging point, it must participate in the subscribed coordinated charging system. The algorithm would calculate the best charging power scheme, and carry out the charging to reach the EV energy requirement in the remaining time. The EV will start the charging immediately, then at each time step the system checks if there is another EVs access to update the power distribution for the whole fleet.

The flowchart illustrated in Figure 4.6 shows the most important computational steps of the algorithm with the above equations.

4.3.5 Simulations results

The EV charging coordination considers a time lapse of 24 hours divided in 96 time steps of 15 minutes each. The time of arrival and time of departure of the EVs are assumed to be generated by a random function following a Poisson distribution as shown in Figure 4.7. The maximum power of the charging point is selected randomly from the values of the vector $[3.2, 7.4, 11, 22, 43]$ kW. The charging points in the charging station have the following ratios: [30%, 25%, 20%, 15%, 10%] respectively.

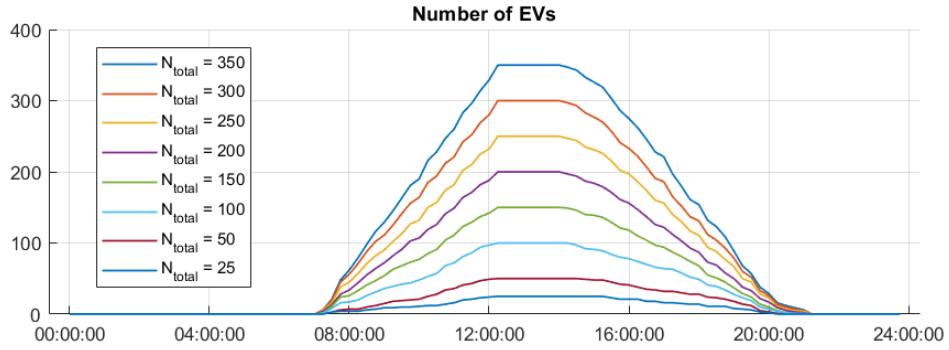

Figure 4.7 – Number of EVs plugged-in per hour

Figure 4.8 shows the charging profile of the 9-th EV using the proposed method with 350 EVs per day and a transformer's power of $300kW$. It is also observed from Figure 4.8 that the EV reached the desired SOC of 0.86 before its departure time with a maximum power allowed by the charging point of $7.4kW$. When compared to the uncoordinated or the uncontrolled charging strategy, the 9-th EV did not reach the desired SOC. As the number of EVs plugged-in at the charging station decreases, the EV receives more charging power to reach the requested SOC before 8 p.m.

In Figure 4.9, it can be observed that the transformer of the charging station is fully loaded from 8 a.m to 8 p.m because of the high number of EVs in the charging station. The EVs start leaving the charging station at 8 p.m, therefore, the transformer load decreases.

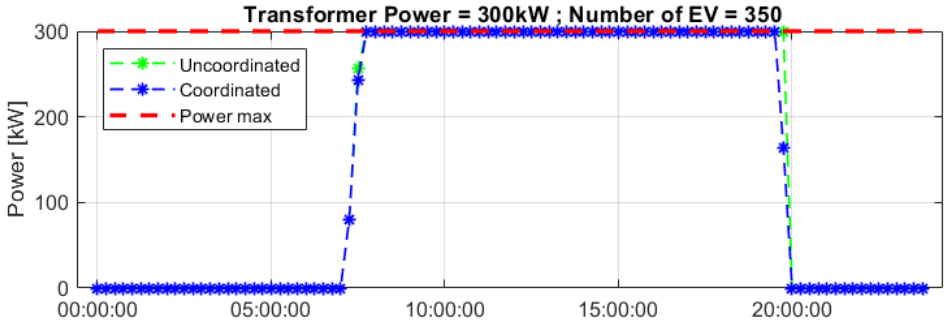

Figure 4.9 – Charging total power

To evaluate the efficiency of the proposed approach to accomplish the charging of the EVs, a quantitative study is done to evaluate the maximum number of EVs that can be supported by the charging station. Considering EV users satisfaction as an important aspect, an EV users satisfaction level indicator is suggested in the Equation (4.20):

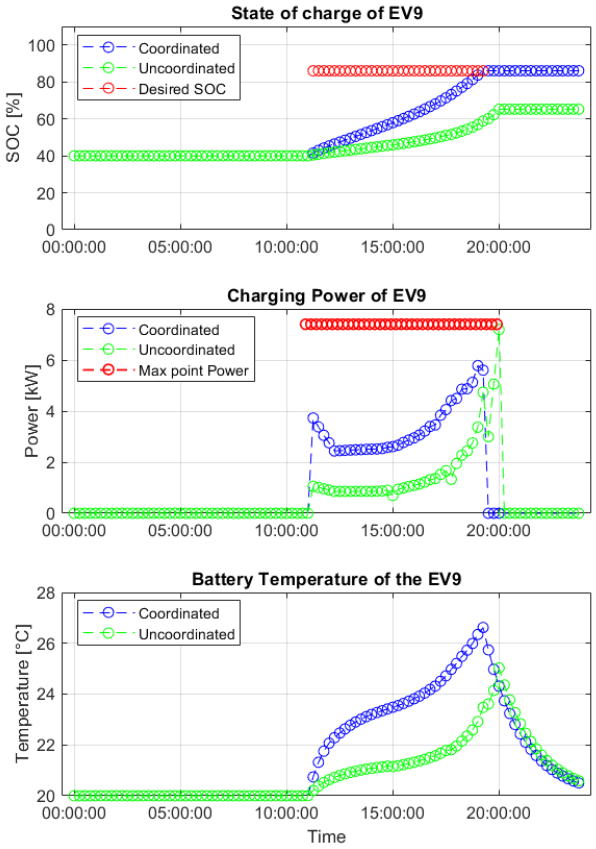

Figure 4.8 – 9-th EV charging profile

$$S_{level} = \frac{SOC_{final} - SOC_{initial}}{SOC_{target} - SOC_{initial}} \tag{4.20}$$

if $SOC_{final} > SOC_{target}$ then $S_{level} = 1$, where the SOC_{final} is the value effectively reached at the end of charging.

The average EV users satisfaction for the total EV number per day $S_{average}$ is expressed in the Equation (4.21):

$$S_{average} = \sum_{j=1}^{N_{total}} S_{level}^{j} \times \frac{N^{j}}{N_{total}} \tag{4.21}$$

where S_{level}^{j} is the mean value of each S_{level} interval $S_{level}^{j} = [0.05, 0.15, ..., 0.85, 0.95]$, N^{j} is the obtained value of each S_{level}^{j} interval, and N_{total} is the total EVs treated per day.

Table 4.2 – The EV satisfaction level

	Total EVs treated per day N_{total}															
	350		300		250		200		150		100		50		25	
S_{level}	Coo	Unc	Coo	Unc	Coo	Unc	Coo	Unc	Coo	Unc	Coo	Unc	Coo	Unc	Coo	Unc
[0,0.1]	9	10	7	13	4	5	3	4	2	3	1	1	1	1	1	1
]0.1,0.2]	25	28	14	22	7	8	0	7	0	3	0	1	0	0	0	0
]0.2,0.3]	27	46	9	27	4	13	1	8	0	4	0	0	0	0	0	0
]0.3,0.4]	31	36	24	27	2	20	0	6	0	1	0	1	0	0	0	0
]0.4,0.5]	17	29	19	25	9	19	4	13	0	2	0	0	0	0	0	0
]0.5,0.6]	25	16	9	18	15	11	2	12	1	6	0	0	0	0	0	0
]0.6,0.7]	16	23	23	10	9	20	7	8	1	5	0	0	0	0	0	0
]0.7,0.8]	45	11	25	19	6	8	2	6	0	2	0	0	0	0	0	0
]0.8,0.9]	35	9	48	13	29	5	4	9	0	4	0	0	0	0	0	0
]0.9,1]	120	142	122	126	165	141	177	127	146	120	99	97	49	49	24	24
S_{level} [%]	66.0	61.8	72.3	64.3	82.8	73.4	90.5	77.9	93.3	85.5	94.1	92.7	93.2	93.2	91.4	91.4
Diff. [%]	4.2		8.1		9.4		12.6		7.8		1.4		0.0		0.0	

Table 4.2 compares the results obtained with the coordinated (Coo) and uncoordinated (Unc) strategies. It summarizes the number of EVs for each satisfaction interval using a maximal transformer power of $300kW$. Table 4.2 clearly indicates that the average satisfaction level decreases when the number of total EVs increases. However, despite the increase in the number of EVs, the average satisfaction remains acceptable with a mean value of 85.5%. The proposed strategy performs the charging of EVs with a good efficiency compared to the uncontrolled charging method with an average improvement of 5.4 %.

At a low number of EVs, the transformer power remains sufficiently large, therefore the satisfaction level is high and it is the same for both two strategies. However, when the number of coordinated EVs per day hits the 200 mark for $300kW$ of transformer power, the satisfaction level of the coordinated charging is excellent compared to the uncoordinated charging.

Exceeding 300 EVs, there are less EVs in $[0.9, 1]$ S_{level} range for Coo compared to Unc. The Coo strategy aims to improve $S_{average}$ by sacrificing by those EVs that have almost reached their SOC_{target} to charge the lowest priority EVs before the departing time.

In the end, in order to guarantee a level of satisfaction higher than 80%, the number of EVs treated per day should not exceed an average of 250 for a transformer power of 300kW.

4.4 Centralized Electric Vehicle Fleet Bidirectional Charging Algorithm with Frequency Regulation Service

As the EV penetration level grows and the battery capacity of EVs increases, the charging station becomes a very big energy storage system. EVs are capable to deliver immediate power through V2G feature and to adjust the charging power level in G2V mode. Thus, EVs are able to offer ancillary services such as frequency regulation. EV batteries are different from conventional energy storage systems in the sense that the EV owners energy requirement constraint should be respected while their vehicles even participate in the frequency control. To address this problem, an optimization problem has been defined considering both EV owner's satisfaction and frequency regulation performances. The idea of the proposed contribution is to keep the total available energy stored in EVs in an optimal moving region in which EVs keep maximal regulation up capacity and regulation down capacity. Moreover, the EVs charging power will be maintained above a certain threshold to keep charging highest priority EVs. The problem is expressed as a multi-objective optimization with time depending references. This section presents a bidirectional energy management strategy for frequency regulation, describes a concept of optimal time depending SOC for EV charging requests, and considers the EV charger' efficiency dependence on power.

This contribution is an extension of the previous work presented in Section 4.3, which has been significantly improved to take into consideration the bidirectional charging and the charger efficiency dependence on power. It corresponds to the content of my second article presented in the section 5. The contributions of the proposed strategy are highlighted by:

— Maximization of the regulation reserve using an EV charging algorithm based on preventive actions by replacing a scheduling problem by one on the fly.

— Avoiding the use of hard constraints, decreasing the number of decision variables and the number of constraints to reduce the computation time and memory use.

— Taking into account the charger's efficiency and its dependence on power and therefore maximizing the charging efficiency.

— Considering the dependence of the regulation capacity on the SOC and temperature and maintaining the total regulation capacity in the optimal zone.

— Controlling the bidirectional EV charging (V2G) considering both the grid operator's power demand and the satisfaction of the EV's users SOC target.

4.4.1 Optimization Problem Modeling

The problem of EV charging dispatch is divided into two sub-problems:

— (P1) Without frequency disturbance ($f = 50$Hz): The scope is to keep charging the EVs with maintaining the regulation up capacity and regulation down capacity in the optimal region

— (P2) With frequency disturbance ($f \neq 50$Hz, power request): It aims to match the grid power demand to the charging demand

When there is no power request, the minimization problem is expressed as a quadratic multi-objective optimization problem. The formulation of the objective function is a weighted sum expressed in the Equation (4.22):

$$F_1 = w_1 C_1^2 + w_2 C_2^2 \tag{4.22}$$

The setting of the parameters w_1 and w_2 depends on the choice of the aggregator. For our study, the $w_1 = 1$ and $w_2 = 0.3$.

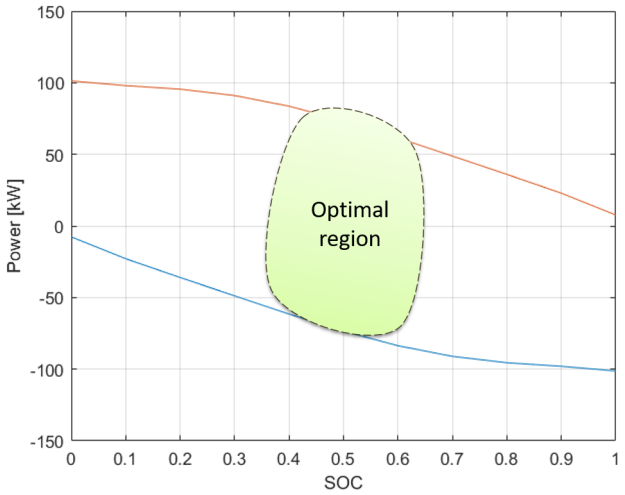

Figure 4.10 – Lithium-ion battery charging and discharging capability depending on the SOC

The idea of C_1 is to maintain the total available energy stored in the EVs within the optimal region in which the regulation up capacity and regulation down capacity are highest (see Figure 4.10), so as to maintain the total available energy charge above a certain threshold until the end of the day. C_1 quantifies the deviation from the tracking reference E_i^{ref}, in order to adjust the charging power of the EV P_i^j as presented in the Equation (4.23):

$$C_1 = (E_{i-1} + \sum_{j=1}^{N_{EV}} P_i^j \Delta t) - E_i^{ref} \tag{4.23}$$

The E_i is calculated by the given Equation (4.24):

$$E_i = \sum_{j=1}^{N_{EV}} SOC_i^j \cdot E_{batt}^j \cdot SOH^j \tag{4.24}$$

The E_i^{ref} should be tracked to keep the regulation up/down capacity at the maximal value The definition of the capacity for regulation up/down is given in Figure 4.11.

$$E_i^{ref} = \sum_{j=1}^{N_{EV}} SOC_i^{ref} \cdot E_{batt}^j \cdot SOH^j \tag{4.25}$$

Regarding the dependence of the charging/discharging power of lithium-ion batteries on SOC, the optimal SOC for both maximal charging/discharging can be found between 0.4 and 0.6. At $SOC = 0.5$ the charging rate is 80kW and discharging rate is -80kW for this example in the Figure 4.10 . At this point, the EV charging/discharging capacities are both high, thus optimal to track the power request. Giving priority to the charging of the EVs over the discharging of the EVs, the optimal SOC can be set to 0.6.

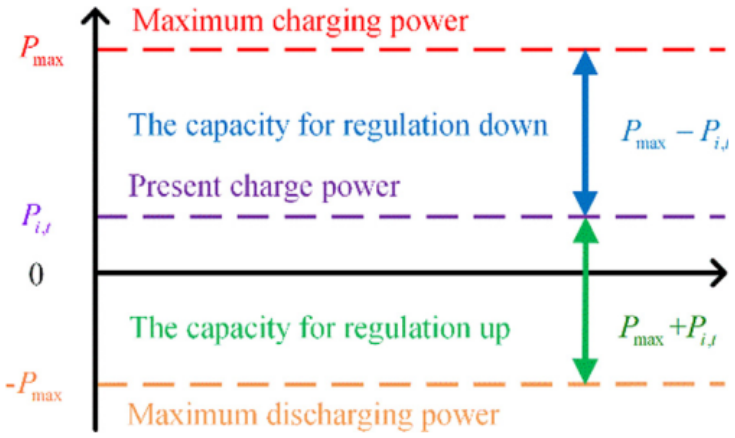

Figure 4.11 – Definition of the capacity for regulation up and regulation down [6]

Charging the EV fleet involves many nuanced subtleties to consider conflicting objectives of maximizing the EV's battery SOC at the end of the day, maintaining the total available energy within the optimal region and improving the frequency regulation response performance.

The time of the frequency deviation is unpredictable and its duration is also unknown in advance. This is why the EV fleet must be prepared at all times to respond to these disturbances, taking into account two contradictory objectives as shown in Figure 4.12:

— To maximize the SOC of the EV battery in order to satisfy EV user's needs (with rather high SOCs 0.6 - 0.9)

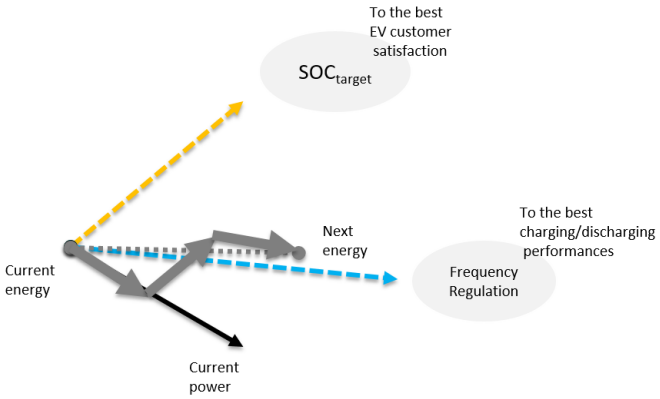

Figure 4.12 – An illustration of two conflicting objectives

— To keep the SOC within the optimal region for charging/discharging (with a SOC between 0.4 and 0.6) which improves the response performance of frequency control.

All this without the possibility to schedule the charging/discharging and executing a recalculation in real-time. This method allows a better power management of the EV fleet charging and a quick response to the power request in case of a frequency deviation.

The purpose of C_2 defined in Equation (4.26) is to keep the EV charging, so the total power approaches to P_i^{ref}, thus the total available energy stored in the EVs increases gradually to the maximal capacity of the EV's battery at the end of the day (cf. Figure 4.13). The strategy of increasing the EVs' SOC at the end of the day is fully justified because of high power demand during the peak period between 6 p.m. and 10 p.m. thus, the necessity to discharge EVs for power grid's relief.

$$C_2 = (\sum_{j=1}^{N_{EV}} P_i^j) - P_i^{ref} \tag{4.26}$$

The P_i^{ref} is defined in Equation (4.28) as the average power that must be used to reach $E^{saturation}$ at the end of the day, with a total station opening time of t_{op} hours. The detailed expression of P_i^{ref} is given in the following equations:

$$E^{saturation} = \sum_{j=1}^{N_{EV}} SOC^{limit} \cdot E_{batt}^j \cdot SOH^j \tag{4.27}$$

$$\begin{cases} E_i^{remain} = E^{saturation} - E_i \\ P_i^{ref} = \frac{E_i^{remain}}{t_{op}} \end{cases} \tag{4.28}$$

The (P1) aims to prepare the EV fleet to respond to any power request by keeping the average SOC of the EV fleet into the optimal region (where the capacities for regulation up/down are maximal) and charging the EVs with higher priority. However, the objective of (P2) is to minimize the tracking error between the requested power and the used charging power, and to maximize the charging efficiency of the fleet.

When there is a power request, the (P2) is activated and the optimization problem expressed as a multi-objective minimization.

$$F_2 = w_3 C_3^2 + w_4 C_4 \tag{4.29}$$

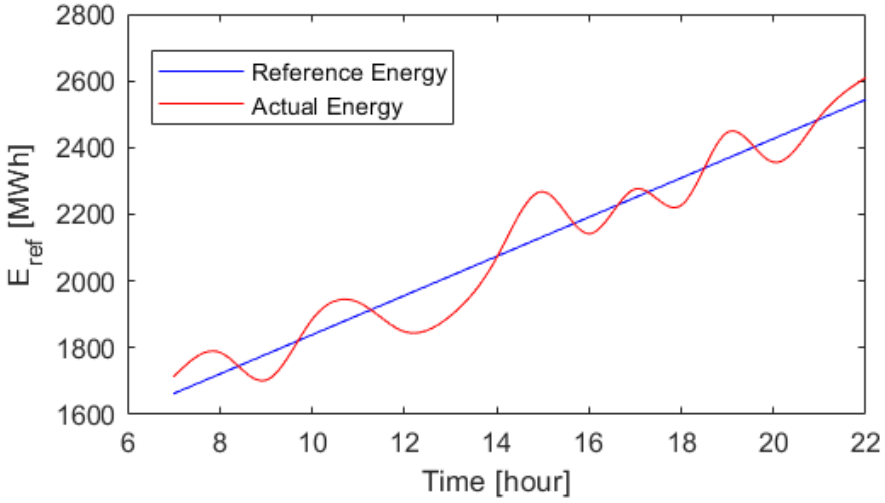

Figure 4.13 – Example of a time depending references $E(t)^{ref}$

The purpose of C_3 defined in Equation (4.30) is to have a best response to the power request with reducing the tracking error $P - P^{request}$

$$C_3 = (\sum_{j=1}^{N_{EV}} P_i^j) - P_i^{request} \tag{4.30}$$

The setting of the parameters w_1 and w_2 depends on the choice of the aggregator. For our study, the $w_3 = 1$ and $w_4 = 0.1$.

The C_4 includes the dependence of the charger efficiency, the objective of Equation(4.31) is to use the EV chargers in their maximum efficiencies. Maximizing the charger efficiency η corresponds to minimizing the charging loses $(1-\eta)P$

$$C_4 = \sum_{j=1}^{N_{EV}} P_i^j (1 - \eta(P_i^j)) \tag{4.31}$$

The two sub-problems (P1) and (P2) are subject to the same constraints.

The global constraints related to the upper and the lower bounds of the charging/discharging power are expressed in Equation (4.32):

$$\begin{aligned} P_i^j &\leq C_i^j \\ P_i^j &\geq D_i^j \end{aligned} \tag{4.32}$$

The definition of C_i^j and D_i^j is given by the Equations (4.33) :

$$\begin{aligned} C_i^j &= s_i^j \cdot \alpha_i^{j,ub} \cdot P_i^{j,max+} \\ D_i^j &= s_i^j \cdot \alpha_i^{j,lb} \cdot P_i^{j,max-} \end{aligned} \tag{4.33}$$

where $P_i^{j,max+}$ and $P_i^{j,max-}$ are the maximum charging power that take the limitation of the three elements (the charger, the charging point, the battery) defined in Equation (4.34):

$$\begin{aligned} P_i^{j,max+} &= min(P_{chpt+}^j, P_{Charger+}^j, P_{i,Bat+}^j) \\ P_i^{j,max-} &= max(P_{chpt-}^j, P_{Charger-}^j, P_{i,Bat-}^j) \end{aligned} \tag{4.34}$$

s_i^j, $\alpha_i^{j,ub}$, and $\alpha_i^{j,ub}$ are defined in the Equations (4.35), Equations (4.36), and Equations (4.37) as follow:

$$s_i^j = \begin{cases} 1, & \text{pluged-in} \\ 0, & \text{pluged-out} \end{cases} \tag{4.35}$$

$$\alpha_i^{j,ub} = \begin{cases} 1, & SOC_i^j < SOC_{maxi} \\ 0, & SOC_i^j \geq SOC_{maxi} \end{cases} \tag{4.36}$$

$$\alpha_i^{j,lb} = \begin{cases} 1, & SOC_i^j \geq SOC_{mini} \\ 0, & SOC_i^j < SOC_{mini} \end{cases} \tag{4.37}$$

In order to prevent the transformer from any overloading power, an inequality constraint has been expressed in Equation (4.38):

$$\sum_{j=1}^{N_{EV}} P_i^j \leq P_{total} \tag{4.38}$$

The dynamic monitoring of the SOC is given by Equation (4.39):

$$\begin{aligned} &\text{In charging mode: } P_i^j \geq 0 \\ &SOC_{i+1}^j = SOC_i^j + \frac{\eta(P_i^j) P_i^j \cdot \Delta t}{E_{batt}^j \cdot SOH^j} \\ &\text{In discharging mode: } P_i^j < 0 \\ &SOC_{i+1}^j = SOC_i^j + \frac{(P_i^j / \eta(P_i^j)) \cdot \Delta t}{E_{batt}^j \cdot SOH^j} \end{aligned} \tag{4.39}$$

For simplification purposes, this works considers an evenly distributed joule heat generation, and a temperature of the battery cell uniformly distributed. Thus, the temperature estimation is a first order model expressed as in Equation (4.17). The joule power is formulated as a linear model in terms of charging and discharging power defined in Equation (4.18). The convective power is modeled by the Newton law showed in Equation (4.19).

4.4.2 Simulations and results

In order to demonstrate the effectiveness of the presented EV charging management strategy, the results were obtained with *fmincon* MATLAB optimization solver, Table 4.3 shows the used parameters in all simulations.

Table 4.3 – Simulation parameters of EVs

Parameters	
Sampling time	$5min$
Maximum EV number	20
Battery capacity	$60kWh$
Initial SOC	$[0.1, 0.6]$
Desired SOC	$[0.3, 0.9]$
SOC_{maxi} / SOC_{mini}	$0.9/0.2$

4.4.2.1 The effect of charger efficiency

In this section the impact of the charger's efficiency will be studied. The consideration of a constant number of EVs in the charging station in Table 4.4, allows us to evaluate the real impact of the proposed strategy on the tracking error. The impact of the EVs arrival and departure time will be studied in the section 4.4.2.2.

Table 4.4 – Simulation parameters of 4.4.2.1

Parameters	
EVs arrival time	$8h$
EVs departure time	$18h$

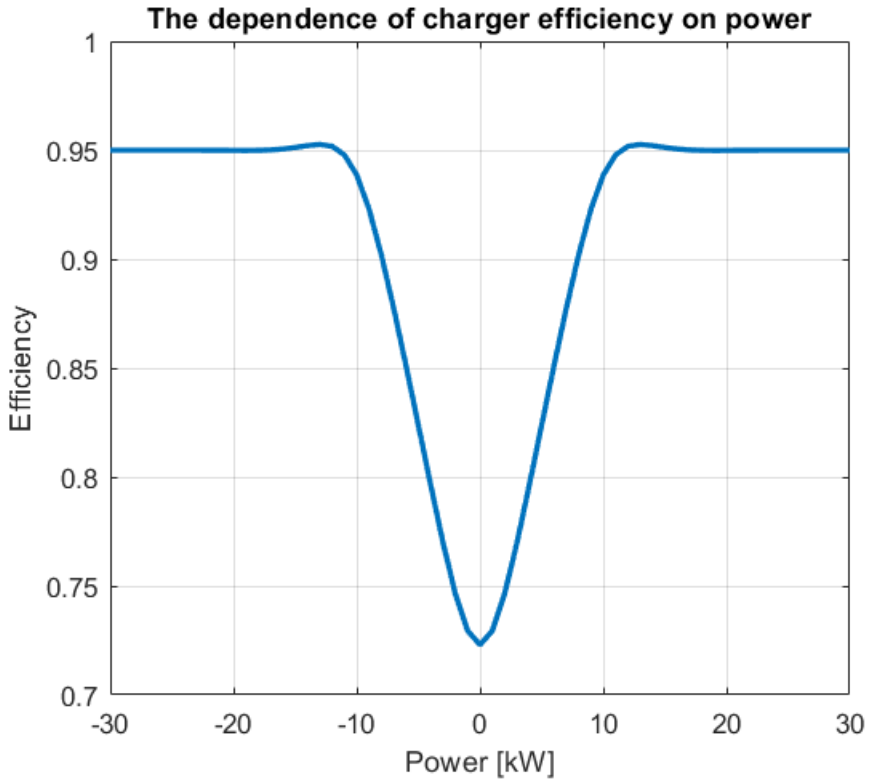

Figure 4.14 – EV charger efficiency [7]

A tracking error is observed in both VEs responses in the Figure 4.15. However, by taking into account the variation in efficiency of the charger as a function of power presented in Figure 4.14, the tracking error was significantly reduced to the 10^{-3} scale, i.e. to the accuracy of the Watt instead of the kW.

4.4.2.2 The effect of the number of the EVs on the tracking error

Table 4.5 – Simulation parameters of 4.4.2.2

Parameters	
EVs arrival time	$\mathcal{N}(9,0.5)$
EVs departure time	$\mathcal{N}(17,0.5)$

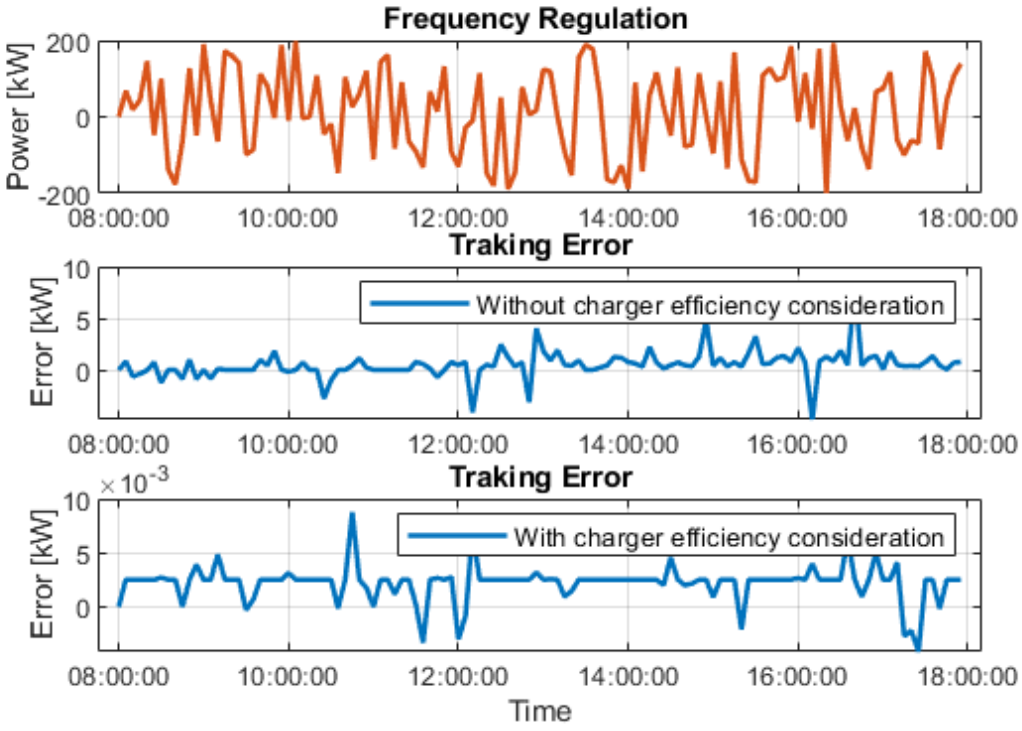

Figure 4.15 – Frequency regulation (FR) Signal, and impact of charger efficiency response error

High tracking error is observed in the Figure 4.16 in the time interval of [8h,9h] and [17h,18h], this problem is caused by the low regulation capacity due to the low number of EVs in the charging station. However, outside this two periods the error is near to zero with the help of the available EVs offering high regulation reserve. As shown on the Figure 4.16, when the number of vehicles exceeds 10, the tracking error becomes zero. In brief, the EVs arrival and departure time affect the tracking error, so the charging station should keep a minimum number of EVs in the charging station, otherwise include energy storage solutions to compensate this lack of EVs in these periods.

4.4.2.3 Long period of frequency drop and the effect of the charging point maximum rate

The purpose of this simulation is to show how can EVs take a leading role in supporting the power grid in difficult situations such as a high frequency drop caused by a power plant shutdown or a high grid power demand in peak period.

Figure 4.17 shows that the EVs can feed power into the grid by discharging the EVs' battery and absorb the surplus of power from the grid to maintain the frequency. The simulation shows the ability of EVs to withstand a special event for a remarkable period of time, approximately 3 hours for this case. Therefore, the charging station with plugged-in EVs can react as energy storage to support the grid.

Despite the long period of disturbance and its high magnitude, almost all EVs respect the minimum SOC limit of 0.2 as shown in Figure 4.18.

In this simulation the rated power of the charging points will be reduced from $22kW$ to $[3.2, 7.4, 11, 22]kW$, to study its effect on sustaining the grid support. The maximum charging/discharging power of the charging point will be selected randomly from the values of the vector $[3.2, 7.4, 11, 22]kW$. The charging points in the charging station have the following ratios: $[30\%, 30\%, 20\%, 20\%]$ respectively.

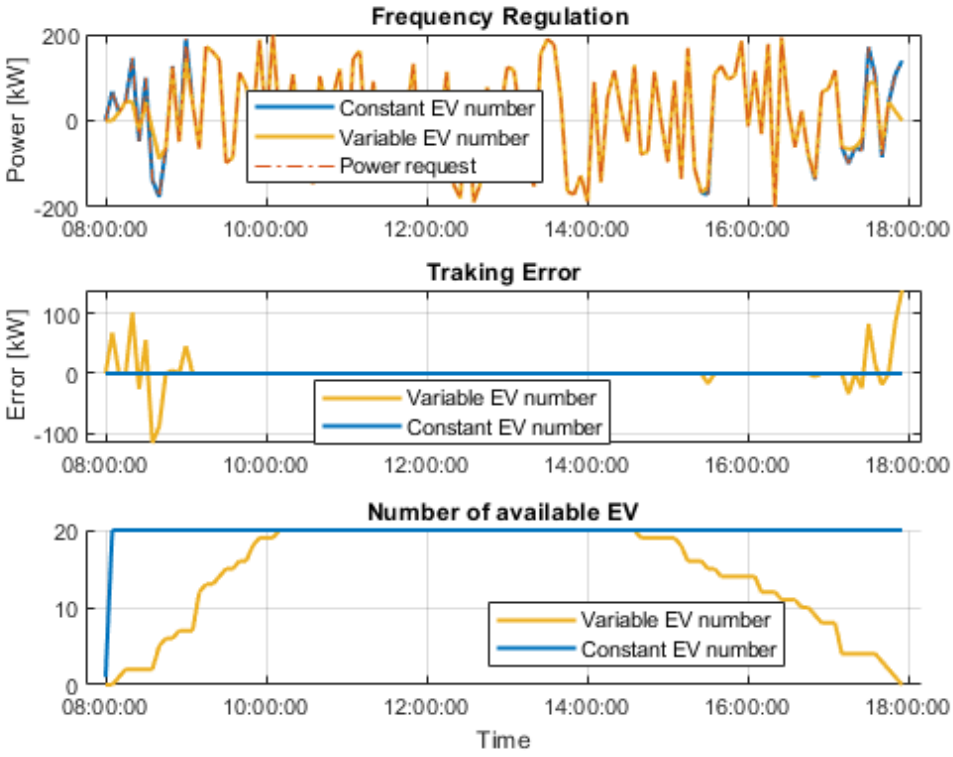

Figure 4.16 – FR Signal, response error, and EV availability

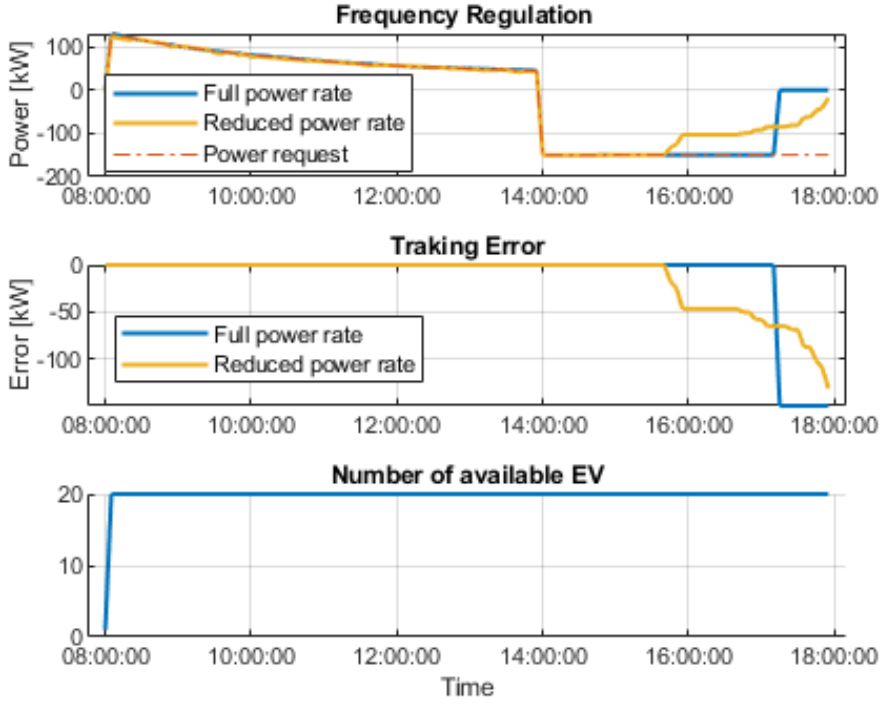

Figure 4.17 – FR Signal, response error, and EV availability

The effect of the maximum power of charging point is observed in the Figure 4.19 where the charging slop and the discharging slop of some EVs are low compared to the Figure 4.18. Moreover, this point affects directly the EVs considered as fast response energy storage system.

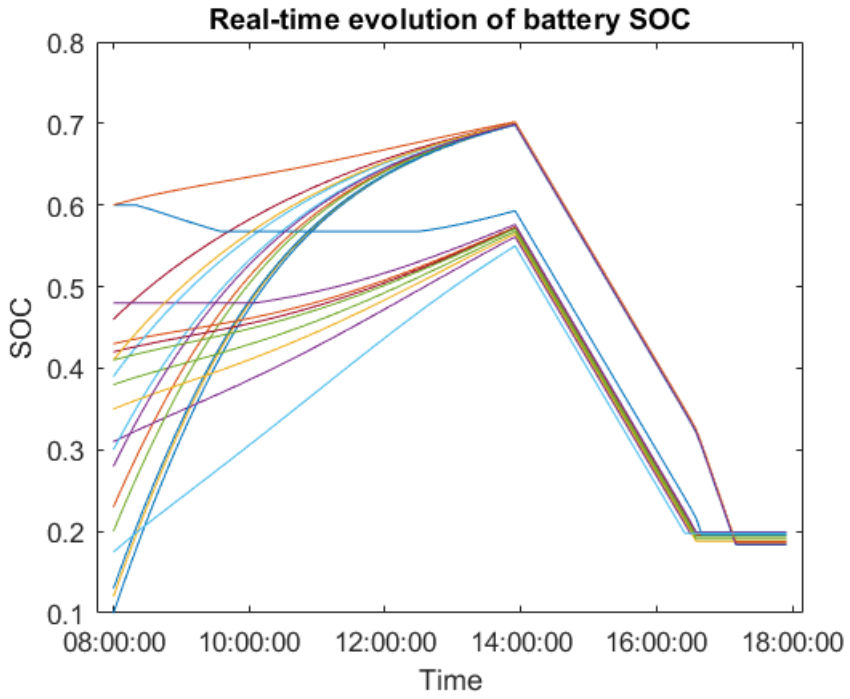

Figure 4.18 – The SOC evolution of every EV in the charging station for full power rate $22kW$

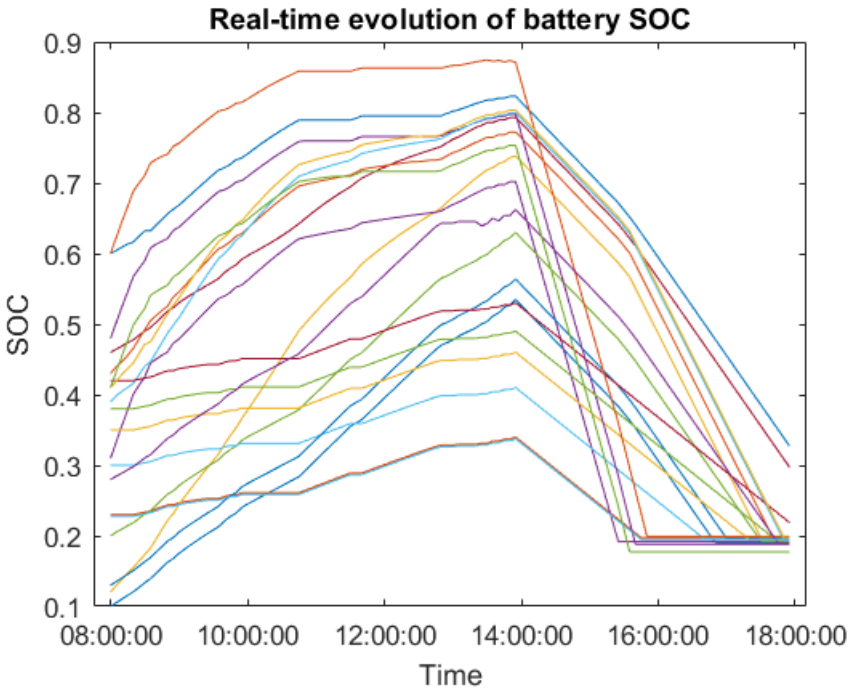

Figure 4.19 – The SOC evolution of each EV in the charging station for reduced power rate

Because of the power limitation of some charging points the charging station can not maintain the constant power injection in the grid and their power delivery decrease due to the low discharging rate of some charging points. The power was maintained by the EVs with high power of their charging point $22kW$ until $15h45min$, when approaching to the minimal SOC of 0.2 those EVs can not longer participate in the grid support. In fact, with the constraint of the power limitation of the rest of the charging points, the holding of the grid supply is far from perfect for the rest of the EV fleet due to the low charging speed of the charging points.

To summarise, as the SOC of EVs connected to the fast charging points ($22kW$ and $11kW$) is gradually depleted, the tracking error increases step by step as shown in Figure 4.17.

4.4.2.4 Synthesis of EV position in frequency regulation market

The two previous examples show the possibility of scaling up the participation of EVs in the ancillary services market. However, the conditions of participation in the primary and secondary reserve are not the same. In general the conditions may change from country to another but the most common conditions are presented on the Table 4.6.

According to the Table 4.6 and the results of simulations, the participation of the EVs in primary reserve can be more suitable if the charging station contains a limited number of charging points but with high charging rate in order to reach the minimum required power of $1MW$. Also the randomly arrival time, the uncertain departure time and short availability of the EVs is not a big constraint. The most important thing is to ensure the minimum contracted reserve. Moreover, the maximum duration of the reserve activation in primary control is $15min$, so the charging station can interrupt the charging of EVs for this period of time and resume the charging of the EVs after the frequency incident to fulfill the energy requirement of the EVs' owner. Furthermore, the discharging of the EVs for a period of time of $15min$ can offer an attractive profit from V2G feature that will compensate the battery cycling caused by this operation.

Table 4.6 – Characteristics of primary and secondary reserve [10]

	Primary reserve	Secondary reserve
Activation dynamic	50% of the reserve within $15s$ and 100% of the reserve enabled within $30s$	100% of the reserve activated within $5min$
Activation duration	The reserve must be kept activated for $15min$ maximum	The activation duration could be unlimited during the duration of the contract
Minimum power	$1MW$	$5MW$
Power direction	Positive **AND** Negative	Positive **OR** Negative

The secondary frequency control needs a larger capacity compared to the primary reserve and the activation of the reserve could be for a long duration. Therefore, the charging stations with a high number of charging points, strong attendance rates, and long periods of availability of the EVs are more appropriate to the secondary reserve. Although the geographical remoteness, small charging stations can be grouped together to form one virtual charging station supervised by one aggregator to participate in secondary reserve. In addition, a mix of fast charging stations and slow charging stations with high capacity can perfectly ensure the secondary frequency regulation requirement. Finally, the case of long frequency drop confirms the long solicitation of EVs leading to high EV batteries DOD. Considering the high impact of DOD on EV's Li-ion batteries lifetime and the low economical profit from V2G operation can make the involvement of EVs in the secondary frequency market less tolerated by the EVs owners.

4.5 Conclusion

In this chapter, a detailed state of the art about EV fleet charging algorithm was conducted. After, two EV fleet energy management strategies has been proposed. The first strategy covers the

unidirectional charging of large numer of EVs considering the charging infrastructure limit. The second one deals with the bidirectional charging of EVs with frequency regulation considering the charger efficiency dependence on power.

The section of the state of the art presents the most important studies about the charging management of the EV fleet. Firstly, the discussion was about the coordinated charging strategy, in which the control of the charging can be done by the number of EVs in charge in TCC strategy and by the charging power in PCC strategy. Secondly, the discussion was turned to unidirectional charging strategies that use a priority criterion to dispatch the available power, considered as the first step of the full EV charging problem. Thirdly, the focus was given to the bidirectional charging strategies, in which the EVs play the role of flexible energy sources by offering several ancillary services to the power grid such as frequency regulation.

The first contribution of this chapter is a solution to the problem of unidirectional coordinated charging for a high number of EVs and a limited power available at the transformer where the charging station is connected. The charging strategy is based on the evaluation of the EV's priority level corresponding to the EV's energy requirement, the duration of EV plug-in time at the charging station and the power available at the charging point. The design of the charging strategy allows an optimal integration of the EVs to the distribution power grid. Moreover, the proposed strategy takes into account the distribution infrastructure constraints, the charging system limitations and the constraints related to EV users' satisfaction. A detailed comparative study was conducted to demonstrate the efficiency of the coordinated charging algorithm. The results show that with a high number of EVs per day, the power coordination algorithm can ensure a very high level of satisfaction compared to the uncoordinated charging. Exceeding a given threshold of a total number of EVs per day, EVs lose the possibility of being charged before the departure time. Despite the centralized aspect of the proposed algorithm, all issues related to high computational cost was avoided, compared to solving an optimization problem in the same context of massive integration of EVs into the grid.

The unidirectional coordination charging strategy was the first step towards a full bidirectional charging strategy implementation. The second step was the integration of V2G functionality in the coordinated charging to offer more services to the power grid such as primary frequency regulation. In the second part of this chapter, the problem of EV frequency regulation service has been studied through EV charging with V2G feature. First, the optimization problem modeling considers both EV's users satisfaction and frequency regulation performance such as tracking error and regulation capacity. Then, the problem was divided into two sub-problems (P1) in normal day time when the frequency is 50Hz and (P2) in case of frequency deviation. A multi-criteria optimization was used in the formulation of the two sub-problems. A numerical analysis was carried out to demonstrate the effect of EV arrival and departure distributions on the regulation capacity and on the tracking precision. Simulation results confirm the importance of taking into account the dependence of the charger efficiency on power in reducing the tracking error.

5

General Conclusion and Perspectives

General Conclusion

Global warming is driving the countries' policies and car manufacturers to accelerate the integration of the electric vehicles. The EVs are considered as a big step towards a sustainable society. However, there are several challenges to be addressed, such as those related to Li-ion battery technologies and the deployment of the charging infrastructure in a large scale. Currently, the EV charging is considered as uncontrolled due to the low market penetration of EVs. However, it is expected that, in the medium to long term, EVs will have a significant level of penetration in the light-duty vehicle vehicle market. The integration of a large number of EVs will lead to significant impacts on the power grid, such as increased energy losses and peak power, overloading of lines and transformers, voltage drops, reduction of the life of distribution transformers, etc., unless an action is taken. Controlling the charging of EVs is the only way to prevent the distribution networks from suffering these problems without having a major upgrade on the network's infrastructure.

In addition to the ability of EVs to adjust the charging power, the EV batteries can deliver the energy to the grid in real-time due to the V2G feature. Therefore, EVs can support the grid in the peak hour demand, reduce the impact of intermittence in renewable power production and provide ancillary services to the grid. In this context, the improving of the EV charging methods can provide both technical and economical benefits. The concept of smart charging and EV fleet management are the key to achieve this high level objective. The main conclusion of this work can be expressed in different parts, each dedicated to the contributions of this PhD thesis.

Li-ion battery modeling and temperature consideration: This part began by presenting the state-of-the-art of the battery modeling approaches: electrochemical models, empirical models and equivalent circuit models. The main advantages and limitations of each modeling method in terms of accuracy and the complexity are highlighted. The comparison of the three modeling technique conclude that the empirical models and equivalent circuit models are the two suitable for EV simulations. However, the choice of the optimal battery model is a tradeoff between the desired accuracy and the complexity of parameter' identification. In addition, the level of battery modeling and the desired modeling time scale should be taken into consideration. Due to the thermal issues of Li-ion batteries and the effect of temperature on Li-ion batteries performances,

the estimation of the temperature was a crucial point to consider. Therefore, a thermal modeling has been discussed in order to build a electro-thermal model that combine a Rint model with a 1D lumped thermal model. Finally, a Least square estimation was carried out to identify the thermal parameters of the Li-ion battery model. The proposed electro-thermal model will be use in the next chapters to evaluate the temperature and evaluate the battery SOC.

Smart charging strategies by decentralized onboard controller: In order to provide an economic benefit to EV users, a couple of charging strategies have been proposed in this work with the objective of reducing the total charging cost for the final user. These smart charging strategies consist of shifting the charging from the peak period to a low power demand period in which the energy prices are more attractive. Moreover, the EVs can offer more profitable gains when considering the V2G feature, by discharging the EV to the grid at high peak demand the EV owner can earn money and reduce his/her charging bill. By shifting the charging from the evening when the energy prices and power demand are the highest to the night, a major problem occurs especially with Li-ion batteries when the temperature could drop in some regions to subzero temperatures as revealed in the state of the art. To deal with this problem, a decentralized smart charging strategy considering cost minimization and temperature has been proposed. The scheduling strategy considers TOU energy prices, the initial SOC, the final SOC desired by the EV user, the maximum power of the charging infrastructure, the power limitation the Li-ion battery, the initial battery temperature and the outside temperature. The scheduling algorithm calculates the optimal power profile to reach the desired SOC by the EV user's without neglecting the effect of temperature on the charging performances of Li-ion batteries. The results show the impact of the temperature consideration on the SOC estimation, specially in cold weather conditions and the choice of the value of the minimal authorized SOC is a tradeoff between the maximization of the profit from the V2G feature and battery degradation.

When assuming the high variations in energy prices the first smart charging strategy can not perform the scheduling due to high number of decision variables and the high number of constraints. The added value of the second proposed smart charging algorithm is the use of a dynamic optimized time step taken as a decision variable, contrary to the first one that uses a constant time step as a fixed parameter. The proposed algorithm can perform the power scheduling despite the high fluctuation of energy prices in a reduced time and low computational capacities such as those available on an onboard controller. Taking into account the same consideration as in the first algorithm, the second smart charging algorithm outperforms the first one in terms of computing time and the charging cost reduction.

EV fleet charging coordination strategies in a centralized framework: The task of developing a real-time coordinated charging management algorithm of an EVs fleet has been successfully achieved in this thesis. The topic of a massive integration of EV in distribution network has been studied by proposing an unidirectional coordinated charging algorithm in order to manage the charging of a large number of EVs in a charging station with limited transformer power without any reinforcement of the grid infrastructure. To address this problem, a priority criterion was proposed. This criterion takes into account mainly the current infrastructure of the electric distribution network, the EV user's satisfaction, the charging constraint and the battery power limitation constraints. The main features of the proposed algorithm are: the optimal distribution of the total available power, information on whether the EV has reached the requested state of charge in the allowed time and the priority given to the EVs charged. This study is carried out under the assumption of a large number of EVs per day, random arrivals and departures, and a power demand considerably higher than the available transformer power. The results show that the charging of a large number of EVs is performed in spite of a limited total available

power. Moreover, the charging efficiency of the station and the satisfaction level of EV users are respected while the power is limited. By preventing the transformer from overloading, the lifespan of the transformer serving the charging station can be extended.

The concept of bidirectional charging has been considered to improve the first algorithm by considering the potential of the V2G feature in offering ancillary services to the power grid such as the frequency regulation. Due to the high power density and energy density of Li-ion batteries, EVs can provide an immediate power to the grid as an energy storage system. However, EVs have an additional constraint that should be taken into account while the EVs are participating in grid services. The mobility energy requirement is considered as the most important short term need. In this context, an optimization problem has been defined considering both EV owner's satisfaction and frequency regulation services. The purpose of the proposed strategy is maintain the total stored energy in the EV batteries in an optimal moving region in which both frequency regulation capacities and SOC are higher. Despite the importance of frequency regulation request the charging power will be maintained for EVs with a higher priority. In addition to the bidirectional power flow, this strategy considers also the EV charger's efficiency dependence on power. By taking into account this aspect, the accuracy of tracking the TSO power request is enhanced. To achieve this goal, a multi-objective optimization with the concept of optimal time depending references is introduced. The simulations conclude that there is an impact on the reduction of the tracking error when the charger's efficiency variation is considered. Finally, a comparative study confirms that the participation of EVs in primary frequency control is more appropriate for preventing the EV batteries from high DOD when considering the battery lifespan as an important point.

Finally, it can be highlighted that the results obtained during the development of this PhD thesis have been valorized in the form of conferences papers, articles of journals and patents:

Conference papers :

— Y. Dahmane, M. Ghanes, R. Chenouard, and M. Alvarado-Ruiz, "Decentralized control of electric vehicle smart charging for cost minimization considering temperature and battery health," in 2019 IEEE International Conference on Communications, Control, and Computing Technologies for Smart Grids (SmartGridComm), October 21-23, Beijing, China, 2019.

— Y. Dahmane, R. Chenouard, M. Ghanes, and M. Alvarado-Ruiz, "Coordinated charging of large electric vehicle fleet in a charging station with limited transformer power," in 2020 IEEE Conference on Control Technology and Applications (CCTA), August 24-26, Montreal, Canada, 2020

Journal papers :

— Y. Dahmane, M. Ghanes, R. Chenouard, and M. Alvarado-Ruiz, "Optimized Time Step for Electric Vehicle Charging Optimization Considering Cost and Temperature", ELSEVIER Sustainable Energy, Grids and Networks (Under Review)

— Y. Dahmane, M. Ghanes, R. Chenouard, and M. Alvarado-Ruiz, "Optimal Electric Vehicle Fleet Charging Management With Frequency Regulation Service", IEEE Transaction on Smart Grid (Under Review)

Patents :

— Y. Dahmane, M. Ghanes, R. Chenouard, and M. Alvarado-Ruiz : Procédé d'optimisation de la recharge et/ou de la décharge de batteries pour un véhicule automobile électrique : (FR1911756), 2019, application nationale (in the process of validation)

— Y. Dahmane, M. Ghanes, R. Chenouard, and M. Alvarado-Ruiz : Procédé de gestion de recharge avec V2G d'une flotte de véhicules électriques avec service de régulation de fréquence (in the process of validation)

Perspectives

On the basis of the development carried out in this thesis, different research axes and horizons have been opened for smart charging technology. Nowadays, many researchers are working on these topics and many improvements have been made in recent years, however, much work is still needed at the experimental level. A big challenge that should be better analyzed is the effect of V2G technology on the degradation of Li-ion batteries, due to the large depth of discharge and a long running time. A degradation model has not been considered in this thesis and is very important to have a good prediction of the battery performance at the cell and pack level. Battery performance, such as energy and power capacity and lifetime, are also strongly influenced by the thermal behavior of the cell, its influence on the heating of neighboring cells, and the cooling and heating strategies. In this work, these effects have not been evaluated, but thermal modeling, especially at the pack level, can greatly improve the accuracy of performance evaluation.

The future work of this thesis should consider the exploration and development of an economic model that describes the economic flow between the grid operators and EVs aggregators. This will help to identify the benefits of both grid operators and EVs owners for each charging strategy. A business model must be designed to take into account all aspects of the smart grid ecosystem in which renewable energy producers, EVs aggregators, car manufacters, aggregators and grid operators interact in order to evaluate the cost-benefit for each participant.

Bibliography

[1] T. Woehrle, "Lithium-ion cell," in *Lithium-Ion Batteries: Basics and Applications*. Springer, 2018, pp. 101–111. 9, 13, 14

[2] *Internatinal Energy agency (IEA): Global EV Outlook 2020 - Entering the decade of electric drive?*, 2020. [Online]. Available: https://www.iea.org/reports/global-ev-outlook-2020 9, 14, 15, 16

[3] K. Smith and C.-Y. Wang, "Solid-state diffusion limitations on pulse operation of a lithium ion cell for hybrid electric vehicles," *Journal of Power Sources*, vol. 161, no. 1, pp. 628 – 639, 2006. [Online]. Available: http://www.sciencedirect.com/science/article/pii/S0378775306006161 9, 20

[4] H. He, R. Xiong, and J. Fan, "Evaluation of lithium-ion battery equivalent circuit models for state of charge estimation by an experimental approach," *Energies*, vol. 4, no. 4, pp. 582–598, 2011. 9, 21, 22, 23

[5] H. E. Perez, X. Hu, S. Dey, and S. J. Moura, "Optimal charging of li-ion batteries with coupled electro-thermal-aging dynamics," *IEEE Transactions on Vehicular Technology*, vol. 66, no. 9, pp. 7761–7770, Sep. 2017. 9, 27

[6] H. Liu, J. Qi, J. Wang, P. Li, C. Li, and H. Wei, "Ev dispatch control for supplementary frequency regulation considering the expectation of ev owners," *IEEE Transactions on Smart Grid*, vol. 9, no. 4, pp. 3763–3772, 2018. 10, 71, 84

[7] C. Ziras, A. Zecchino, and M. Marinelli, "Response accuracy and tracking errors with decentralized control of commercial v2g chargers," in *2018 Power Systems Computation Conference (PSCC)*. IEEE, 2018, pp. 1–7. 10, 71, 88

[8] M. A. Alvarado Ruiz, "An innovative system for electrical vehicular charging in urban zone : conception, dimensioning, and performance evaluation," Theses, Télécom ParisTech, Sep. 2015. [Online]. Available: https://pastel.archives-ouvertes.fr/tel-01569067 11, 76

[9] D. Q. Hung, Z. Y. Dong, and H. Trinh, "Determining the size of phev charging stations powered by commercial grid-integrated pv systems considering reactive power support," *Applied Energy*, vol. 183, pp. 160 – 169, 2016. [Online]. Available: http://www.sciencedirect.com/science/article/pii/S0306261916312776 11, 76

[10] Z. Maxime, B. Sebastian, C. Dago, G. Alexis, and B. Edward, "Flexibility within the electrical systems through demand side response: Introduction to balancing products and markets in germany, france, and the uk," European Commission, Tech. Rep. number, 2017. [Online]. Available: https://ec.europa.eu/research/participants/documents/downloadPublic?documentIds=080166e5b2c00111&appId=PPGMS 11, 92

[11] H. Nazaripouya, B. Wang, and D. Black, "Electric vehicles and climate change: Additional contribution and improved economic justification," *IEEE Electrification Magazine*, vol. 7, no. 2, pp. 33–39, 2019. 13

[12] *Internatinal Energy agency (IEA): CO2 Emissions from Fuel Combustion 2019 Highlights*, 2019. 13

[13] M. Ehsani, Y. Gao, S. Longo, and K. Ebrahimi, *Modern electric, hybrid electric, and fuel cell vehicles*. CRC press, 2018. 13

[14] R. Yazami and P. Touzain, "Composes ioniques du graphite avec nicl2, bf- 4 et k+ pour le stockage electrochimique de l'energie," *Solid State Ionics*, vol. 9, pp. 489–494, 1983. 14

[15] K. Mizushima, P. Jones, P. Wiseman, and J. B. Goodenough, "Lixcoo2 (0< x<-1): A new cathode material for batteries of high energy density," *Materials Research Bulletin*, vol. 15, no. 6, pp. 783–789, 1980. 14

[16] J. Jaguemont, L. Boulon, P. Venet, Y. Dubé, and A. Sari, "Lithium-ion battery aging experiments at subzero temperatures and model development for capacity fade estimation," *IEEE Transactions on Vehicular Technology*, vol. 65, no. 6, pp. 4328–4343, 2016. 15, 25, 42

[17] H. Liu, Z. Wei, W. He, and J. Zhao, "Thermal issues about li-ion batteries and recent progress in battery thermal management systems: A review," *Energy conversion and management*, vol. 150, pp. 304–330, 2017. 15, 25, 42

[18] J. Y. Yong, V. K. Ramachandaramurthy, K. M. Tan, and N. Mithulananthan, "A review on the state-of-the-art technologies of electric vehicle, its impacts and prospects," *Renewable and Sustainable Energy Reviews*, vol. 49, pp. 365 – 385, 2015. [Online]. Available: http://www.sciencedirect.com/science/article/pii/S1364032115004001 16

[19] E. Sortomme and M. A. El-Sharkawi, "Optimal scheduling of vehicle-to-grid energy and ancillary services," *IEEE Transactions on Smart Grid*, vol. 3, no. 1, pp. 351–359, 2012. 16, 40, 42

[20] R. Mehta, D. Srinivasan, A. Trivedi, and J. Yang, "Hybrid planning method based on cost-benefit analysis for smart charging of plug-in electric vehicles in distribution systems," *IEEE Transactions on Smart Grid*, vol. 10, no. 1, pp. 523–534, Jan 2019. 16, 40, 42

[21] C. Le Floch, E. C. Kara, and S. Moura, "Pde modeling and control of electric vehicle fleets for ancillary services: A discrete charging case," *IEEE Transactions on Smart Grid*, vol. 9, no. 2, pp. 573–581, 2018. 16, 40, 42

[22] Z. Liu, Q. Wu, S. Huang, L. Wang, M. Shahidehpour, and Y. Xue, "Optimal Day-ahead Charging Scheduling of Electric Vehicles through an Aggregative Game Model," *IEEE Transactions on Smart Grid*, vol. 3053, no. c, pp. 1–1, 2017. [Online]. Available: http://ieeexplore.ieee.org/document/7879192/ 16, 40, 51

[23] G. Wang, H. Li, H. Wang, X. Zhang, and F. Zhang, "A decentralized power allocation strategy for the ev charging network," in *2018 IEEE Innovative Smart Grid Technologies - Asia (ISGT Asia)*, May 2018, pp. 1305–1310. 16, 40, 42, 68

[24] L. Gan, U. Topcu, and S. H. Low, "Optimal Decentralized Protocol for Electric Vehicle Charging," *IEEE Transactions on Power Systems*, vol. 28, no. 2, pp. 940–951, 2013. 16, 40, 42, 68

[25] H. Turker, "Optimal charging of plug-in electric vehicle (pev) in residential area," in *2018 IEEE Transportation Electrification Conference and Expo (ITEC)*. IEEE, 2018, pp. 243–247. 16, 40, 42

[26] D. A. Chekired, L. Khoukhi, and H. T. Mouftah, "Decentralized cloud-sdn architecture in smart grid: A dynamic pricing model," *IEEE Transactions on Industrial Informatics*, vol. 14, no. 3, pp. 1220–1231, March 2018. 16, 40, 51

[27] A. Fotouhi, D. J. Auger, K. Propp, S. Longo, and M. Wild, "A review on electric vehicle battery modelling: From lithium-ion toward lithium–sulphur," *Renewable and Sustainable Energy Reviews*, vol. 56, pp. 1008–1021, 2016. 19, 21

[28] F. Ciucci, "Modeling electrochemical impedance spectroscopy," *Current Opinion in Electrochemistry*, vol. 13, pp. 132–139, 2019. 19

[29] W. Gu and C.-Y. Wang, "Thermal and electrochemical coupled modeling of a lithium-ion cell," in *Proceedings of the ECS*, vol. 99, 2000, pp. 748–762. 19

[30] A. P. Schmidt, M. Bitzer, Á. W. Imre, and L. Guzzella, "Experiment-driven electrochemical modeling and systematic parameterization for a lithium-ion battery cell," *Journal of Power Sources*, vol. 195, no. 15, pp. 5071–5080, 2010. 19

[31] L. Zheng, J. Zhu, G. Wang, D. D.-C. Lu, and T. He, "Lithium-ion battery instantaneous available power prediction using surface lithium concentration of solid particles in a simplified electrochemical model," *IEEE Transactions on Power Electronics*, vol. 33, no. 11, pp. 9551–9560, 2018. 19

[32] L. Saw, K. Somasundaram, Y. Ye, and A. Tay, "Electro-thermal analysis of lithium iron phosphate battery for electric vehicles," *Journal of Power Sources*, vol. 249, pp. 231–238, 2014. 20

[33] I. Baghdadi, O. Briat, A. Eddahech, J. Vinassa, and P. Gyan, "Electro-thermal model of lithium-ion batteries for electrified vehicles applications," in *2015 IEEE 24th International Symposium on Industrial Electronics (ISIE)*. IEEE, 2015, pp. 1248–1252. 20, 25

[34] K. A. Smith, C. D. Rahn, and C.-Y. Wang, "Control oriented 1d electrochemical model of lithium ion battery," *Energy Conversion and management*, vol. 48, no. 9, pp. 2565–2578, 2007. 20

[35] A. Jokar, B. Rajabloo, M. Désilets, and M. Lacroix, "Review of simplified pseudo-two-dimensional models of lithium-ion batteries," *Journal of Power Sources*, vol. 327, pp. 44–55, 2016. 20

[36] S. Santhanagopalan, Q. Guo, P. Ramadass, and R. E. White, "Review of models for predicting the cycling performance of lithium ion batteries," *Journal of power sources*, vol. 156, no. 2, pp. 620–628, 2006. 20

[37] M. Doyle, T. F. Fuller, and J. Newman, "Modeling of galvanostatic charge and discharge of the lithium/polymer/insertion cell," *Journal of the Electrochemical society*, vol. 140, no. 6, p. 1526, 1993. 20

[38] C. Lin and A. Tang, "Simplification and efficient simulation of electrochemical model for li-ion battery in evs," *Energy Procedia*, vol. 104, pp. 68–73, 2016. 20

[39] X. Huang, H. Yu, J. Chen, Z. Lu, R. Yazami, and H. H. Hng, "Ultrahigh rate capabilities of lithium-ion batteries from 3d ordered hierarchically porous electrodes with entrapped active nanoparticles configuration," *Advanced materials*, vol. 26, no. 8, pp. 1296–1303, 2014. 20

[40] J. Meng, G. Luo, M. Ricco, M. Swierczynski, D.-I. Stroe, and R. Teodorescu, "Overview of lithium-ion battery modeling methods for state-of-charge estimation in electrical vehicles," *Applied sciences*, vol. 8, no. 5, p. 659, 2018. 20, 21

[41] M. Guo, G. Sikha, and R. E. White, "Single-particle model for a lithium-ion cell: Thermal behavior," *Journal of The Electrochemical Society*, vol. 158, no. 2, p. A122, 2010. 20

[42] N. Lotfi, J. Li, R. G. Landers, and J. Park, "Li-ion battery state of health estimation based on an improved single particle model," in *2017 American Control Conference (ACC)*. IEEE, 2017, pp. 86–91. 20

[43] X. Han, M. Ouyang, L. Lu, and J. Li, "Simplification of physics-based electrochemical model for lithium ion battery on electric vehicle. part i: Diffusion simplification and single particle model," *Journal of Power Sources*, vol. 278, pp. 802–813, 2015. 20

[44] G. L. Plett, "Extended kalman filtering for battery management systems of lipb-based hev battery packs: Part 2. modeling and identification," *Journal of power sources*, vol. 134, no. 2, pp. 262–276, 2004. 21

[45] H. He, R. Xiong, H. Guo, and S. Li, "Comparison study on the battery models used for the energy management of batteries in electric vehicles," *Energy Conversion and Management*, vol. 64, pp. 113–121, 2012. 21

[46] J. Jacob, B. Rosca, and S. Wilkins, "Battery pack modelling from the perspective of battery management systems," in *European Electric Vehicle Congress*, 2014. 24

[47] Z. Yang, D. Patil, and B. Fahimi, "Electrothermal modeling of lithium-ion batteries for electric vehicles," *IEEE Transactions on Vehicular Technology*, vol. 68, no. 1, pp. 170–179, 2018. 25, 26

[48] D. Bernardi, E. Pawlikowski, and J. Newman, "A general energy balance for battery systems," *Journal of the electrochemical society*, vol. 132, no. 1, p. 5, 1985. 25, 26

[49] S. Ayche, M. Daboussy, and E.-H. Aglzim, "Modeling and experimenting the thermal behavior of a lithium-ion battery on a electric vehicle," in *2018 Third International Conference on Electrical and Biomedical Engineering, Clean Energy and Green Computing (EBECEGC)*. IEEE, 2018, pp. 16–22. 25

[50] G. Berckmans, J. Jaguemont, M. Soltani, A. Samba, M. Boninsegna, N. Omar, O. Hegazy, J. Van Mierlo, and J. Ronsmans, "Lithium-ion capacitor-optimization of thermal management from cell to module level," in *2016 IEEE Vehicle Power and Propulsion Conference (VPPC)*. IEEE, 2016, pp. 1–6. 25, 26

[51] W. Mohammed, E. Kamal, A. Aitouche, and A. A. Sobaih, "Development of electro-thermal model of lithium-ion battery for plug-in hybrid electric vehicles," in *2018 7th International Conference on Systems and Control (ICSC)*. IEEE, 2018, pp. 201–206. 25

[52] S. Skoog, "Electro-thermal modeling of high-performance lithium-ion energy storage systems including reversible entropy heat," in *2017 IEEE Applied Power Electronics Conference and Exposition (APEC)*. IEEE, 2017, pp. 2369–2373. 25, 26

[53] T. Mesbahi, P. Bartholomeus, N. Rizoug, R. Sadoun, F. Khenfri, and P. Lemoigne, "Advanced model of hybrid energy storage system integrating lithium-ion battery and supercapacitor for electric vehicle applications," *IEEE Transactions on Industrial Electronics*, 2020. 25, 26

[54] M. V. Morganti, S. Longo, M. Tirovic, C.-Y. Blaise, and G. Forostovsky, "Multi-scale, electro-thermal model of nmc battery cell," *IEEE Transactions on Vehicular Technology*, vol. 68, no. 11, pp. 10 594–10 606, 2019. 25, 26

[55] K.-K. Xu, H.-X. Li, and H.-D. Yang, "Local-properties-embedding-based nonlinear spatiotemporal modeling for lithium-ion battery thermal process," *IEEE Transactions on Industrial Electronics*, vol. 65, no. 12, pp. 9767–9776, 2018. 25, 26

[56] L. Jiang, S. Yuan, H. Wu, C. Yin, and W. Miao, "Electro-thermal modeling and experimental verification for 18650 li-ion cell," in *2016 IEEE Vehicle Power and Propulsion Conference (VPPC)*. IEEE, 2016, pp. 1–5. 25, 26

[57] N. Sato, "Thermal behavior analysis of lithium-ion batteries for electric and hybrid vehicles," *Journal of power sources*, vol. 99, no. 1-2, pp. 70–77, 2001. 26

[58] M. Salameh, S. Wilke, B. Schweitzer, P. Sveum, S. Al-Hallaj, and M. Krishnamurthy, "Thermal state of charge estimation in phase change composites for passively cooled lithium-ion battery packs," *IEEE Transactions on Industry Applications*, vol. 54, no. 1, pp. 426–436, Jan 2018. 26

[59] "Online parameterization of lumped thermal dynamics in cylindrical lithium ion batteries for core temperature estimation and health monitoring," *IEEE Transactions on Control Systems Technology*, vol. 21, no. 5, pp. 1745–1755, 2013. 26, 27

[60] S. N. Motapon, A. Lupien-Bedard, L. Dessaint, H. Fortin-Blanchette, and K. Al-Haddad, "A generic electrothermal li-ion battery model for rapid evaluation of cell temperature temporal evolution," *IEEE Transactions on Industrial Electronics*, vol. 64, no. 2, pp. 998–1008, Feb 2017. 27

[61] T. Zheng and J. Dahn, "Hysteresis observed in quasi open-circuit voltage measurements of lithium insertion in hydrogen-containing carbons," *Journal of power sources*, vol. 68, no. 2, pp. 201–203, 1997. 28

[62] F. Baronti, W. Zamboni, N. Femia, R. Roncella, and R. Saletti, "Experimental analysis of open-circuit voltage hysteresis in lithium-iron-phosphate batteries," in *IECON 2013-39th Annual Conference of the IEEE Industrial Electronics Society*. IEEE, 2013, pp. 6728–6733. 28

[63] L. Zhu, Z. Sun, H. Dai, and X. Wei, "A novel modeling methodology of open circuit voltage hysteresis for lifepo4 batteries based on an adaptive discrete preisach model," *Applied Energy*, vol. 155, pp. 91–109, 2015. 28

[64] Y. Xing, W. He, M. Pecht, and K. L. Tsui, "State of charge estimation of lithium-ion batteries using the open-circuit voltage at various ambient temperatures," *Applied Energy*, vol. 113, pp. 106–115, 2014. 28

[65] A. Barai, W. D. Widanage, J. Marco, A. McGordon, and P. Jennings, "A study of the open circuit voltage characterization technique and hysteresis assessment of lithium-ion cells," *Journal of Power Sources*, vol. 295, pp. 99–107, 2015. 28

[66] B. Pattipati, B. Balasingam, G. Avvari, K. Pattipati, and Y. Bar-Shalom, "Open circuit voltage characterization of lithium-ion batteries," *Journal of Power Sources*, vol. 269, pp. 317–333, 2014. 28

[67] Y. Zhang, R. Xiong, H. He, and W. Shen, "Lithium-ion battery pack state of charge and state of energy estimation algorithms using a hardware-in-the-loop validation," *IEEE Transactions on Power Electronics*, vol. 32, no. 6, pp. 4421–4431, 2016. 29

[68] Y. Wang, C. Zhang, and Z. Chen, "A method for joint estimation of state-of-charge and available energy of lifepo4 batteries," *Applied energy*, vol. 135, pp. 81–87, 2014. 29

[69] X. Liu, J. Wu, C. Zhang, and Z. Chen, "A method for state of energy estimation of lithium-ion batteries at dynamic currents and temperatures," *Journal of Power Sources*, vol. 270, pp. 151–157, 2014. 29

[70] C. Zhang, W. Allafi, Q. Dinh, P. Ascencio, and J. Marco, "Online estimation of battery equivalent circuit model parameters and state of charge using decoupled least squares technique," *Energy*, vol. 142, pp. 678–688, 2018. 30

[71] V.-H. Duong, H. A. Bastawrous, K. Lim, K. W. See, P. Zhang, and S. X. Dou, "Online state of charge and model parameters estimation of the lifepo4 battery in electric vehicles using multiple adaptive forgetting factors recursive least-squares," *Journal of Power Sources*, vol. 296, pp. 215–224, 2015. 30

[72] G. K. Prasad and C. D. Rahn, "Model based identification of aging parameters in lithium ion batteries," *Journal of power sources*, vol. 232, pp. 79–85, 2013. 30

[73] Q. Kang, J. Wang, M. Zhou, and A. C. Ammari, "Centralized charging strategy and scheduling algorithm for electric vehicles under a battery swapping scenario," *IEEE Transactions on Intelligent Transportation Systems*, vol. 17, no. 3, pp. 659–669, 2016. 40

[74] L. Zhang, Z. Yan, D. Feng, G. Wang, S. Xu, N. Li, and L. Jing, "Centralized and decentralized optimal scheduling for charging electric vehicles," *CoRR*, vol. abs/1410.3899, 2014. 40, 41

[75] H. Nafisi, S. M. M. Agah, H. A. Abyaneh, and M. Abedi, "Two-stage optimization method for energy loss minimization in microgrid based on smart power management scheme of phevs," *IEEE Transactions on Smart Grid*, vol. 7, no. 3, pp. 1268–1276, 2016. 40, 41

[76] D. M. Anand, R. T. de Salis, Y. Cheng, J. Moyne, and D. M. Tilbury, "A hierarchical incentive arbitration scheme for coordinated pev charging stations," *IEEE Transactions on Smart Grid*, vol. 6, no. 4, pp. 1775–1784, July 2015. 40

[77] B. Alinia, "Optimal resource allocation strategies for electric vehicles in smart grids," Ph.D. dissertation, Institut National des Télécommunications, 2018. 40

[78] H. Turker, "Véhicules électriques Hybrides Rechargeables : évaluation des Impacts sur le Réseau électrique et Stratégies Optimales de recharge," Theses, Université de Grenoble, Dec. 2012. [Online]. Available: https://tel.archives-ouvertes.fr/tel-00966055 40

[79] Z. Ma, D. S. Callaway, and I. A. Hiskens, "Decentralized Charging Control of Large Populations of Plug-in Electric Vehicles," *IEEE Transactions on Control Systems Technology*, vol. 21, no. 1, pp. 67–78, 2013. 40

[80] M. Liu, P. K. Phanivong, Y. Shi, and D. S. Callaway, "Decentralized charging control of electric vehicles in residential distribution networks," *IEEE Transactions on Control Systems Technology*, no. 99, pp. 1–16, 2017. 40, 41

[81] M. Moeini-Aghtaie, A. Abbaspour, M. Fotuhi-Firuzabad, and P. Dehghanian, "Phevs centralized/decentralized charging control mechanisms: Requirements and impacts," in *2013 North American Power Symposium (NAPS)*. IEEE, 2013, pp. 1–6. 40

[82] J. García-Villalobos, I. Zamora, J. I. San Martín, F. J. Asensio, and V. Aperribay, "Plug-in electric vehicles in electric distribution networks: A review of smart charging approaches," *Renewable and Sustainable Energy Reviews*, vol. 38, pp. 717–731, 2014. [Online]. Available: http://dx.doi.org/10.1016/j.rser.2014.07.040 40, 41

[83] D. S. Callaway and I. A. Hiskens, "Achieving controllability of electric loads," *Proceedings of the IEEE*, vol. 99, no. 1, pp. 184–199, 2011. 40

[84] R. Mehta, D. Srinivasan, A. Trivedi, and J. Yang, "Hybrid Planning Method Based on Cost-Benefit Analysis for Smart Charging of Plug-in Electric Vehicles in Distribution Systems," *IEEE Transactions on Smart Grid*, vol. 3053, no. c, pp. 1–11, 2017. 41

[85] J. C. Mukherjee and A. Gupta, "A review of charge scheduling of electric vehicles in smart grid," *IEEE Systems Journal*, vol. 9, no. 4, pp. 1541–1553, 2014. 41

[86] S. Hutterer, M. Affenzeller, and F. Auinger, "Evolutionary optimization of multi-agent control strategies for electric vehicle charging," in *Proceedings of the 14th annual conference companion on Genetic and evolutionary computation*, 2012, pp. 3–10. 41

[87] M. E. Khodayar, L. Wu, and M. Shahidehpour, "Hourly coordination of electric vehicle operation and volatile wind power generation in scuc," *IEEE Transactions on Smart Grid*, vol. 3, no. 3, pp. 1271–1279, 2012. 41

[88] Q. Li, T. Cui, R. Negi, F. Franchetti, and M. D. Ilic, "On-line decentralized charging of plug-in electric vehicles in power systems," *arXiv preprint arXiv:1106.5063*, 2011. 41

[89] E. Sortomme, M. M. Hindi, S. J. MacPherson, and S. Venkata, "Coordinated charging of plug-in hybrid electric vehicles to minimize distribution system losses," *IEEE transactions on smart grid*, vol. 2, no. 1, pp. 198–205, 2010. 41, 68

[90] S. Deilami, A. S. Masoum, P. S. Moses, and M. A. Masoum, "Real-time coordination of plug-in electric vehicle charging in smart grids to minimize power losses and improve voltage profile," *IEEE Transactions on Smart Grid*, vol. 2, no. 3, pp. 456–467, 2011. 41, 42

[91] A. T. Al-Awami and E. Sortomme, "Coordinating vehicle-to-grid services with energy trading," *IEEE Transactions on smart grid*, vol. 3, no. 1, pp. 453–462, 2011. 42, 68

[92] C. Jin, S. Member, J. Tang, P. Ghosh, and S. Member, "Optimizing Electric Vehicle Charging : A Customer ' s Perspective," *IEEE Transactions on Vehicular Technology*, vol. 62, no. 7, pp. 2919–2927, 2013. 42

[93] C. G. Hoehne and M. V. Chester, "Optimizing plug-in electric vehicle and vehicle-to-grid charge scheduling to minimize carbon emissions," *Energy*, vol. 115, pp. 646–657, 2016. 42

[94] I. Rahman, P. Vasant, B. S. M. Singh, and M. Abdullah-Al-Wadud, "Hybrid swarm intelligence-based optimization for charging plug-in hybrid electric vehicle," in *Asian Conference on Intelligent Information and Database Systems*. Springer, 2015, pp. 22–30. 42

[95] S. Dimitrov and R. Lguensat, "Reinforcement learning based algorithm for the maximization of ev charging station revenue," in *2014 International Conference on Mathematics and Computers in Sciences and in Industry*. IEEE, 2014, pp. 235–239. 42

[96] Ö. Okur, N. Voulis, P. Heijnen, and Z. Lukszo, "Aggregator-mediated demand response: Minimizing imbalances caused by uncertainty of solar generation," *Applied Energy*, vol. 247, pp. 426–437, 2019. 42

[97] Z. Qu, J. Song, Y. Liu, H. Lv, K. Hu, J. Sun, M. Li, W. Liu, M. Cui, and W. Wang, "Optimization model of ev charging and discharging price considering vehicle owner response and power grid cost," *Journal of Electrical Engineering & Technology*, vol. 14, no. 6, pp. 2251–2261, 2019. 42

[98] Y. Liu, Y. Xiang, Y. Tan, B. Wang, J. Liu, and Z. Yang, "Optimal allocation model for ev charging stations coordinating investor and user benefits," *IEEE Access*, vol. 6, pp. 36 039–36 049, 2018. 42

[99] S. Ayyadi and M. Maaroufi, "Optimal framework to maximize the workplace charging station owner profit while compensating electric vehicles users," *Mathematical Problems in Engineering*, vol. 2020, 2020. 42

[100] E. Sortomme and M. A. El-sharkawi, "Optimal Charging Strategies for Unidirectional Vehicle-to-Grid," *IEEE Transactions on Smart Grid*, vol. 2, no. 1, pp. 131–138, 2011. 42, 51, 68

[101] G. Ram, C. Mouli, S. Member, M. Kefayati, R. Baldick, P. Bauer, and S. Member, "Integrated PV Charging of EV Fleet Based on Energy Prices , V2G , and Offer of Reserves," *IEEE Transactions on Smart Grid*, vol. 10, no. 2, pp. 1313–1325, 2019. 42

[102] S. Ayyadi, H. Bilil, and M. Maaroufi, "Optimal charging of electric vehicles in residential area," *Sustainable Energy, Grids and Networks*, vol. 19, p. 100240, 2019. 42

[103] S. Guo, R. Xiong, K. Wang, and F. Sun, "A novel echelon internal heating strategy of cold batteries for all-climate electric vehicles application," *Applied Energy*, vol. 219, no. 5, pp. 256–263, 2018. [Online]. Available: https://doi.org/10.1016/j.apenergy.2018.03.052 42

[104] A. Pesaran, "Battery Thermal Management in EVs and HEVs : Issues and Solutions," *Advanced Automotive Battery Conference*, no. January, p. 10, 2001. 42

[105] J. Jaguemont, L. Boulon, and Y. Dubé, "Characterization and modeling of a hybrid-electric-vehicle lithium-ion battery pack at low temperatures," *IEEE Transactions on Vehicular Technology*, vol. 65, no. 1, pp. 1–14, Jan 2016. 42

[106] Y. Ji and C. Y. Wang, "Heating strategies for Li-ion batteries operated from subzero temperatures," *Electrochimica Acta*, vol. 107, pp. 664–674, 2013. 42

[107] J. Jaguemont, L. Boulon, and Y. Dubé, "A comprehensive review of lithium-ion batteries used in hybrid and electric vehicles at cold temperatures," *Applied Energy*, vol. 164, pp. 99–114, 2016. [Online]. Available: http://dx.doi.org/10.1016/j.apenergy.2015.11.034 42

[108] Y. Dahmane, M. Ghanes, R. Chenouard, and M. Alvarado-Ruiz, "Decentralized control of electric vehicle smart charging for cost minimization considering temperature and battery health," in *2019 IEEE International Conference on Communications, Control, and Computing Technologies for Smart Grids (SmartGridComm)*. IEEE, 2019, pp. 1–6. 42, 51

[109] L. Zhang and Y. Li, "Optimal Management for Parking-Lot Electric Vehicle Charging by Two-Stage Approximate Dynamic Programming," *IEEE Transactions on Smart Grid*, vol. 8, no. 4, pp. 1722–1730, 2017. 51

[110] H. Ramadan, A. Ali, and C. Farkas, "Assessment of plug-in electric vehicles charging impacts on residential low voltage distribution grid in hungary," in *2018 6th International Istanbul Smart Grids and Cities Congress and Fair (ICSG)*, April 2018, pp. 105–109. 67

[111] S.-A. Amamra and J. Marco, "Vehicle-to-grid aggregator to support power grid and reduce electric vehicle charging cost," *IEEE Access*, vol. 7, pp. 178 528–178 538, 2019. 67, 71

[112] K. N. Kumar, B. Sivaneasan, and P. L. So, "Impact of priority criteria on electric vehicle charge scheduling," *IEEE Transactions on Transportation Electrification*, vol. 1, no. 3, pp. 200–210, 2015. 68, 69

[113] R. Mehta, D. Srinivasan, A. M. Khambadkone, J. Yang, and A. Trivedi, "Smart charging strategies for optimal integration of plug-in electric vehicles within existing distribution system infrastructure," *IEEE Transactions on Smart Grid*, vol. 9, no. 1, pp. 299–312, Jan 2018. 68

[114] R. Jiang, Z. Zhang, J. Li, Y. Zhang, and Q. Huang, "A coordinated charging strategy for electric vehicles based on multi-objective optimization," in *2017 2nd International Conference on Power and Renewable Energy (ICPRE)*, Sep. 2017, pp. 823–827. 68

[115] M. Liu, P. K. Phanivong, Y. Shi, and D. S. Callaway, "Decentralized charging control of electric vehicles in residential distribution networks," *IEEE Transactions on Control Systems Technology*, vol. 27, no. 1, pp. 266–281, Jan 2019. 68

[116] M. Ansari, A. T. Al-Awami, M. Abido, and E. Sortomme, "Optimal charging strategies for unidirectional vehicle-to-grid using fuzzy uncertainties," in *2014 IEEE PES T&D Conference and Exposition*. IEEE, 2014, pp. 1–5. 68

[117] L. Luo, Z. Wu, W. Gu, H. Huang, S. Gao, and J. Han, "Coordinated allocation of distributed generation resources and electric vehicle charging stations in distribution systems with vehicle-to-grid interaction," *Energy*, vol. 192, p. 116631, 2020. 68

[118] Y. Zheng and L. Jian, "Smart charging algorithm of electric vehicles considering dynamic charging priority," in *2016 IEEE International Conference on Information and Automation (ICIA)*. IEEE, 2016, pp. 555–560. 68, 69

[119] M. M. Islam, X. Zhong, Z. Sun, H. Xiong, and W. Hu, "Real-time frequency regulation using aggregated electric vehicles in smart grid," *Computers & Industrial Engineering*, vol. 134, pp. 11–26, 2019. 68, 71

[120] J. Hu, S. You, M. Lind, and J. Østergaard, "Coordinated charging of electric vehicles for congestion prevention in the distribution grid," *IEEE Transactions on Smart Grid*, vol. 5, no. 2, pp. 703–711, 2013. 68, 70

[121] F. J. G. Villalobos, "Optimized charging control method for plug-in electric vehicles in lv distribution networks," Ph.D. dissertation, Universidad del País Vasco-Euskal Herriko Unibertsitatea, 2016. 68

[122] J. Clairand, J. Rodríguez-García, and C. Álvarez-Bel, "Smart charging for electric vehicle aggregators considering users' preferences," *IEEE Access*, vol. 6, pp. 54 624–54 635, 2018. 68

[123] R. Wang, P. Wang, and G. Xiao, "Two-stage mechanism for massive electric vehicle charging involving renewable energy," *IEEE Transactions on Vehicular Technology*, vol. 65, no. 6, pp. 4159–4171, June 2016. 69

[124] D. A. Chekired, L. Khoukhi, and H. T. Mouftah, "Fog computing based energy storage in smart grid: A cut-off priority queuing model for plug-in electrified vehicles charging," *IEEE Transactions on Industrial Informatics*, 2020. 69

[125] Z. J. Lee, D. Johansson, and S. H. Low, "Acn-sim: An open-source simulator for data-driven electric vehicle charging research," in *2019 IEEE International Conference on Communications, Control, and Computing Technologies for Smart Grids (SmartGridComm)*. IEEE, 2019, pp. 1–6. 69

[126] Z. J. Lee, T. Li, and S. H. Low, "Acn-data: Analysis and applications of an open ev charging dataset," in *Proceedings of the Tenth ACM International Conference on Future Energy Systems*, ser. e-Energy '19. New York, NY, USA: Association for Computing Machinery, 2019, p. 139–149. [Online]. Available: https://doi.org/10.1145/3307772.3328313 69

[127] Adaptive charging network research portal (acn-portal). [Online]. Available: https://ev.caltech.edu/index 69

[128] J. A. Stankovic, M. Spuri, K. Ramamritham, and G. C. Buttazzo, *Deadline scheduling for real-time systems: EDF and related algorithms*. Springer Science & Business Media, 2012, vol. 460. 70

[129] N. B. Arias, S. Hashemi, P. B. Andersen, C. Træholt, and R. Romero, "Distribution system services provided by electric vehicles: recent status, challenges, and future prospects," *IEEE Transactions on Intelligent Transportation Systems*, vol. 20, no. 12, pp. 4277–4296, 2019. 70

[130] S. Sarabi, "Contribution du Vehicle-to-Grid (V2G) à la gestion énergétique d'un parc de Véhicules Électriques sur le réseau de distribution," Theses, Ecole nationale supérieure d'arts et métiers - ENSAM, Nov. 2016. [Online]. Available: https://pastel.archives-ouvertes.fr/tel-01514175 70

[131] C. S. Ioakimidis, D. Thomas, P. Rycerski, and K. N. Genikomsakis, "Peak shaving and valley filling of power consumption profile in non-residential buildings using an electric vehicle parking lot," *Energy*, vol. 148, pp. 148–158, 2018. 70

[132] N. Chen, C. W. Tan, and T. Q. Quek, "Electric vehicle charging in smart grid: Optimality and valley-filling algorithms," *IEEE Journal of Selected Topics in Signal Processing*, vol. 8, no. 6, pp. 1073–1083, 2014. 70

[133] Z. Wang and S. Wang, "Grid power peak shaving and valley filling using vehicle-to-grid systems," *IEEE Transactions on power delivery*, vol. 28, no. 3, pp. 1822–1829, 2013. 70

[134] K. Zhang, L. Xu, M. Ouyang, H. Wang, L. Lu, J. Li, and Z. Li, "Optimal decentralized valley-filling charging strategy for electric vehicles," *Energy conversion and management*, vol. 78, pp. 537–550, 2014. 70

[135] M. Uddin, M. F. Romlie, M. F. Abdullah, S. Abd Halim, T. C. Kwang *et al.*, "A review on peak load shaving strategies," *Renewable and Sustainable Energy Reviews*, vol. 82, pp. 3323–3332, 2018. 70

[136] A. S. Masoum, S. Deilami, P. S. Moses, M. A. Masoum, and A. Abu-Siada, "Smart load management of plug-in electric vehicles in distribution and residential networks with charging stations for peak shaving and loss minimisation considering voltage regulation," *IET generation, transmission & distribution*, vol. 5, no. 8, pp. 877–888, 2011. 70

[137] J. Y. Lee and S. G. Choi, "Linear programming based hourly peak load shaving method at home area," in *16th International Conference on Advanced Communication Technology*. IEEE, 2014, pp. 310–313. 70

[138] J. Y. Yong, V. K. Ramachandaramurthy, K. M. Tan, and N. Mithulananthan, "Bi-directional electric vehicle fast charging station with novel reactive power compensation for voltage regulation," *International Journal of Electrical Power & Energy Systems*, vol. 64, pp. 300–310, 2015. 70

[139] N. Zou, L. Qian, and H. Li, "Auxiliary frequency and voltage regulation in microgrid via intelligent electric vehicle charging," in *2014 IEEE International Conference on Smart Grid Communications (SmartGridComm)*. IEEE, 2014, pp. 662–667. 70

[140] M. Kesler, M. C. Kisacikoglu, and L. M. Tolbert, "Vehicle-to-grid reactive power operation using plug-in electric vehicle bidirectional offboard charger," *IEEE Transactions on Industrial Electronics*, vol. 61, no. 12, pp. 6778–6784, 2014. 71

[141] J. Wang, G. R. Bharati, S. Paudyal, O. Ceylan, B. P. Bhattarai, and K. S. Myers, "Coordinated electric vehicle charging with reactive power support to distribution grids," *IEEE Transactions on Industrial Informatics*, vol. 15, no. 1, pp. 54–63, 2018. 71

[142] M. Latifi, R. Sabzehgar, and M. Rasouli, "Reactive power compensation using plugged-in electric vehicles for an ac power grid," in *IECON 2018-44th Annual Conference of the IEEE Industrial Electronics Society*. IEEE, 2018, pp. 4986–4991. 71

[143] M. C. Kisacikoglu, "Vehicle-to-grid (v2g) reactive power operation analysis of the ev/phev bidirectional battery charger," PhD diss, University of Tennessee, 2013. 71

[144] A. BOUALLAGA, "Gestion énergétique d'une infrastructure de charge intelligente de véhicules électriques dans un réseau de distribution intégrant des énergies renouvelables. ," Theses, Université Lille 1 Sciences et Technologies, Jun. 2015. [Online]. Available: https://tel.archives-ouvertes.fr/tel-01222648 71

[145] H. N. Nguyen, C. Zhang, and J. Zhang, "Dynamic demand control of electric vehicles to support power grid with high penetration level of renewable energy," *IEEE Transactions on Transportation Electrification*, vol. 2, no. 1, pp. 66–75, 2016. 71

[146] S. Tabatabaee, S. S. Mortazavi, and T. Niknam, "Stochastic scheduling of local distribution systems considering high penetration of plug-in electric vehicles and renewable energy sources," *Energy*, vol. 121, pp. 480–490, 2017. 71

[147] F. Mwasilu, J. J. Justo, E.-K. Kim, T. D. Do, and J.-W. Jung, "Electric vehicles and smart grid interaction: A review on vehicle to grid and renewable energy sources integration," *Renewable and sustainable energy reviews*, vol. 34, pp. 501–516, 2014. 71

[148] M. Rahmani-andebili, "Spinning reserve supply with presence of electric vehicles aggregator considering compromise between cost and reliability," *IET Generation, Transmission & Distribution*, vol. 7, no. 12, pp. 1442–1452, 2013. 71

[149] J. Zhao, C. Wan, Z. Xu, and K. P. Wong, "Spinning reserve requirement optimization considering integration of plug-in electric vehicles," *IEEE Transactions on Smart Grid*, vol. 8, no. 4, pp. 2009–2021, 2016. 71

[150] W. Zhang, K. Spence, R. Shao, and L. Chang, "Optimal scheduling of spinning reserve and user cost in vehicle-to-grid (v2g) systems," in *2018 IEEE Energy Conversion Congress and Exposition (ECCE)*. IEEE, 2018, pp. 1058–1064. 71

[151] G. R. C. Mouli, M. Kefayati, R. Baldick, and P. Bauer, "Integrated pv charging of ev fleet based on energy prices, v2g, and offer of reserves," *IEEE Transactions on Smart Grid*, vol. 10, no. 2, pp. 1313–1325, 2017. 71

[152] Y. Mu, J. Wu, J. Ekanayake, N. Jenkins, and H. Jia, "Primary frequency response from electric vehicles in the great britain power system," *IEEE Transactions on Smart Grid*, vol. 4, no. 2, pp. 1142–1150, 2012. 71

[153] S. Han, S. Han, and K. Sezaki, "Development of an optimal vehicle-to-grid aggregator for frequency regulation," *IEEE Transactions on smart grid*, vol. 1, no. 1, pp. 65–72, 2010. 71

[154] H. Liu, Z. Hu, Y. Song, and J. Lin, "Decentralized vehicle-to-grid control for primary frequency regulation considering charging demands," *IEEE Transactions on Power Systems*, vol. 28, no. 3, pp. 3480–3489, 2013. 71

[155] X. Xu, C. Zhang, and L. Gu, "Decentralized primary frequency regulation control strategy for vehicle-to-grid," in *2016 3rd International Conference on Systems and Informatics (ICSAI)*. IEEE, 2016, pp. 217–222. 71

[156] S. Izadkhast, P. Garcia-Gonzalez, and P. Frías, "An aggregate model of plug-in electric vehicles for primary frequency control," *IEEE Transactions on Power Systems*, vol. 30, no. 3, pp. 1475–1482, 2015. 71

[157] H. Liu, K. Huang, Y. Yang, H. Wei, and S. Ma, "Real-time vehicle-to-grid control for frequency regulation with high frequency regulating signal," *Protection and Control of Modern Power Systems*, vol. 3, no. 1, p. 13, 2018. 71

[158] E. Yao, V. W. Wong, and R. Schober, "Robust frequency regulation capacity scheduling algorithm for electric vehicles," *IEEE Transactions on Smart Grid*, vol. 8, no. 2, pp. 984–997, 2016. 71

[159] G. Wenzel, M. Negrete-Pincetic, D. E. Olivares, J. MacDonald, and D. S. Callaway, "Real-time charging strategies for an electric vehicle aggregator to provide ancillary services," *IEEE Transactions on Smart Grid*, vol. 9, no. 5, pp. 5141–5151, 2018. 71

[160] H. Liu, K. Huang, N. Wang, J. Qi, Q. Wu, S. Ma, and C. Li, "Optimal dispatch for participation of electric vehicles in frequency regulation based on area control error and area regulation requirement," *Applied energy*, vol. 240, pp. 46–55, 2019. 71

[161] K. Kaur, N. Kumar, and M. Singh, "Coordinated power control of electric vehicles for grid frequency support: Milp-based hierarchical control design," *IEEE Transactions on Smart Grid*, vol. 10, no. 3, pp. 3364–3373, 2019. 71

[162] K. Kaur, M. Singh, and N. Kumar, "Multiobjective optimization for frequency support using electric vehicles: An aggregator-based hierarchical control mechanism," *IEEE Systems Journal*, vol. 13, no. 1, pp. 771–782, 2019. 71

[163] H. Jeong, M. Jeong, and S. Lee, "Vehicle-to-grid based frequency regulation method in an isolated microgrid considering charging requests of electric vehicles," in *2019 International Conference and Exhibition on Electricity Distribution (CIRED)*. AIM, 2019, pp. 1–5. 71

[164] M. Wang, Y. Mu, F. Li, H. Jia, X. Li, Q. Shi, and T. Jiang, "State space model of aggregated electric vehicles for frequency regulation," *IEEE Transactions on Smart Grid*, 2019. 71

[165] M. H. Khooban and M. Gheisarnejad, "A novel deep reinforcement learning controller based type-ii fuzzy system: Frequency regulation in microgrids," *IEEE Transactions on Emerging Topics in Computational Intelligence*, 2020. 71

[166] X. Chen, K.-C. Leung, A. Y. Lam, and D. J. Hill, "Online scheduling for hierarchical vehicle-to-grid system: Design, formulation, and algorithm," *IEEE Transactions on Vehicular Technology*, vol. 68, no. 2, pp. 1302–1317, 2018. 71

[167] Y. Dahmane, R. Chenouard, M. Ghanes, and M. Alvarado-Ruiz, "Coordinated charging of large electric vehicle fleet in a charging station with limited transformer power," in *2020 IEEE Conference on Control Technology and Applications (CCTA)*. IEEE, 2020, pp. 1054–1059. 71, 72

[168] X. Ye, T. Ji, M. Li, and Q. Wu, "Optimal control strategy for plug-in electric vehicles based on reinforcement learning in distribution networks," in *2018 International Conference on Power System Technology (POWERCON)*. IEEE, 2018, pp. 1706–1711. 71

[169] E. Yao, V. W. S. Wong, and R. Schober, "Robust frequency regulation capacity scheduling algorithm for electric vehicles," *IEEE Transactions on Smart Grid*, vol. 8, no. 2, pp. 984–997, 2017. 71

CENTRALE NANTES

Titre : Gestion d'énergie optimisée étendue véhicules infrastructures

Mot clés : : Voiture électrique, optimisation, batteries Li-ion, effet de la température, algorithmes de planification, gestion d'énergie de flotte, réseau intelligent, V2G, régulation de fréquence.

Résumé :

Cette thèse de doctorat s'inscrit dans le cadre de la chaire Renault/Centrale Nantes sur l'amélioration des performances des véhicules électriques (EV/HEV). Elle est dédiée à la problématique de la gestion de la recharge des véhicules électriques, en utilisant des algorithmes d'optimisation et des stratégies de recharge intelligentes. Dans ce cadre, plusieurs contributions ont été proposées sur les sujets de la recharge intelligente d'une voiture électrique et la gestion de la recharge d'une flotte de véhicules électriques, en considérant les contraintes de mobilités (SOC désiré à la fin de la recharge et heure de départ), la température des batteries Li-ion, les infrastructures de recharge, et le réseau électrique.

Sur le sujet de la recharge intelligente d'une voiture électrique, les contributions se sont concentrées sur le développement des algorithmes embarqués permettant la planification du profil de la puissance de recharge afin de réduire le coût de la recharge. Les algorithmes proposés prennent en compte les besoins de mobilités des utilisateurs de véhicules électriques, et l'effet de la température sur la puissance de recharge des batteries Li-ion.

Sur le sujet de la gestion de recharge de flotte de véhicules, les contributions portent essentiellement sur les algorithmes centralisés dans les stations de recharge de véhicules électriques. Un algorithme de recharge unidirectionnelle a été proposé afin d'évaluer le nombre optimal de véhicules électriques à recharger avec un bon niveau de satisfaction des contraintes de mobilités et sans aucun renforcement de l'infrastructure. Le passage à l'algorithme bidirectionnel est fait grâce à l'exploitation de la fonctionnalité V2G qui permettra la participation des véhicules électriques dans la régulation de fréquence.

Les contributions proposées sur le premier sujet ont l'avantage d'augmenter la précision d'estimation de SOC final en très basse température, et d'être embarquable sur le véhicule grâce à la légèreté des algorithmes et la rapidité d'exécution. D'autre part, les algorithmes de gestion de recharge de flotte de véhicules permettent une intégration des véhicules électriques à grande échelle sur le réseau et montrent le potentiel des voitures électriques dans la contribution à la stabilité du réseau électrique.

Les algorithmes et les stratégies développées ont été testés en simulation et seront testés sur un système de recharge de voiture électrique. Les résultats obtenus ont permis de mettre en évidence l'avantage de la recharge intelligente sur la réduction des coûts, les bienfaits sur le réseau et l'importance de la gestion de la recharge des flottes de véhicules électriques dans développement des services réseaux.

Title: Optimized Energy Management for Electric Vehicles and Infrastructures

Keywords: Electric vehicle, optimization, Li-ion battery charging, temperature effect, scheduling algorithms, EV fleet energy management, smart grid, V2G, frequency regulation.

Abstract: This PhD thesis is part of the Renault/Centrale Nantes chair on improving the performance of electric vehicles (EV/PHEV). It is dedicated to the problem of the charging management of electric vehicles, using optimization algorithms and smart charging strategies. In this framework, several contributions have been proposed on the topics of smart charging of an EV and the smart energy management of an EV fleet, considering the mobility constraints (desired SOC at the end of the charging and departure time), the temperature of the Li-ion batteries, the charging infrastructures, and the power grid.

On the subject of smart charging of an EV, the contributions focused on the development of embedded algorithms allowing the scheduling of the charging power profile in order to reduce the charging cost. The proposed algorithms take into account the mobility needs of electric vehicle users, and the effect of temperature on the charging power of Li-ion batteries. On the subject of fleet energy management, the contributions focus on centralized algorithms in electric vehicle charging stations. An unidirectional recharging algorithm has been proposed in order to evaluate the optimal number of electric vehicles to be recharged with a good level of satisfaction of mobility constraints and without any infrastructure reinforcement. The switch to the bidirectional algorithm is due to the exploitation of the V2G functionality, which will allow the participation of electric vehicles in frequency regulation.

The proposed contributions on the first topic have the advantage of increasing the estimation accuracy of final SOC in very low temperature, and to be embedded on the EV due to the low computational capacity of the algorithms and the speed of execution. On the other hand, the EV fleet charging management algorithms allow the possibility of large-scale integration of electric vehicles on the grid and show the potential of EVs in contributing to the stability of the power grid by offering ancillary services such as frequency regulation.

The algorithms and strategies developed have been tested in simulation and will be tested on an EV charging system. The results obtained have highlighted the benefits of smart charging on cost reduction and grid benefits and the importance of electric vehicle fleet charging management in the development of grid services.